United States
Environmental Protection
Agency

Office of Air Quality
Planning and Standards
Research Triangle Park NC 27711

EPA-450/4-82-009
June 1982

Air

EPA

An Evaluation of the Empirical Kinetic Modeling Approach Using the St. Louis RAPS Data Base

EPA-450/4-82-009

An Evaluation of the Empirical Kinetic Modeling Approach Using the St. Louis RAPS Data Base

By
Gerald L. Gipson
Air Management Technology Branch
Monitoring and Data Analysis Division

U.S ENVIRONMENTAL PROTECTION AGENCY
Office of Air Quality Planning and Standards
Research Triangle Park, North Carolina 27711

June 1982

This report has been reviewed by the Office of Air Quality Planning and Standards, EPA, and approved for publication. Mention of trade names or commercial products is not intended to constitute endorsement or recommendation for use.

Publication No. EPA-450/4-82-009

TABLE OF CONTENTS

TABLE OF CONTENTS (Continued)

PREFACE

The Urban Airshed Model Simulations described in this report were conducted by the Source Receptor Analysis Branch (SRAB) of the Office of Air Quality Planning and Standards in EPA. The author gratefully acknowledges the invaluable assistance of Conrad Newberry and Gerald Moss of SRAB in providing the Airshed Modeling information needed to conduct this project. In addition, the author extends special thanks to Robert Kelly, Norman Possiel and Edwin L. Meyer for their numerous contributions and valuable suggestions. Finally, the author is especially grateful to Mrs. Carole Mask for typing and editing the final report.

LIST OF TABLES

LIST OF FIGURES

EXECUTIVE SUMMARY

The Empirical Kinetic Modeling Approach (EKMA) is a technique developed for estimating the degree of emission reduction necessary to achieve the ozone National Ambient Air Quality Standard (NAAQS). The objective of this study has been to investigate several approaches for assessing the validity of the relationships underlying EKMA. The most direct means of validating the model is to compare changes in ozone levels that result from changes in precursor emissions to those predicted by the model. Such an approach requires the existence of well documented trends in both ozone and its precursors over a period of time during which precursor emissions have been appreciably altered. Such data, especially trends in precursors, are generally not available over a time period of sufficient interest to make such comparisons. As a result, three indirect methods for evaluating EKMA have been explored.

The first method entails using the sample, Lagrangian model underlying EKMA to make predictions of peak ozone levels on a given day, and comparing those predictions to observations. For this approach, detailed meteorological, emissions, and air quality data compiled under the Regional Air Pollution Study (RAPS) in St. Louis, Missouri, were used to develop the model inputs. This approach does not answer the key question of how accurately EKMA predicts changes in peak ozone accompanying reductions in precursors. However, successful prediction of observed peaks gives some confidence that the model provides a reasonable approximation of the physical and chemical phenomena leading to ozone formation. This, in turn, should provide greater confidence in using the model to make predictions of changes in ozone occurring because of changes in precursors. The results of using this approach are not particularly encouraging. Substantial underpredictions of peak ozone occurred in a number of cases. However, a detailed assessment of the results suggested that performance could be improved in some cases with revised model inputs. Thus, it is not clear from these results whether the tendency towards underprediction is due to the modeling concepts, or due to uncertainties in the model inputs.

The second method evaluated is very similar to the one just described. Again, the model underlying EKMA is used to make predictions of peak ozone, and these are then compared to observed levels. In this approach, however, a less complex data base is used, with certain simplifying assumptions made in the formulation of the model inputs. Because of limited data, this level of analysis is the more commonly used method of applying EKMA. As with the first approach, the primary question of how well EKMA predicts changes in peak ozone is not directly addressed, but this approach does give some indication of how well the model simulates ozone formation. The results found with this approach are much better than those found using the first approach. In nearly every case, predicted peak ozone concentrations are within ±30% of observations. Furthermore, sensitivity tests indicate that this agreement is not substantially altered by variations in selected input variables. These results suggest that the ozone formation processes are reasonably simulated by the model. Therefore, the possibility exists that the simplified approach may "smooth out" some anomalies associated with the development of the model inputs using the more rigorous approach. However, because of the simplifying assumptions used in deriving the model inputs, the possibility that agreement between observations and predictions may be somewhat fortuitous cannot be entirely ruled out.

The final approach attempts to address more directly the question of how well EKMA predicts changes in peak ozone. In this approach, a number of emission reduction scenarios are simulated with a complex Photochemical Air Quality Simulation Model (PAQSM). These results form the basis for evaluating corresponding EKMA predictions. An important limitation of such an evaluation is that no absolute guarantee exists that the PAQSM predictions are correct. Nevertheless, the PAQSM does represent the state-of-the-art in photochemical modeling and, as such, serves as one means of testing simpler models. However, making such comparisons is complicated by differences in the mode of application of each type of model. EKMA did not agree precisely with the PAQSM in every case. However, when estimates of the degree of control needed to reduce peak ozone to 120 ppb (the level of the ozone NAAQS) were made for each of three days with EKMA and the PAQSM, differences between the estimated emission reductions were less than about 10%. Using the PAQSM as the standard, EKMA was not found to systematically over or underestimate required emission reductions

The findings of the above three approaches for evaluating EKMA have led to several recommendations for future evaluation. First, the trajectory model underlying EKMA should be compared with more complex trajectory models. Also, methodologies for formulating the trajectory model inputs need more study. Additional tests should be conducted to identify potential differences in model predictions that could occur as the result of using various chemical mechanisms. Finally, the relative importance of boundary condition assumptions in the PAQSM and EKMA simulations need additional study.

1.0 INTRODUCTION

The Empirical Kinetic Modeling Approach (EKMA) is a procedure developed by the U.S. Environmental Protection Agency (EPA) to determine emission reductions necessary to achieve the National Ambient Air Quality Standard (NAAQS) for ozone.[1,2] EKMA mathematically relates peak ozone concentrations to its precursors - nonmethane organic compounds (NMOC) and oxides of nitrogen (NO_x). These relationships form the basis for estimating reductions in precursor emissions needed to attain a prescribed reduction in peak ozone concentrations. The objective of this study has been to investigate several approaches for assessing the validity of the O_3-precursor relationships generated by the model underlying EKMA.

When any photochemical model is used to predict changes in ozone levels resulting from changes in precursor emissions, the most direct means of validating that model is to compare the predicted change to that which has actually taken place. Such an approach requires the existence of well documented trends of both ozone and its precursors over a sufficient period of time during which precursor emissions have been appreciably altered. For many areas of the country, sufficient data are available to establish the trends in ozone over a number of years, but changes in precursors that have taken place during that same time are not as well known.[3,4] This uncertainty in precursor trends often introduces large uncertainties in comparing the ozone trends predicted by a photochemical model with those that have been observed. Furthermore, little, if any, ozone trend data are available for areas of the country which have moved from a position of a significant ozone problem to one of compliance with the ozone NAAQS, or vice versa. As a result, the data necessary to validate a model over the range for which it is to be used are not available.

The aforementioned problems associated with direct validation of photochemical models have led to the development of some indirect approaches for assessing the validity of EKMA. The first approach consists of using detailed meteorological, emissions, and air quality data with EKMA to predict observed ozone peaks, rather than changes in peak ozone levels as is usually done. The use of detailed data is commensurate with a Level II analysis

described in Reference 5, and the technique of comparing predicted and observed ozone peaks is similar in concept to the approach normally used to validate more complex photochemical models. Such an approach does not directly answer the key question of how accurately EKMA predicts changes in peak ozone accompanying reductions in precursors. However, successful prediction of observed peaks gives some confidence that the model provides a reasonable approximation of the physical and chemical phenomena leading to ozone formation. This, in turn, leads to greater confidence in using the cause effect relationships contained within the model to make predictions of changes in ozone occurring as a result of changes in precursors.

The second approach investigated for assessing EKMA's validity is nearly identical to the first in that model predictions of peak ozone are compared to observed levels. The difference results from using a less complex data base to formulate model inputs. This approach was taken because the detailed data of the type needed for a Level II analysis are not available for many areas of the country. To test the potential effects of limited data on the predictions of peak ozone, the model inputs used in the Level II analysis were modified such that they are consistent with those required for a Level III analysis, as described in Reference 5. Once again, the comparison of predicted peak ozone levels with those observed does not address the primary question of how well the modeling approach predicts changes in peak ozone, but provides some indication of how well the model represents ozone formation phenomena when a much more limited data base is used.

The final approach attempts to address more directly the problem of how well EKMA predicts changes in peak ozone resulting from changes in precursors, but with some important limitations. In this approach, the EKMA predictions of changes in peak ozone are compared to the predictions of a detailed Photochemical Air Quality Simulation Model (PAQSM). PAQSMs have been identified as having the greatest potential for estimating the changes in ozone levels resulting from changes in precursor levels because of their detailed mathematical representation of chemical and physical processes leading to ozone formation.[1] For this third approach, a number of control strategies in which precursors are changed from existing, or base case, levels are simulated with

the PAQSM and then replicated with the simpler EKMA model. The effects of the control strategies predicted by each model are then compared for consistency. Presumably, the more complex PAQSM should provide the best estimate of the effects of changing precursor levels because of its more detailed nature, and therefore serves as the basis for evaluating the predictions of the simpler EKMA. One important limitation of such an analysis, however, is that no absolute assurance exists that the PAQSM predictions are correct. Nevertheless, the PAQSM does provide state-of-the-art estimates of the effectiveness of potential control programs and, as such, serves as one means of testing simpler approaches.

The data base used to conduct the three analyses just described was compiled during the Regional Air Pollution Study (RAPS) in the Metropolitan St. Louis Area.[6] This particular data base was selected because of the detailed information collected, and because a complex PAQSM had been applied using the data base. With this data base, sufficient information exists not only to apply the different types of models, but it also affords the opportunity to examine several facets of model performance, especially those related to the models' capabilities to simulate existing ozone levels.

The remainder of Section 1 provides background information on EKMA and a more detailed description of the data base used in the study. Sections 2 and 3 describe the Level II and Level III analyses where predictions of peak ozone are compared to measured levels. The comparisons between the PAQSM and EKMA are discussed in Section 4. Finally, conclusions and recommendations arising from the findings of all three analyses are presented in Section 5.

1.1 Background

The application of EKMA involves the use of an ozone isopleth diagram, an example of which is shown in Figure 1-1. In such a diagram, peak hourly average ozone concentrations are plotted as a function of early morning precursor levels. To estimate the emission reductions needed to achieve the ozone NAAQS, the diagrams are used in conjunction with ambient measurements of ozone and precursor concentrations. The diagrams themselves are generated by means of the Kinetics Model and Ozone Isopleth Plotting Package (OZIPP).[7,8]

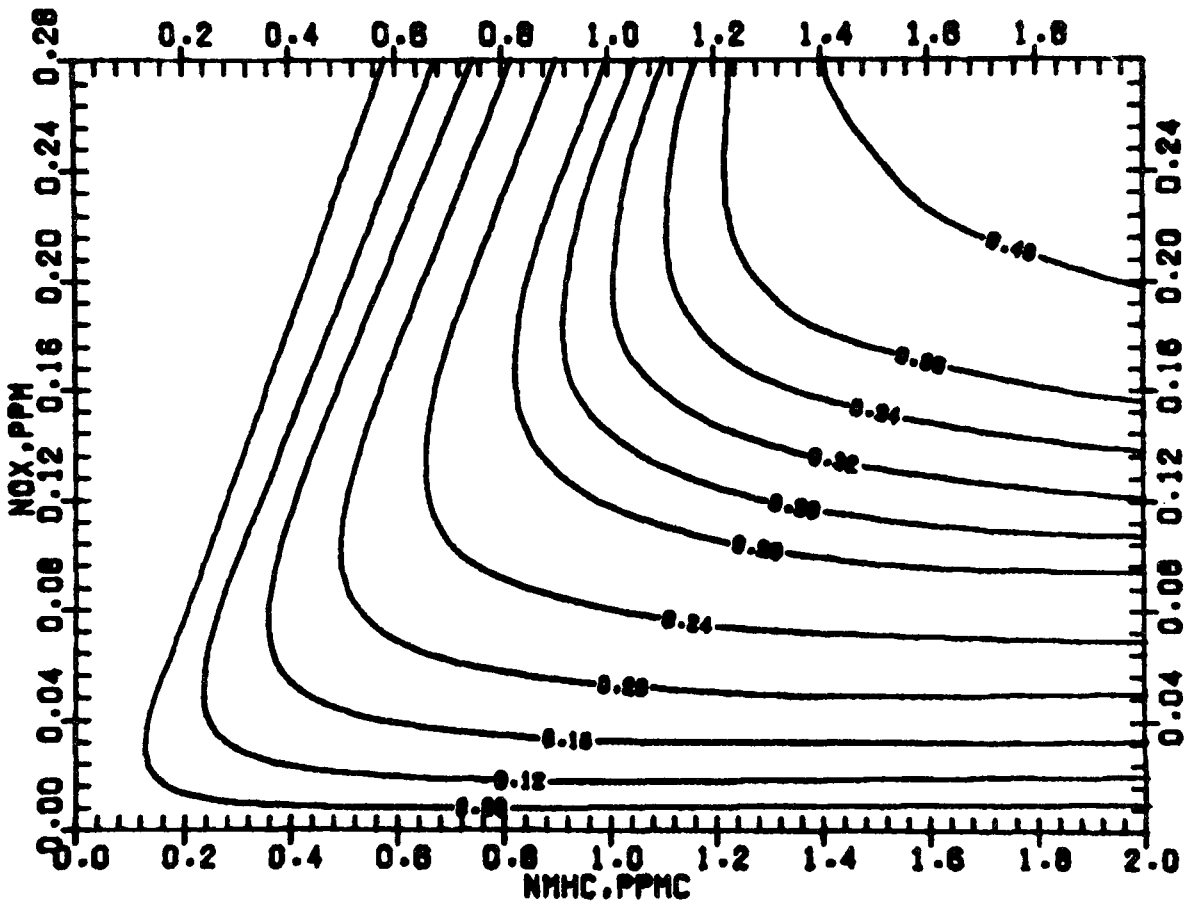

Figure 1-1. Example Ozone Isopleth Diagram.

This computerized program produces an isopleth diagram on the basis of a simplified trajectory model which mathematically simulates ozone formation. In so doing, the trajectory model takes into account the effects of emissions, meteorology and pollutants which may have been transported into an area. Thus, while the isopleths are plotted as a function of early morning precursor levels, the positioning of the isopleths of the diagram are influenced by these other variables as well.

Of the three approaches taken for evaluating EKMA that were previously described, two involve making predictions of peak ozone, and in the other, EKMA is used to make predictions of changes in ozone from some existing, or base case condition. Thus, the first two involve testing the trajectory model underlying EKMA for its ability to predict peak ozone levels that have been observed. The third approach, predicting changes from base case conditions, consists of actually using the isopleth diagram and the EKMA technique. While both have been discussed extensively elsewhere,[1,2,8,9] they are briefly described below.

1.1.1 OZIPP Trajectory Model

The conceptual basis for the simple trajectory model in OZIPP is similar to a Lagrangian photochemical dispersion model (see Figure 1-2). A column of air is advected along a trajectory by the wind. The height of the column is equal to the mixing height (i.e., the column extends from the earth's surface throughout the mixed layer). The horizontal dimensions are selected such that concentration gradients are small, and thus the effects of horizontal exchange of air between the column and its surroundings can be ignored. Within the column, the air is assumed to be uniformly mixed at all times.

Initially, the column contains NMOC, NO_x and possibly ozone resulting from prior emissions and/or possible transport from upwind areas. As the column moves along the trajectory, the height grows in accordance with the temporal variation in mixing height. As the mixing height increases, air above the column is mixed downwind into the column instantaneously, resulting in two phenomena. First, pollutants within the column are diluted due to the

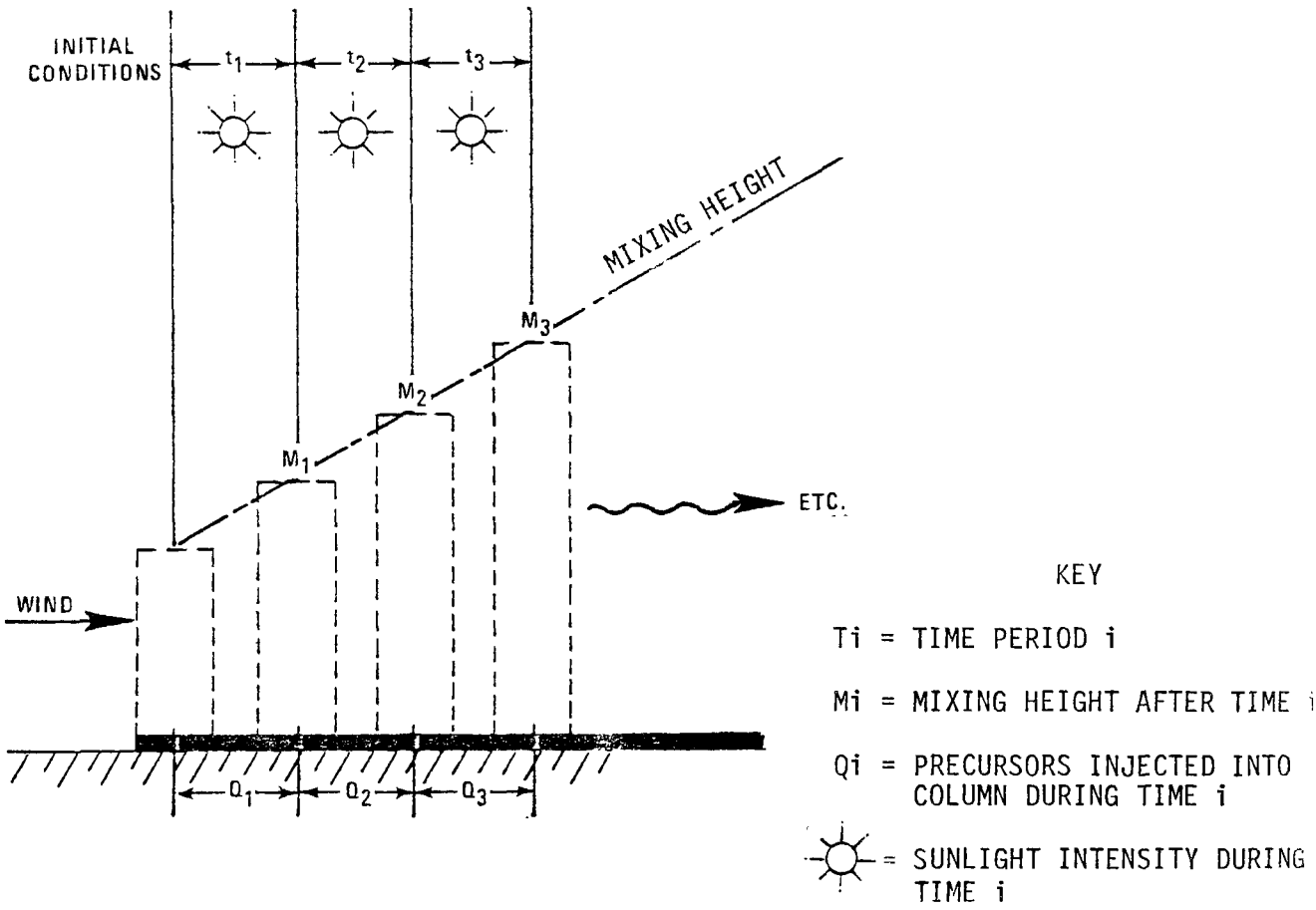

Figure 1-2. Conceptual View of the OZIPP Trajectory Model.

increased volume of the column. Second, entrainment of pollutants from aloft may occur. Several studies have documented that, under certain conditions, significant pollutant concentrations (especially ozone) may exist above the early morning mixed layer.[10,11,12] The trajectory model simulates the effect of entrainment by assuming constant pollutant concentrations aloft, and by assuming their entrainment into the column at a rate proportional to the growth of the mixed layer. In addition to these two effects, the trajectory model also simulates the injection of fresh precursor emissions into the column, which may occur as it moves along the trajectory. Thus, while pollutant concentrations within the column are diluted by the growth of the mixed layer, this effect may be offset somewhat by the entrainment of pollutants from aloft and by the injection of fresh precursor emissions.

In addition to the physical processes described above, the OZIPP trajectory model simulates the chemical interactions taking place among the pollutants within the column. The latter is accomplished by means of a chemical kinetic mechanism which describes the chemical reactions and their corresponding rates of reaction. For those reactions affected by sunlight, the rate constants are determined by a theoretical estimation of the diurnal variation in solar radiation. Thus, the trajectory model calculates the instantaneous concentrations of all reactive species included within the mechanism as a function of time. From the time profile of ozone within the column, the model calculates the maximum one-hour-average concentration occurring during the simulation. The mathematical representation of all the aforementioned processes is summarized in Table 1-1.

The application of the trajectory model in OZIPP requires the extraneous development of a number of specific model inputs. First, the trajectory path which depicts the column movement through time and space must be defined. Once this is done, the pollutant concentrations initially within the column (i.e., at the trajectory starting point) can be approximated, and the emissions occurring along the path can be estimated. Additionally, the growth in the mixed layer and the concentrations of pollutants above the early morning mixed layer must be estimated. The procedures used for developing these inputs for the Level II and Level III analyses are described in Sections 2 and 3,

Table 1-1. Mathematical Representation of the OZIPP Trajectory Model[a].

C_i = the concentrations of the ith chemical species in the mixed volume at time = t

$C_i(@0)$ = the initial concentration of the ith species in the mixed volume at time = 0

C_i^{aloft} = the concentration of the ith species above the mixed volume

$MH = f(t)$	mixing height at time = t
$\frac{dMH}{dt} = f'(t)$	rate of rise at time = t
$K_D = (\frac{1}{MH}) \frac{dMH}{dt}$	dilution rate at time = t
$\left\{\frac{dC_i}{dt}\right\}_{dil} = -K_D C_i$	decrease in species i caused by mixing height rise
$\left\{\frac{dC_i}{dt}\right\}_{ent} = + K_D C_i^{aloft}$	increase in species i caused by entrainment due to mixing height rise
$E_i = h(t)$	mass of species C_i emitted per unit time at time = t (concentration - height units)
$\left\{\frac{dC_i}{dt}\right\}_{emis} = E_i/MH$	increase in species C_i caused by emissions into a mixing volume with unit area and height, MH, at time t
$P_i = \text{func}\ (C_j, j=1,n)$	production of species C_i due to chemical formation at time t
$L_i = \text{func}\ (C_j, j=1,n)$	loss of species C_i due to chemical reaction at time t
$\left\{\frac{dC_i}{dt}\right\}_{chem} = P_i - L_i$	increase or decrease in species C_i caused by chemical reactions of all species at time t

$$\left\{\frac{dC_i}{dt}\right\}_{TOTAL} = \left\{\frac{dC_i}{dt}\right\}_{dil} + \left\{\frac{dC_i}{dt}\right\}_{ent} + \left\{\frac{dC_i}{dt}\right\}_{emis} + \left\{\frac{dC_i}{dt}\right\}_{chem}$$

SOLUTION:

$C_i = C_i(@0) + \int_0^t \left\{\frac{dC_i}{dt}\right\}_{TOTAL}$ numerical integration used to solve initial value, differential equation problem

[a] adopted from Reference 9

respectively. Finally, the OZIPP trajectory model internally generates the information necessary for the chemical mechanism, with only the date of the simulation input in order to derive the appropriate photolytic rate constants.

1.1.2 The EKMA Technique

Following the procedure described in the previous section will lead to the prediction of one time/concentration profile of ozone, from which a single, peak, one-hour average ozone concentration can be calculated. More often than not, the predicted peak level will not agree precisely with the observed ozone concentration. Such disagreement may be due in part to uncertainties in the model inputs, and to the simplistic manner in which the trajectory model simulates ozone formation. (Recall that a number of simplifying assumptions were made in the formulation of the model, including the existence of a well defined column or air parcel, no horizontal dispersion, instantaneous mixing, etc.) The EKMA technique circumvents the potential problem of disagreement between a model prediction and the observed peak when the model is applied for regulatory purposes.

When the OZIPP computer program is used to generate an isopleth diagram, the same basic information described in the preceding section is required as input, except for the initial concentrations of NMOC and NO_x. To generate an isopleth diagram, OZIPP performs repeated simulations with differing assumed initial concentrations of NMOC and NO_x. Thus, a peak one-hour average ozone concentration is calculated for each set of initial concentrations, and the results are plotted as ozone isopleths (i.e., all combinations of NMOC and NO_x that yield a constant level of ozone are connected by a single curve, or isopleth). Note that a particular isopleth diagram inherently incorporates the other information input to the model, i.e., the mixing height growth, the photolytic reaction rates, the levels of pollutants aloft, and the emission pattern. (That is, these factors affect the positioning of the isopleths on the diagram.) The emissions themselves are actually input to the model as factors relative to initial concentrations. Thus, for example, if the initial concentrations are decreased by 50% from one simulation to the next, then the emissions will also be decreased by that same percentage. In effect, then, the isopleth diagram graphically depicts the model predictions of peak

ozone under varying conditions of precursor initial concentrations and precursor emissions, with all other variables held constant. As a consequence, the isopleth diagram can be used to estimate the model predicted effect of changing precursors from one level to another.

In order to use the isopleth diagram to estimate changes in ozone resulting from changes in precursors, a starting point must be established on the diagram to which all changes are related. In the trajectory model application, the absolute initial concentrations of NMOC and NO_x are estimated from available air quality data. If these two values are used to define a starting point, the corresponding ozone level will more than likely not equal the measured peak since the model will not always predict the peak ozone precisely. The EKMA procedure circumvents this problem by using the measured ozone peak and the measured NMOC/NO_x ratio to establish the starting point on the diagram. The starting point itself is the intersection between the NMOC/NO_x ratio line and the ozone isopleth corresponding to the observed ozone concentration. This procedure, in essence, calibrates the model to the observations in order to evaluate changes from existing conditions. Figure 1-3 illustrates the procedure graphically.

With the starting point defined, the isopleth diagram can be used to estimate the effects of changing precursors from existing levels, or to estimate to what degree precursor levels must be changed in order to achieve a prescribed reduction in peak ozone. The latter is illustrated by the example contained in Table 1-2. Note that the changes in precursors are expressed on a relative basis, i.e., as a percent change from existing levels. As previously stated, the precursor changes imply that both initial precursor concentrations and subsequent emissions must be changed by the same degree, with all other variables held constant. As such, the use of a single isopleth diagram provides estimates of the precursor reductions needed to reduce the observed ozone level to the desired goal for only those conditions that led to the observed ozone peak (e.g., dilution, pollutants aloft, sunlight, etc.). For the example problem shown in Table 1-2, the NMOC reduction of 72% is not necessarily the reduction needed to achieve the ozone NAAQS, since the latter is statistical in form and allows, on average, one daily maximum one-hour

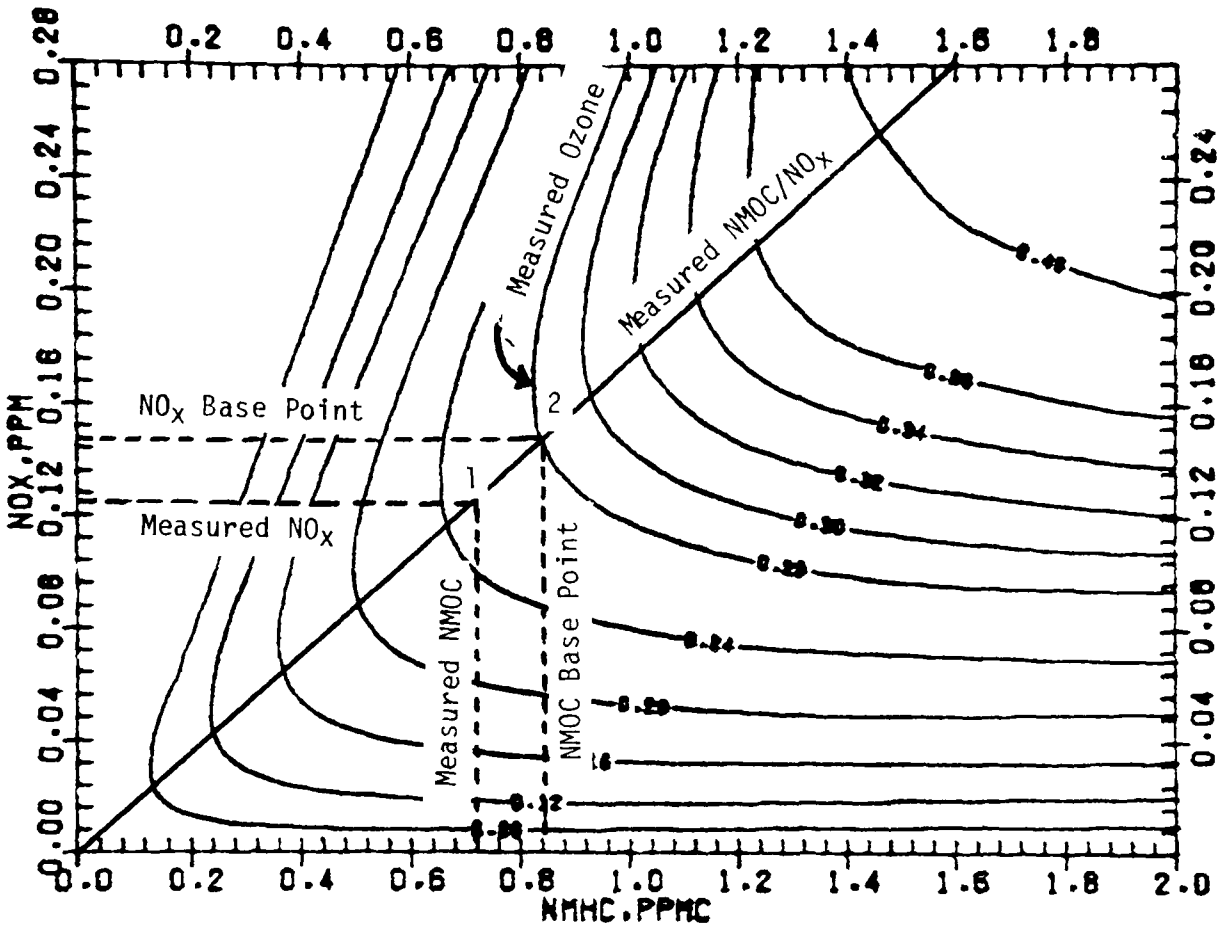

Point 1 corresponds to model prediction of peak ozone

Point 2 corresponds to model calibration to observed peak ozone

Figure 1-3. Illustration of EKMA Procedure.

Table 1-2. Example Emission Reduction Calculation Using a Single Ozone Isopleth Diagram.

GIVEN: O_3 Daily Design Value = .24
Design NMOC/NO_x = 8:1
Anticipated Change in NO_x = -20%
Base case diagram shown below

FIND: Percent reduction in VOC emissions needed to reduce ozone from .24 to 0.12 ppm

SOLUTION:

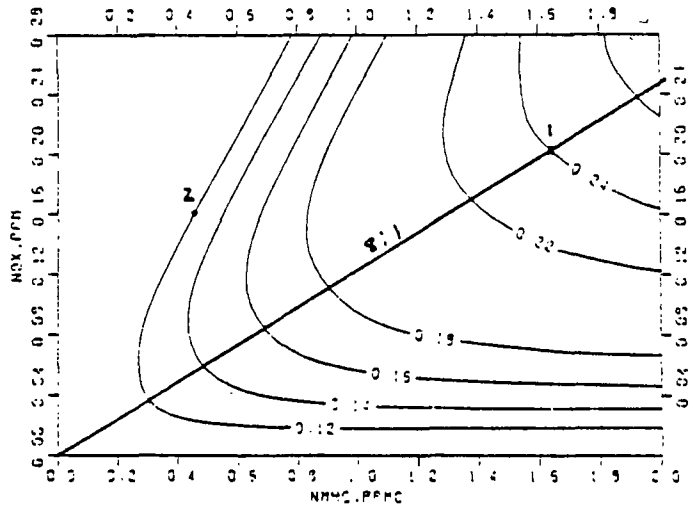

BASE CASE DIAGRAM, O3 ISOPL = .12

STEP 1: The base case point is found by the intersection of the 8:1 NMOC/NO_x ratio line with the .24 ozone isopleth (Point 1) on the diagram. At Point 1, $(NMOC)_1$ = 1.64 and $(NO_x)_1$ = .205

STEP 2: The post-control NO_x coordinate is calcualted as follows:

$$(NO_x)_2 = (.205) \times (1 - \frac{20}{100}) = .164$$

STEP 3: The post-control point is located at the intersection of the .164 NO_x coordinate and the 0.12 ppm ozone isopleth (Point 2). At Point 2, $(NMOC)_2$ = 0.46

STEP 4: The VOC emission reduction is calculated as

$$\% \text{ reduction} = (1 - \frac{.46}{1.64}) \times 100 = 72\%$$

average ozone concentration above 0.12 ppm each year.* In the comparisons of the EKMA procedure with the PAQSM predictions, it must be emphasized that no attempt has been made to establish the prescribed reduction in precursors needed to achieve the ozone NAAQS with either model. Rather, attention is focused on the precursor reductions needed to lower peak ozone on each of three days to a level of 0.12 ppm. This is a subtle, but important point, and will be addressed more completely in Section 4.

1.2 RAPS Data Base

As previously described, an extensive air quality management data base was compiled as part of the Regional Air Pollution Study (RAPS). The data base contains all of the elements needed to evaluate air quality simulation models: air quality, emissions, and meteorological data sufficiently resolved in space and time to develop input data and provide measures for evaluating model performance. The data base as it relates to this study is briefly described below.

The bulk of the air quality data used in the study was collected at 25 Regional Air Monitoring Stations (RAMS) spaced concentrically throughout the study region (see Figure 1-4). These stations were located such that they would not be unduly influenced by any one source or group of sources. At each station, hourly average concentrations of the following pollutants are available: ozone, nitrogen dioxide (NO_2), nitric oxide (NO), total oxides of nitrogen (NO_x), nonmethane organic compounds (NMOC), and carbon monoxide (CO). The size of the network, the quality of the data and the duration of measurements provided the best available temporal and spatial resolution of ambient

---

* Reference 2 describes the procedure for establishing the precursor reductions needed to achieve the ozone NAAQS. In essence, a number of high ozone days are modeled, and the precursor reduction needed to achieve the ozone NAAQS is selected such that it is consistent with the acceptable number of ozone peaks above 0.12 ppm, and other possible changes in existing conditions which may take place (e.g., changes in the levels of pollutants aloft).

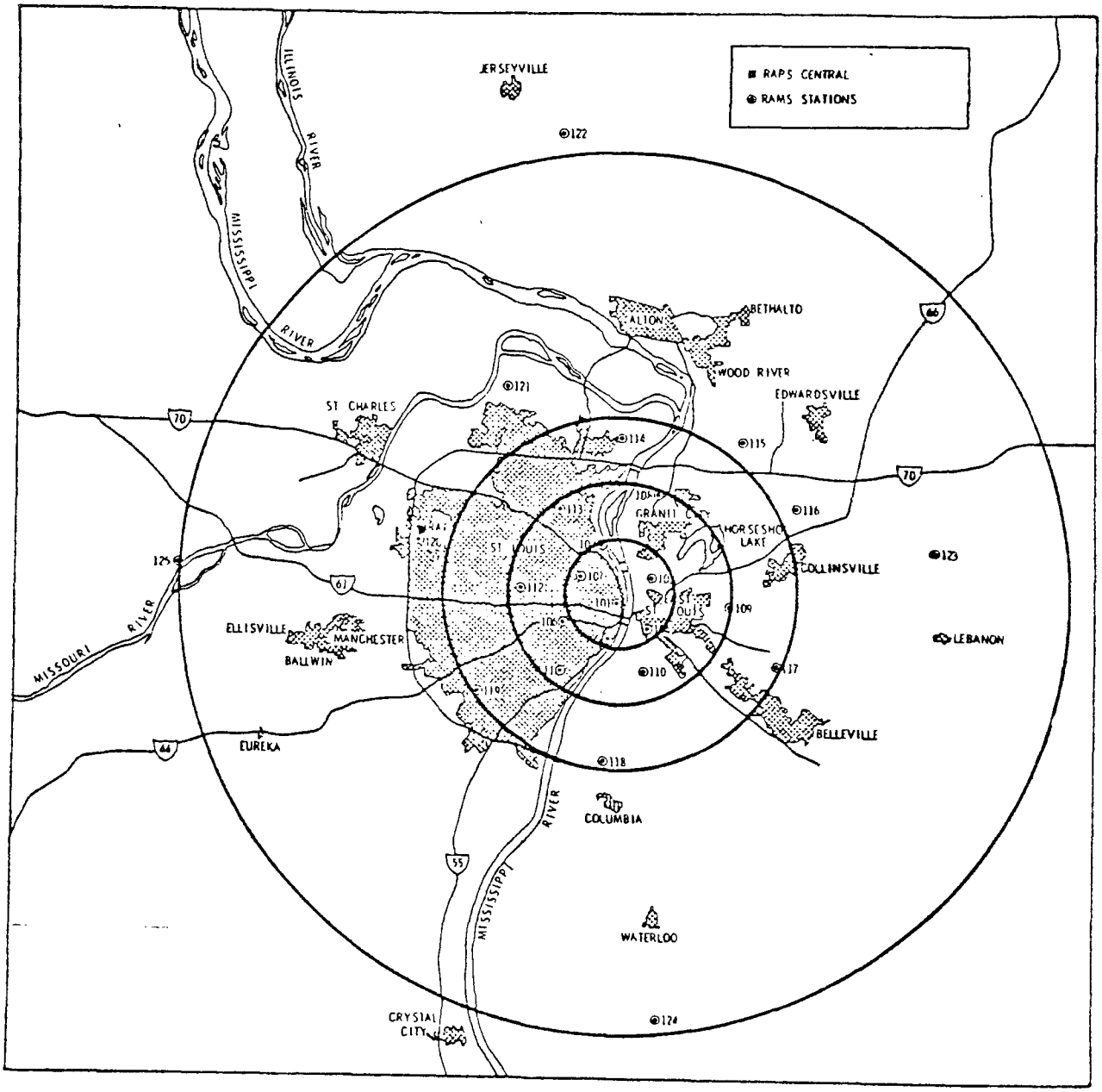

Figure 1-4. RAMS Station Locations.

pollutant levels necessary to evaluate a model such as the trajectory model underlying EKMA.

The emissions data employed in this study include an hourly resolved point and area source emissions inventory for NO_x, CO and Volatile Organic Compounds (VOC). The area source emissions were spatially resolved by means of the RAPS grid system which consists of about 2000 variable-sized grids.[13] Thus, estimates of emission rates from both area and point sources are available by hour and by grid for any day in 1975 and 1976, the principal period for ambient measurements.

The primary source of meteorological data consisted of continuous measurements of wind speed, wind direction and temperature made at each of the 25 RAMS. Additional data were collected from the RAPS Upper Air Sounding Network (UASN). In this program, radiosondes were conducted three times per day, five times per week, at a minimum of two stations. These soundings furnished vertical temperature profiles from which mixing heights could be estimated. The latter were supplemented by data collected in the early morning hours from the operation of sodar instruments.

The data base compiled under the RAPS program has been used by EPA in an in-depth study to evaluate the performance of a number of PAQSMs.[14] One phase of that study consists of applying a complex photochemical dispersion model developed by Systems Applications, Incorporated - the Urban Airshed Model.[16] A number of days have been simulated to evaluate the Airshed Model's performance in characterizing ozone formation under conditions encountered during the data collection period. In addition, a series of detailed sensitivity tests have been conducted for three of these days in order to:

(1) identify those model inputs which most significantly affect model predictions, and subsequently require most care in data collection efforts;

(2) isolate possible sources of error in model inputs or formulation;

(3) estimate the effects of changes in precursor emission levels on predicted ambient ozone levels.

The results of this last set of sensitivity tests provide the basis for evaluating the EKMA predictions of changes in ozone accompanying changes in precursors, and are discussed in Section 4.

2.0 LEVEL II ANALYSIS

As previously described, the trajectory model underlying EKMA has been used with a comprehensive air quality management data base to make predictions of peak ozone for comparison with observed levels. Several criteria were employed to select ten trajectories on nine different days during 1976. Because EKMA will necessarily be used for those days with the highest ozone levels, primary interest focused on predicting the highest ozone levels measured in the region. Further, enough days were selected to insure that the model's performance was evaluated for a variety of atmospheric conditions. A few days with lower ozone concentrations were also included to test for a possible systematic bias in the model's predictions. These considerations led to the selection of the ten test cases summarized in Table 2-1.

In the discussion that follows, the procedures for estimating the model inputs are first described, followed by a comparison of the model predictions of peak ozone with those observed. In addition, a detailed assessment of each simulation is also made. Finally, Section 2.3 describes the results of a series of tests designed to assess the sensitivity of the model predictions to uncertainty in some of the model inputs.

2.1 Methodology for Developing Input Data

The first step in performing a simulation involved deriving an air parcel trajectory corresponding to the time and location of the observed peak ozone concentration. This trajectory represents the path an air parcel would have traveled to reach the site of interest at the specified time (thereby representing the movement of the theoretical column described in Section 1.1.1). Once the column movement had been defined, the remaining information necessary to simulate a test case could then be developed: the initial concentrations, emissions, boundary conditions (e.g., ozone aloft), and dilution data. Methodologies used to develop each of these are described below.

2.1.1 Air Parcel Trajectory

Air parcel trajectories were calculated for each of the test cases from the minute-by-minute measurements of wind speed and wind direction taken

Table 2-1. Model Test Cases

Date	Julian Day	RAMS Site	Time of Peak O_3, Local Daylight Time	Peak O_3, Concentration, ppm
10/1/76	275	102	1500-1600	.24
7/13/76	195	114	1600-1700	.22
6/8/76	160	115	1700-1800	.22
6/7/76	159	122	1600-1700	.20
6/8/76	160	103	1400-1500	.19
8/25/76	238	115	1400-1500	.19
10/2/76	276	115	1700-1800	.19
9/17/76	261	118	1300-1400	.15
7/19/76	201	122	1300-1400	.15
8/8/76	221	125	1800-1900	.12

at each of the 25 RAMS. First, ten minute vector averages of wind speed and direction were calculated for each of the 25 sites. The individual site averages were then averaged to obtain an overall regional average wind speed and direction for each ten minute period. The regional average wind speed and direction were used to track a trajectory backwards from the site and time of the observed peak ozone concentration until 0800 Central Daylight Time (CDT). Figure 2-1 illustrates the back trajectory for the July 19th test case, with the hourly segments of the trajectory shown along the path.

2.1.2 Initial Concentrations

The initial concentrations of nonmethane organic compounds (NMOC), total oxides of nitrogen (NO_x), and ozone represent the pollutant levels initially within the theoretical model column at 0800 CDT. They were estimated from the hourly-averaged concentrations at the three RAMS stations nearest the trajectory starting point. The first step in the procedure was to select the three RAMS sites closest to the trajectory starting point. At these three sites, instantaneous concentrations corresponding to the simulation starting time were computed by averaging the hourly pollutant levels for the hour immediately preceding the starting time and the hour following the starting time. For example, the 0800 CDT instantaneous concentration for a pollutant at one site would be calculated by averaging the 0700-0800 and the 0800-0900 hourly levels. The initial column concentrations were then computed as a weighted average of the three instantaneous levels, with the weighting factors equal to the square of the reciprocal of the distance between each RAMS site and the trajectory starting point (i.e., $1/r^2$). In performing these calculations, any concentrations below the minimum detectable limit of an analyzer were set equal to the following lower limits: .005 ppm for NO_x; 0.1 ppmC for NMOC; and .005 ppm for ozone.

2.1.3 Emissions

The trajectory model also simulates the impact of precursor emissions occurring after the simulation starting time. The RAPS emissions inventory was used to estimate hourly emission rates for nonmethane organic compounds (NMOC) and for NO_x. However, the emissions encountered by the column during

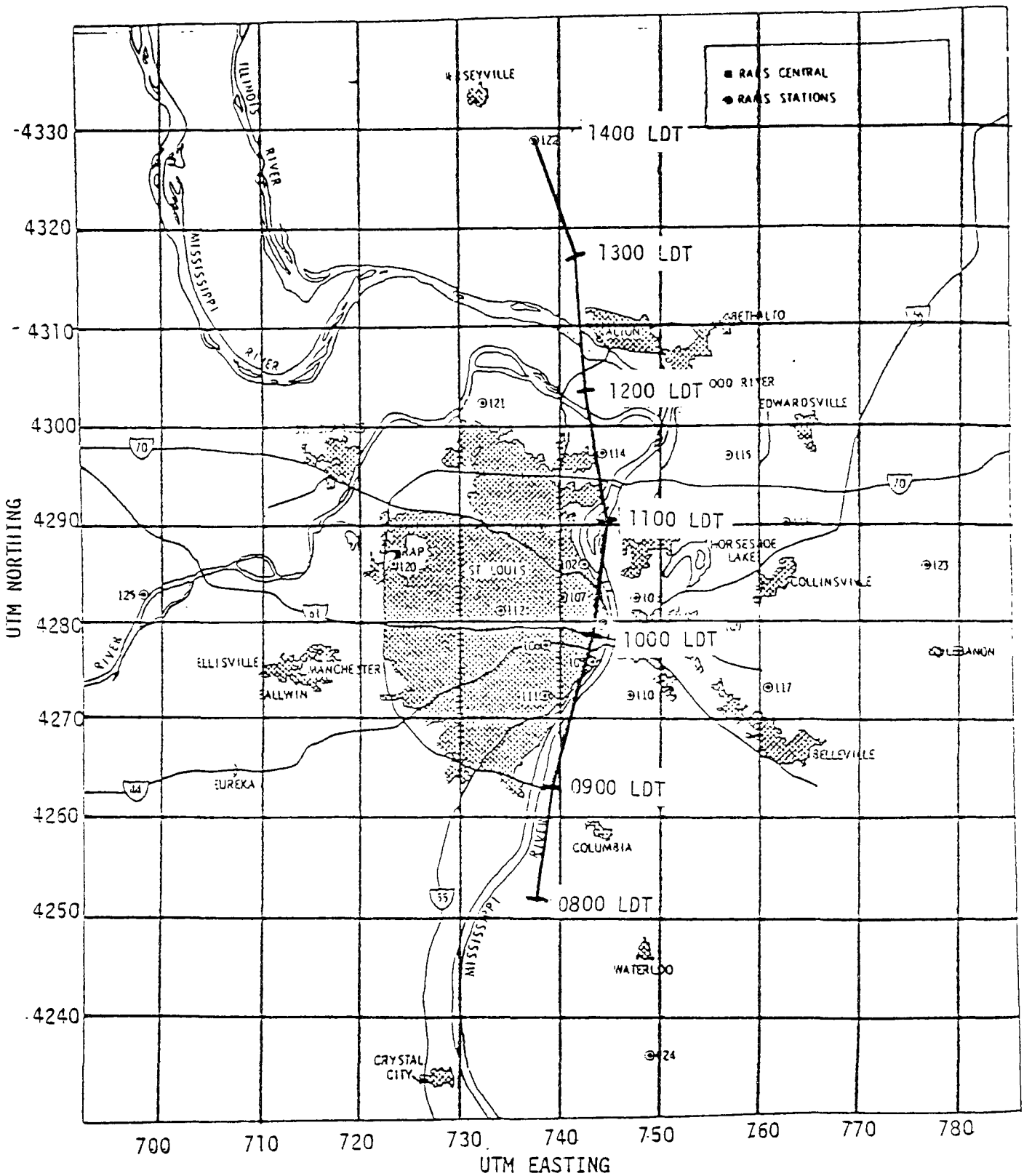

Figure 2-1. Air Parcel Trajectory for July 19 Test Case.

each hour are actually input to the model as fractions of initial concentration of NMOC or NO_x. As described below, the fractions themselves were computed by comparing the emission densities encountered by the column of air during each hour to the pollutant density initially in the column.

From the RAPS emission inventory, an average emission density for each hour of the column trajectory path could be computed. This was done by (1) establishing the 10 km x 10 km grid network shown in Figure 2-2; (2) summing the hourly point and area source emissions occurring within each grid square encountered by a trajectory segment; (3) dividing the total emissions in each grid square by the area of that grid square (i.e., 100 km^2); and (4) weighting the resulting emission densities consistently with the proportion of the trajectory segment in each grid square. For example, consider the trajectory path shown in Figure 2-2. An emission density for the first hour would be calculated from the total emissions occurring between 0800 and 0900 LDT within grid squares (1) and (2). Since roughly 2/3 of the trajectory segment between 0800 and 0900 occurs in grid square (2), the emission density in (2) is weighted by a factor of "0.67," whereas the emission density in grid square (1) is weighted by a factor of "0.33."

The actual fractions input to the OZIPP model were calculated for both organic compounds and NO_x using the following expression:

$$e_i = \frac{Qi}{Ho\ Co\ \rho} \qquad (2\text{-}1)$$

where

e_i = fraction of initial concentration to be added during hour i to represent emissions occurring during hour i

Qi = emission density* for hour i, moles/m^2

---

* Emissions derived from the RAPS inventory were expressed on a mass basis (e.g., kilograms). To convert to a molar (or ppm) basis, the following conversion factors were used: 46 gm/mole for NO_x and 14.5 for NMOC. For NO_x, the inventory gives NO_x as equivalent NO_2, and for NMOC, one ppmC is assumed equivalent to $CH_{2.5}$.

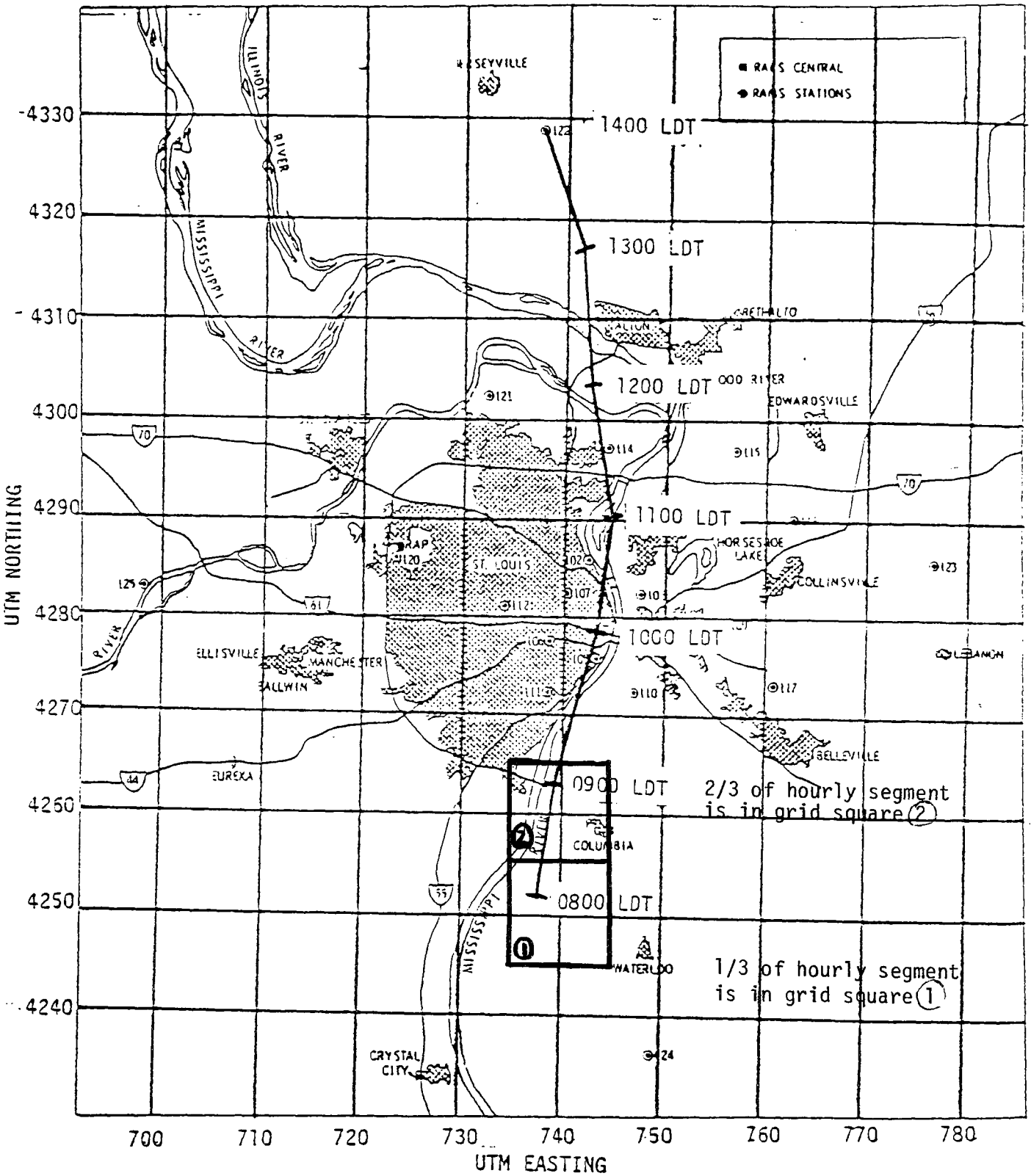

Figure 2-2. Air Parcel Trajectory for July 19 Test Case Demonstrating How Fresh Precursor Emissions are Considered.

Ho = initial morning mixing height (described in Section 2.1.5), m

Co = initial pollutant concentration, ppm or ppmC

ρ = density of air, 41 moles/m^3

Equation 2-1 represents the ratio of the emission density at a particular hou to a hypothetical column density based on the initial column conditions.

This procedure has the effect of assuming that the absolute mass of emissions occurring during any one hour is instantaneously dispersed throughout the theoretical model column. Note that, in equation 2-1, the area of the column does not appear. However, this term is implicitly accounted for by the emission density term, Qi. Hence, it is possible to vary the impact of fresh emissions simply by changing the size of the grid squares used in the modeling exercise. As subsequently described, model sensitivity tests to grid square size were performed.

2.1.4 Boundary Conditions

Boundary conditions for the trajectory model include pollutant concentrations found in the layer above the early-morning mixed layer. A procedure used to estimate the level of ozone aloft has been described in Reference 1 and was used in this study. Hourly ozone concentrations measured between 1100 and 1300 CDT at upwind, rural-type monitors were averaged to obtain an estimate of the levels aloft. Precursor pollutants aloft were assumed to be negligible.

2.1.5 Dilution

Dilution in the trajectory model results from the change in mixing height which occurs during the day. In the OZIPP model, the mixing height is assumed to rise as a function of the time after sunrise in accordance with a "characteristic curve" derived empirically from data taken during the RAPS study.[15] Because of the existence of detailed radiosonde and sodar data, the OZIPP program was modified such that a day specific mixing height profile could be used in place of the characteristic curve. (Use of the characteristic curve is considered in the sensitivity analysis portion of the discussion.)

Radiosonde measurements were taken at the four Upper Air Network (UAN) stations shown in Figure 2-3. For every day except October 2, soundings were taken at stations 41 and 42 at about 0500, 1100 and 1700 CDT. On some of the days, additional soundings were taken at the other locations. The vertical temperature profiles corresponding to each radiosonde were used to estimate the height to which pollutants emitted near the ground would be likely to mix radpidly (i.e., the mixed layer).* The mixing heights derived from radiosondes taken at different sites but at approximately the same time were averaged to obtain a regional average mixing height in early morning, mid-morning and afternoon. These estimates were supplemented by measurements taken by SODAR to better establish the mixing height as a function of time during the early morning. In this fashion, mixing heights were estimated at hourly intervals throughout the morning hours, and the profile for each day derived by fitting a monotonically increasing smooth curve through the data points.

2.1.6 Chemical Mechanism

The chemical kinetics mechanism currently incorporated in OZIPP was used in all ten tests. The NO_2/NO_x fraction corresponding to observed initial concentrations of NO_2 and NO were used in all cases. The hydrocarbon reactivity factors recommended in References 1 and 2 were also used.

2.2 Peak Ozone Predictions

The model inputs developed in accordance with the previously described procedures are summarized for each test case in Appendix A. The peak ozone concentrations predicted with these inputs are graphically compared with the observed ozone concentrations in Figure 2-4. The solid 45 degree line emanating from the origin represents perfect agreement between observed peak hourly ozone concentrations (abscissa) and predicted peaks (ordinate). The

---

* In some cases, subjective interpretations of the radiosonde data were invoked to arrive at the best estimate of the mixing height. For October 2, only radiosondes conducted at the Salem, Illinois National Weather Service Radiosonde Station were used since RAPS radiosonde data were not available.

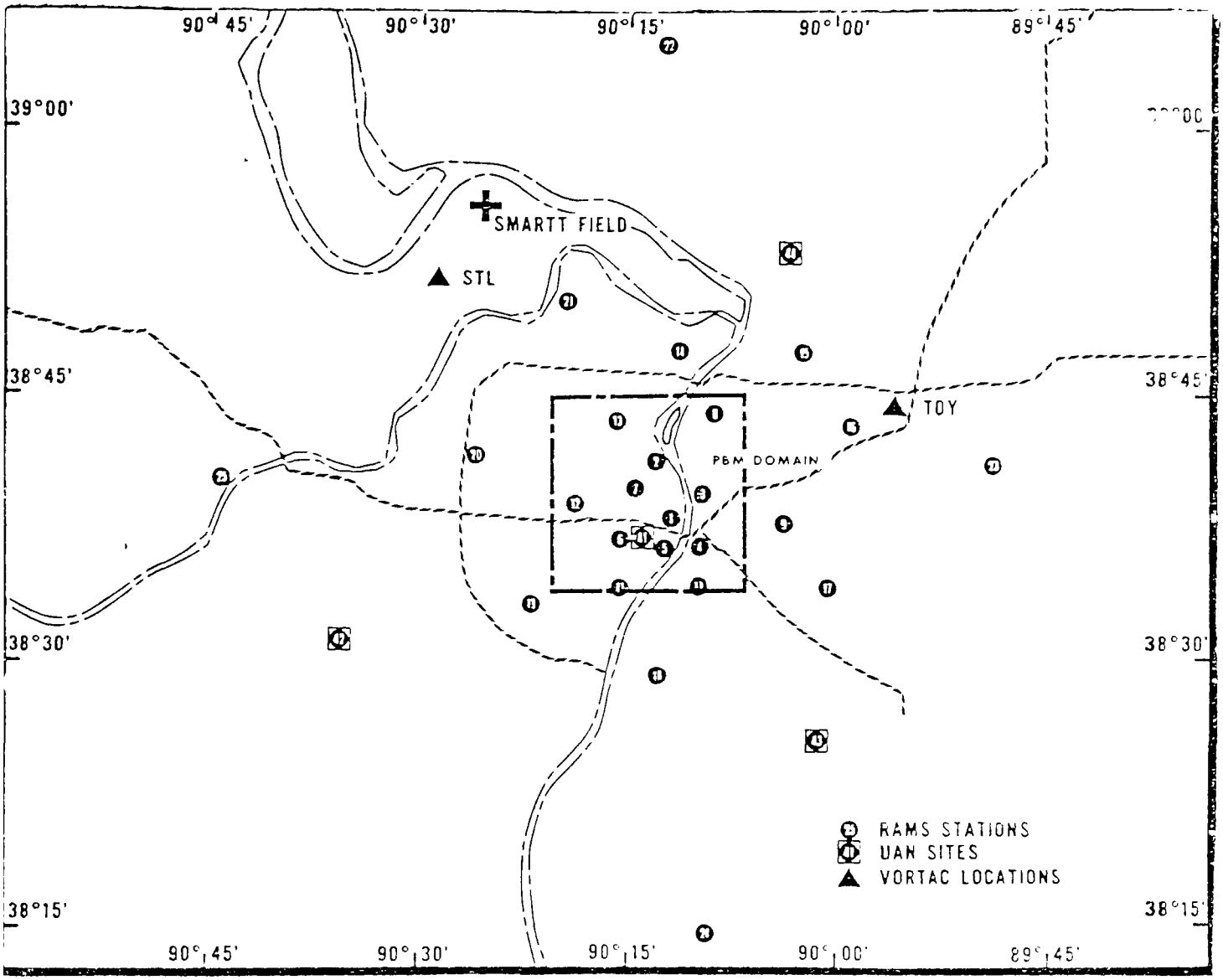

Figure 2-3. Location of Upper Air Network Stations

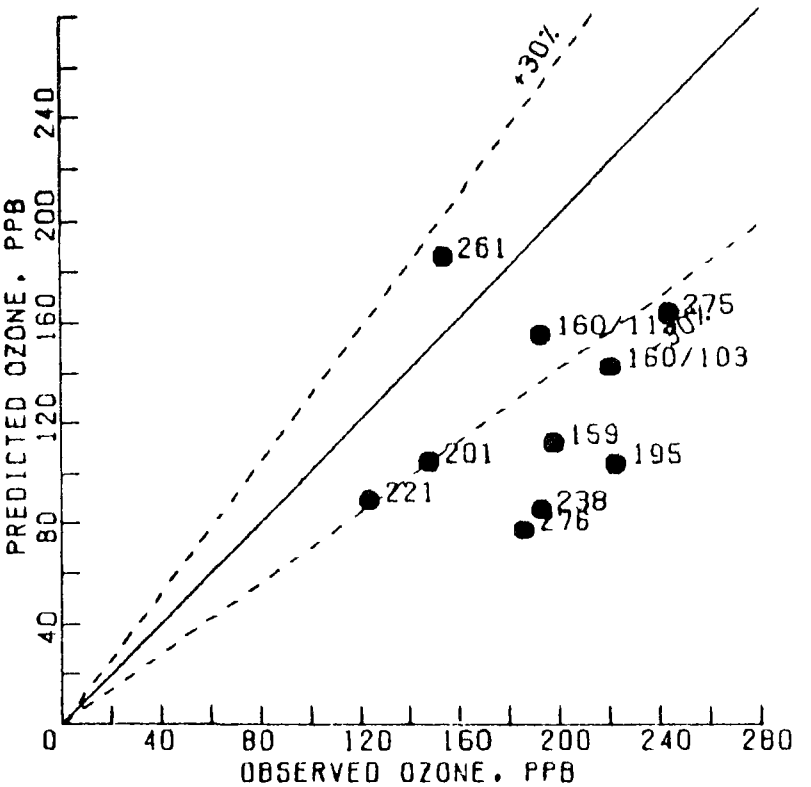

Figure 2-4. Level II Predictions Versus Observations of Peak Ozone.

dashed lines on either side of this line represent agreement to within ±30%, and the numbers on the graph indicate the Julian day corresponding to each of the ten test cases. Of the ten simulations performed, only four are within ±30% of the observed peak. In practically every case, the observed peak ozone concentration is underpredicted, sometimes by a substantial amount.

To examine potential causes for the tendency towards underprediction, a detailed examination of each simulation was undertaken. The goal of the analysis is to compare the temporal patterns of ozone, key precursors and related variables (such as the NMOC/NO_x) predicted by the model with measured levels. In addition, the relatively inert pollutant carbon monoxide (CO) was also modeled to provide supplemental information on the emissions/mixing height relationships used in the analysis. The latter was possible only because the RAMS monitors were sited such that they would not be unduly influenced by any one source or group of sources. In most instances, such an analysis would be inappropriate because CO monitors are normally located to detect peak levels originating from a localized group of sources.

Because the model computes species concentrations in a moving reference frame (i.e., in a moving column of air), and ambient measurements are recorded in a fixed reference frame (i.e., at fixed monitoring sites), some means of transformation is necessary for comparison. The procedure used is similar to that for estimating initial concentrations. Pollutant levels are interpolated on the hour along each trajectory from ambient measurements taken at the fixed RAMS monitoring sites. First, trajectory nodes are established by locating the trajectory position at the start of each hour. Next, the three RAMS sites nearest each node are selected. For each chosen site, the concentrations at the start of an hour are obtained by averaging the hourly average level for the preceding hour with the hourly-average for the following hour (e.g., the 1100-1200 CDT average ozone level would be averaged with the 1200-1300 CDT average ozone level to obtain an estimate of the ozone concentration occurring precisely at 1200 CDT). Finally, the concentrations at the start of an hour are combined into a weighted average using the square of the reciprical distance between the node and the site. In a sense, the concentrations computed at each node represent instantaneous levels, and are directly comparable to the

model predicted instantaneous levels. It should be noted, however, that some situations may arise in which the interpolated values might not be representative of the column concentrations. For example, some situations may occur in which the interpolated value may be based on measurements taken 20-40 kilometers from a trajectory node. In general, these occurrences are rare, and the use of interpolated measurements provides one means of comparing concentration calculated in a Lagrangian reference frame with those measured in a fixed frame.

The model predicted temporal patterns of ozone, NO_x, NMOC, NO, NO_2, $NMOC/NO_x$, NO_2/NO_x, and CO versus the interpolated values for each simulation are contained in Appendix B. The interpolated averages are represented as the circle, and the range of values used in calculating a particular interpolated value is indicated by the vertical bars. The solid line is the model prediction of a particular variable as a function of time. At a minimum, one might expect the model prediction to fall within the range of values used in the interpolation scheme. Each of the simulations are qualitatively described below.

10/1/76 (Day 275). This day was one of general stagnation, with the trajectory meandering within the urban area. The temporal pattern of CO predicted by the model agreed fairly well with the interpolated pattern, although the absolute levels were underpredicted in the morning. The results for NMOC were similar, in that mid-morning levels were underpredicted. NO_x, NO, and NO_2 predictions agreed reasonably well with interpolated values. Predictions of ozone corresponded extremely well with interpolated levels up to about 1400 CDT, after which ozone was underpredicted.

7/13/76 (Day 195). The trajectory for this day led from the rural area southeast of the city, passed through the urban area about mid-day, and ended slightly north of the city at 1600 CDT. Precursor concentrations, both predicted and interpolated, were at or near minimum levels throughout the morning. The interpolated levels of CO, NMOC and NO_x all increased in the afternoon (corresponding to passage of the trajectory through the urban area), although the absolute levels of each were still relatively low. Model predictions of these three pollutants were all lower than interpolated levels throughout the afternoon period. Ozone predictions agreed with observations until early afternoon, after which the model underpredicted the interpolated ozone levels.

6/8/76 (Day 160, Site 115). The peak ozone on this day was measured at 1600-1700 CDT slightly northeast of the city. The trajectory begins northwest of the city, passes through the city in later morning, and veers north-

east to the site of maximum ozone. The interpolated NMOC, NO_x and CO patterns are at the highest levels in early morning, decrease rapidly in mid-morning, and level off to low levels during the afternoon. The same pattern is predicted by the model, but the interpolated concentrations of NMOC and CO from early- to mid-morning are slightly underpredicted. Interpolated and model predicted concentrations of NO_x, NO and NO_2 agree fairly well. The ozone predictions are slightly higher than the interpolated levels up to about noon, after which the model predictions are somewhat lower than the interpolated levels.

6/7/76 (Day 159). The trajectory on this day begins to the northwest of St. Louis, moves slightly southward until mid-morning, and then veers northward passing close to Alton, eventually leading to the site of peak ozone about 40-50 km north of the central St. Louis urban core. Interpolated concentrations of CO, NMOC and NO_x are all on the low side, with the highest levels occurring in the early morning. Model predictions of NMOC and NO_x are somewhat lower than interpolated levels. However, the model predictions of CO track the interpolated levels fairly well, although concentrations tend to be slightly underpredicted in mid-afternoon. Ozone predictions agree with interpolations very well up to about noon, but are significantly lower in the afternoon period.

6/8/76 (Day 160, Site 103). The trajectory for this simulation is similar to that for the 6/8, Site 115 simulation discussed above. The model predictions of CO agree very well with interpolated levels, as do the NMOC and NO_x patterns. In the early morning, the predicted values of NO_x, NO and NO_2 are somewhat higher than the interpolated levels. Ozone predictions are similar to the other days in that interpolated and model predicted levels agree reasonably well, but the predictions fall off more rapidly in the afternoon than the interpolated levels.

8/25/76 (Day 238). The measured peak ozone concentration on this day occurred to the northwest of the city in early afternoon. The trajectory started southeast of the city, and tracked from the southeast to the northwest, passing quite well to the east of the urban area. The model predicted CO levels were lower than the interpolated levels, even though the latter were relatively low. The same pattern was found with NMOC, but NO_x predictions agreed fairly well with interpolated levels. As might be expected, ozone was significantly underpredicted, with the model prediction leveling out in the afternoon.

10/2/76 (Day 276). October 2 was the day following the October 1 stagnation period. Because this was a Saturday, some of the meteorological information normally collected were unavailable, and of course, and it is likely that more uncertainty exists in the emissions estimates for this day than for a weekday. Interpolated concentrations of CO, NMOC and NO_x remained relatively high in the early morning hours and then decreased substantially in late morning. The model predictions of these pollutants followed the same general pattern, but the early morning peak NMOC was underpredicted. Ozone was again substantially underpredicted.

9/17/76 (Day 261). The trajectory on this day started in the general urban area and tracked to the south. The peak occurred about 20 km south of the city in early afternoon. The model predictions of CO, NMOC and NO_x all agreed reasonably well with the interpolated levels, although CO and NMOC were slightly overpredicted in late morning. Ozone predictions were always greater than the interpolated levels, resulting in an overprediction of the one-hour-average peak.

7/19/76 (Day 201). July 19 was marked by persistent and moderate winds out of the south. The trajectory started well south of the city and passed through the urban area in early morning. The measured peak occurred about 50 km to the north in early afternoon. Although model predicted CO concentrations agreed well with interpolated levels, both were quite low, being just slightly above the minimum detectable limit of the analyzers. Late morning to early afternoon concentrations of NMOC predicted by the model are somewhat lower than the interpolated levels, although again both are relatively low being below 0.5 ppmC. Except for a one-hour spike in the interpolated NO_x levels, model predictions and interpolated NO_x concentrations exhibited good agreement. The afternoon ozone concentrations predicted by the model were somewhat less than the interpolated levels.

8/8/76 (Day 221). The trajectory for this day tracked from east to west, passing through the city in mid-morning. The peak ozone, which the lowest of the ten test cases, was measured about 40 km due west of the urban area. Both model predicted and interpolated concentrations of NMOC, CO and NO_x were all near the minimum detectable limits of the analyzers. Ozone levels predicted by the model were somewhat lower than the interpolated levels.

The findings discussed above suggest that one possible reason for the underprediction of peak ozone is that its precursors are also underpredicted, especially NMOC. Often, the inert pollutant CO was underpredicted as well. The one case (Day 261) in which both precursor and CO predictions agreed fairly well with interpolated values, ozone was slightly overpredicted. Possible reasons for the underpredicted precursor levels could be erroneous mixing height profiles, or trajectory paths, since these factors directly affect model predicted concentrations of precursors. This is further addressed in the sensitivity analysis of the following section.

2.3 Sensitivity Tests

In this section, attention is focused on sensitivity tests conducted to examine the relative importance of some of the model input variables. It should be noted, however, that because of the number of test cases and the number of model input variables, a full, factorial design experiment was

beyond the scope of this analysis. Rather, individual tests were chosen to illustrate particular facets of model behavior.

The establishment of the sensitivity of model predictions to individual model inputs is complicated by the interactions among variables. For example, consider the model sensitivity to ozone aloft. If the mixing height does not change during the day, then the levels of ozone aloft will not affect model predictions at all. On the other hand, if the mixing height grows substantially, model predictions will be significantly affected.* Thus, it is not possible to generalize about the sensitivity of the model prediction to the level of ozone aloft. Other such model interactions also occur, and some of those are illustrated in the discussion that follows on the sensitivity of the predictions to key model inputs.

Trajectory. Probably the most important part of the Level II analysis is the derivation of the air parcel trajectory. The approach previously described was based on regional average wind vectors for ten minute periods. Another possible approach would be to derive the trajectories using a $1/r^2$ weighting factor for the stations within a preset scanning radius. Such a technique was employed to generate alternative trajectories for each of the ten test cases, and they are shown in Appendix C (along with the ones previously described). In some cases, the two techniques agree fairly well. In others, the disagreement is more pronounced. For the latter situation, it is not possible to say which is correct.

To illustrate the potential effects of the differing trajectories on the modeling results, consider the two test cases shown in Figure 2-5. For the July 19 case, the two methods yield virtually identical trajectories, and the model predictions of peak ozone are essentially the same (approximately .11 ppm for both simulations). Conversely, the difference in trajectories for October 1 leads to significant differences in model predictions. With the

---

* Note that in the extreme, the model predictions of peak ozone approach the levels of ozone aloft as the growth in mixing height becomes very large.

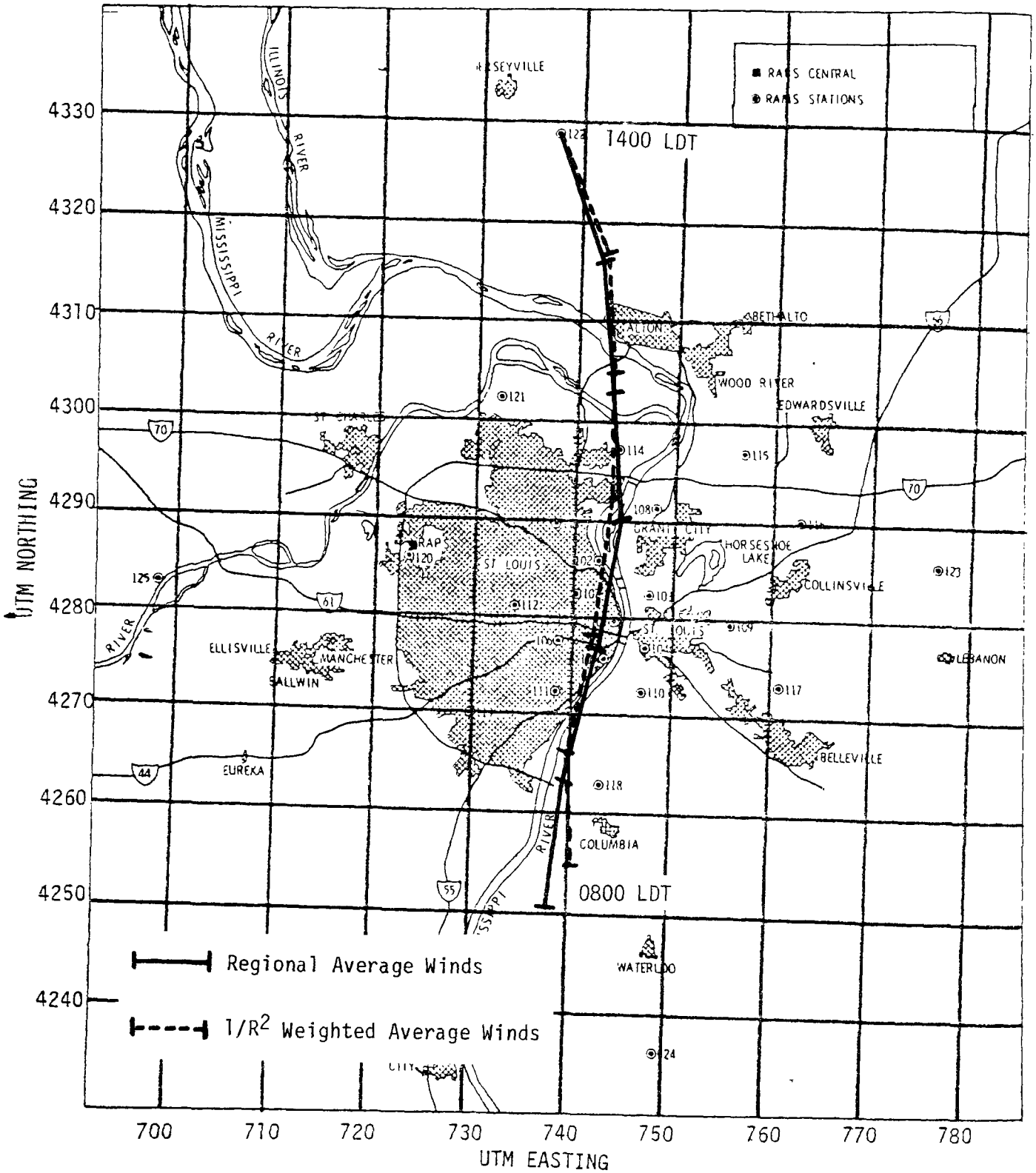

Figure 2-5A. Comparison of Trajectories Calculated by Alternative Methods: July 19 (Day 201)

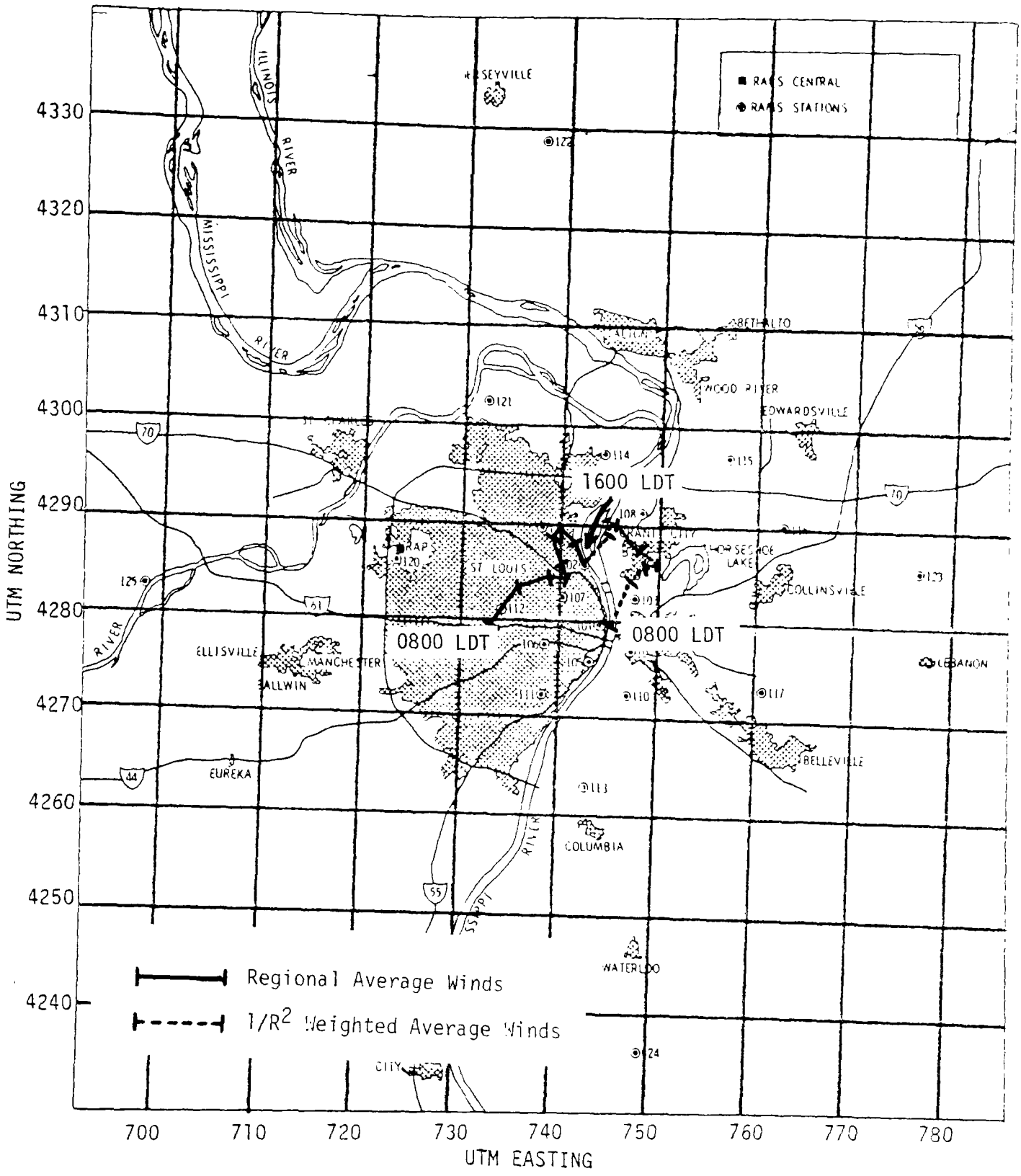

Figure 2-5B. Comparison of Trajectories Calculated by Alternative Methods: October 1 (Day 275)

trajectory based on regional average winds, the predicted peak ozone was 0.165 ppm, which was significantly lower than the observed .244 ppm. When the trajectory based on the $1/r^2$ weighting of the nearest stations is modeled, the model prediction of peak ozone is substantially improved. The $1/r^2$ trajectory leads to higher initial concentrations, which in turn result in a higher predicted ozone peak of .211 ppm. Thus, in one case, the differences in trajectories are unimportant, but in another case they substantially affect model performance.

The two techniques for estimating trajectories that have been considered so far were based on surface level winds (i.e., measurements were taken at a height of 10 meters). Information on the speed and direction of winds aloft (within the mixed layer) are limited, but suggest that in some cases substantial wind shear may exist, i.e, within the mixed layer, differing wind directions are found aloft. Figure 2-6 illustrates the vertical profile of wind direction measured by a midmorning radiosonde taken on June 7 (Day 159) By combining the measurements of winds aloft with the surface measurements, a trajectory such as the one shown in Figure 2-7 could be hypothesized as a more representative wind flow (the original trajectory is shown for reference). It must be emphasized, however, that the measurements of winds aloft are of short duration, taken at discrete points in time, with multi-hour intervals without any measurement. The representativeness of the discrete measurements for intermediate times is open to question. But, if the trajectory based on combined surface/aloft winds is more representative of the wind flow on that day, and were modeled as such, then the model's prediction of peak ozone would increase because of the higher initial precursor concentrations near the new starting point. Thus, model performance on this day would be improved.

The major point to be emphasized here is that using different techniques to derive trajectories can lead to different estimates of air parcel paths. In some cases, the differences in trajectories can lead to substantially different modeling results. Determining which is the "correct" trajectory is difficult because of no standard with which to compare the different results, i.e., the trajectory most representative of the actual parcel path is unknown.

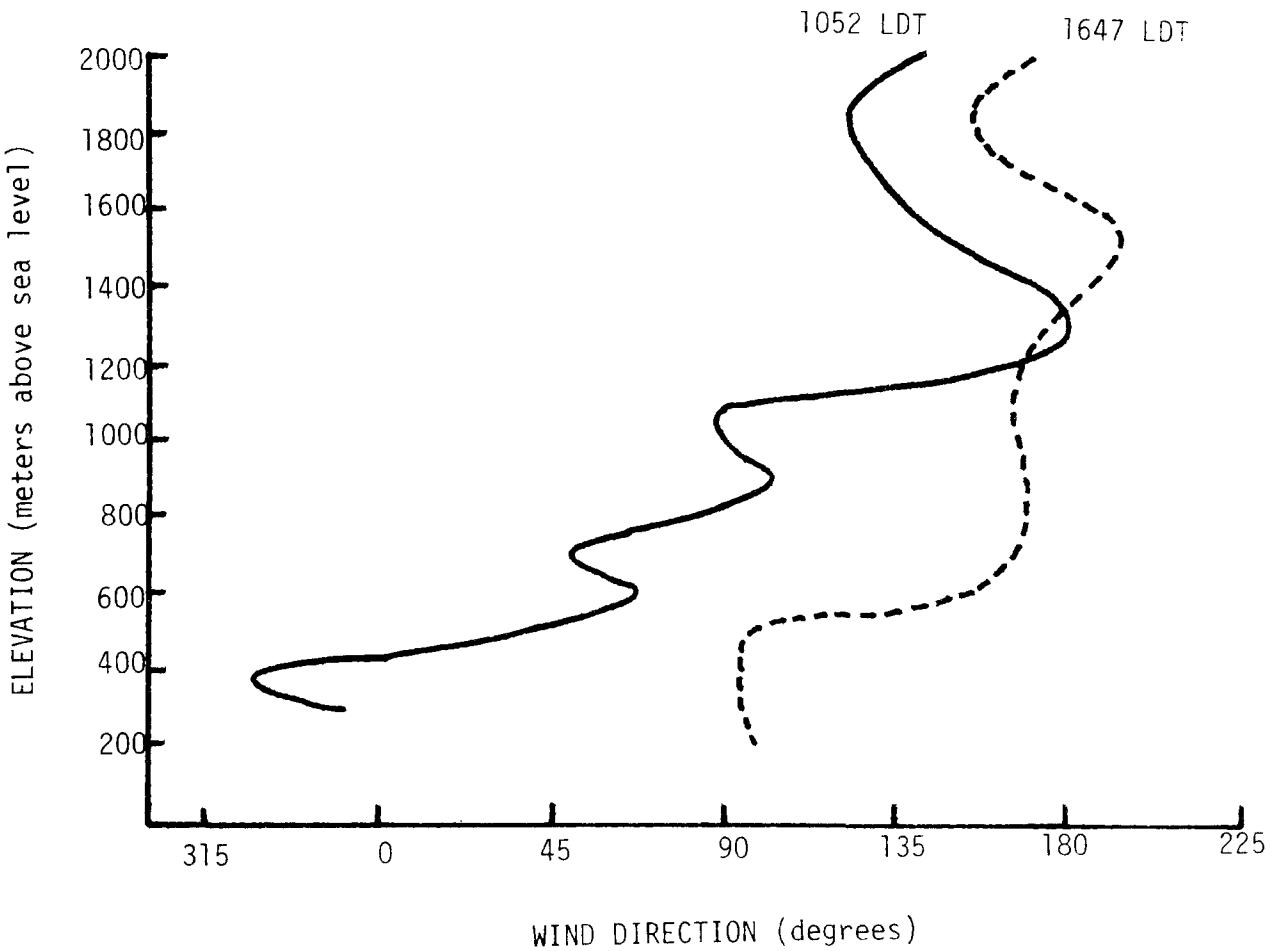

Figure 2-6. Radiosonde Measurements of Wind Direction Aloft for June 7 (Day 159).

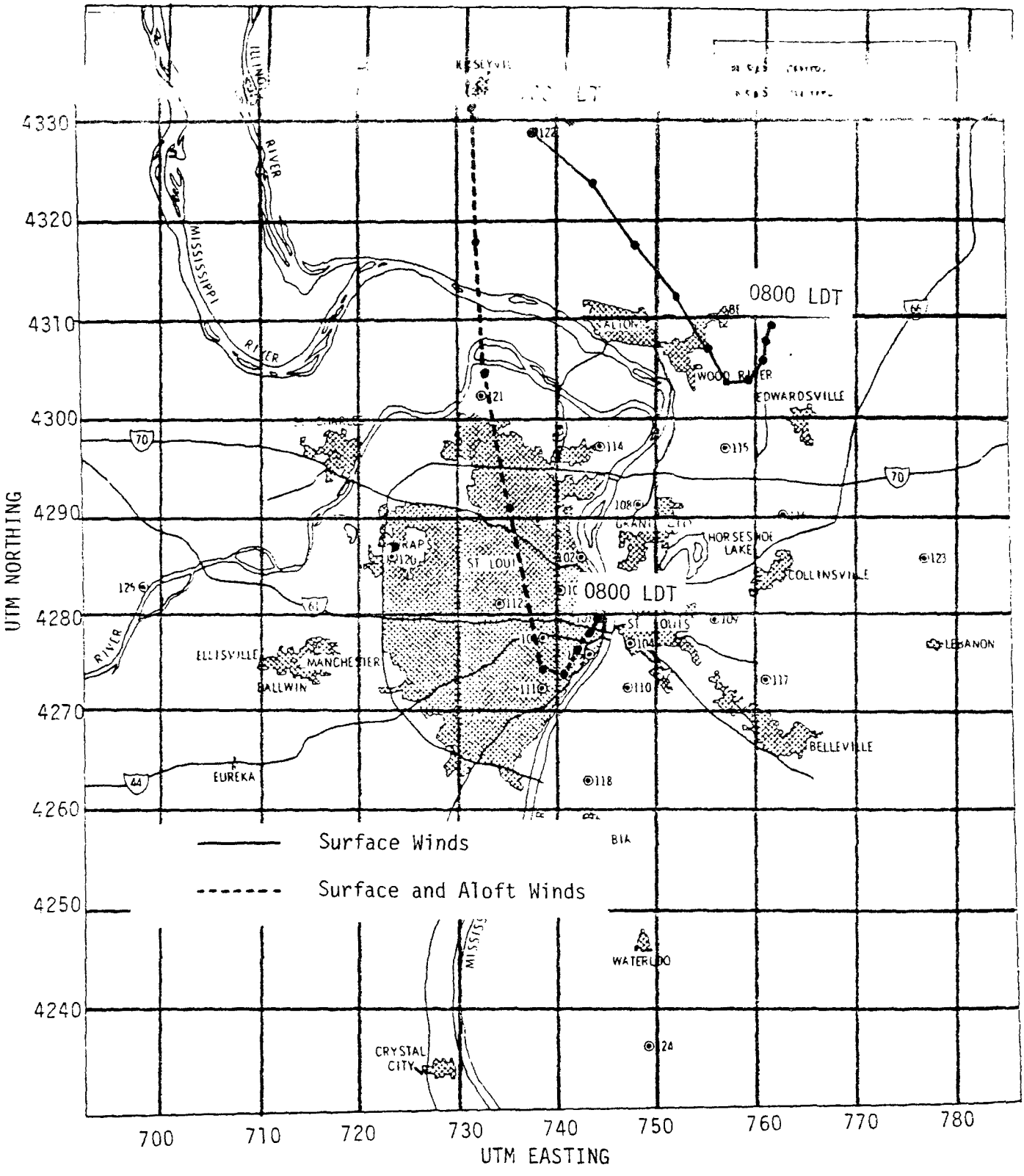

Figure 2-7. Trajectory for June 7 Derived From Surface and Aloft Wind Data.

Dilution. As previously mentioned, uncertainties exist in estimating the mixing height profiles. In OZIPP, the profile is based on a number of days, and the growth of the mixing layer is characterized by a "typical" pattern. To compare the effects of using this characteristic profile rather than the day-specific one, each test case was simulated using the characteristic curve (shown in Figure 2-8) which is incorporated in OZIPP. Table 2-2 summarizes the differences in input and their effect on model predictions. Note that the same afternoon maximum mixing height was used in both cases, but for simulations with the characteristic curve, the mixing height was assumed equal to 150 meters at sunrise in every case. This often leads to significant differences in the mixing height at 0800 LDT, the start of the simulation. Despite these differences, the effects on model predictions of peak ozone were relatively small, the largest one being to increase the peak on one day by only .022 ppm.

Post 0800 Emissions. As indicated in Section 2.1, the post-0800 emissions were derived on the basis of a 10 km x 10 km grid system. The effect of choosing a different sized grid network on predictions of peak ozone was examined by using 5x5 and 20x20 km grid networks, as well. Figure 2-9A summarizes the results when the different grid networks were used with day-specific mixing height profile. The results corresponding to the use of the characteristic curve profile are shown in Figure 2-9B. In each figure, the series of vertical bars depict the range within which model predictions varied when the grid square size was varied. As can be seen, model predictions do not vary substantially with grid square size, suggesting that the spatial resolution of the emissions inventory is not an extremely critical factor.

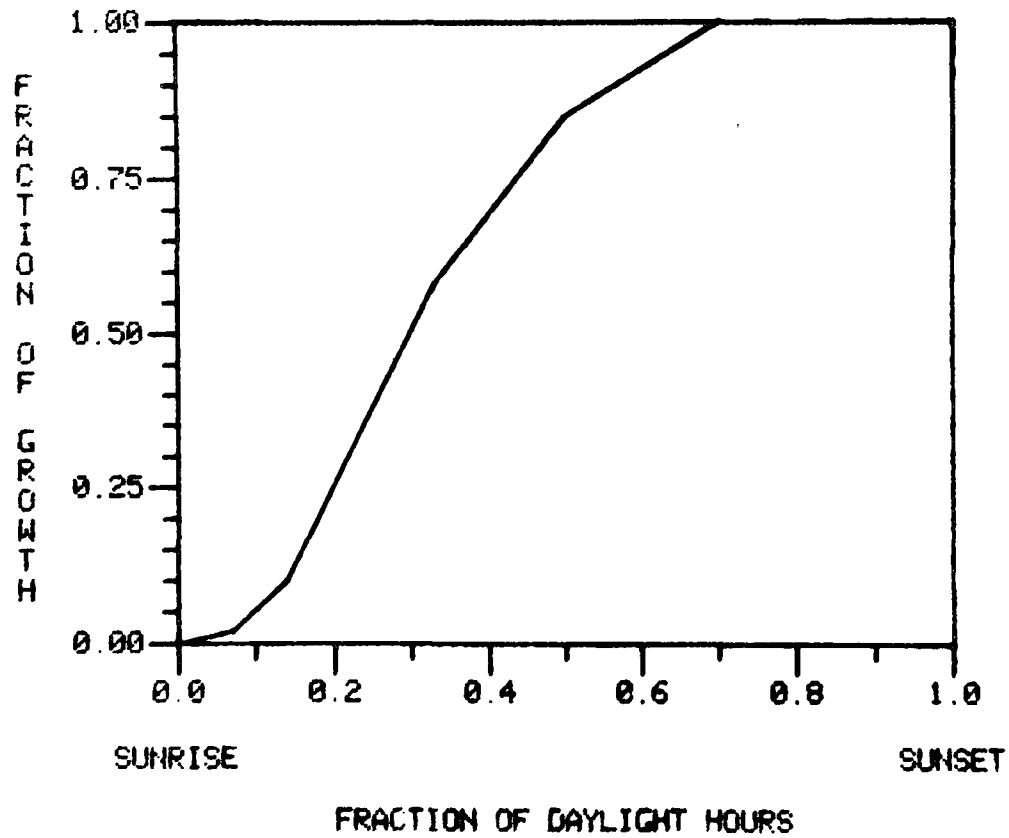

Figure 2-8. Graphical Depiction of Characteristic Curve.

Table 2-2. Example Sensitivity to Mixing Height Profile

Test Case	Mixing Heights, m						Change in Ozone*
	Original Inputs			Characteristic Curve			
	Sunrise	0800 LDT	Maximum	Sunrise	0800 LDT	Maximum	prediction, ppm
10/1/76	100	100	950	150	170	950	+.015
07/13/76	280	280	1670	150	336	1670	-.003
06/8/76 (115)	150	150	2220	150	350	2220	+.011
06/7/76	170	170	1920	150	320	1920	+.002
06/8/76 (103)	150	150	2220	150	150	2220	+.008
08/25/76	100	100	1800	150	250	1800	-.001
10/02/76	100	100	1810	150	190	1810	+.009
09/17/76	110	110	1670	150	200	1670	+.022
07/19/76	100	100	1850	150	300	1850	+.003
08/08/76	100	100	1440	150	250	1440	+.003

* A '+' means that the characteristic curve profile led to a higher predicted peak ozone concentration than did the original inputs.

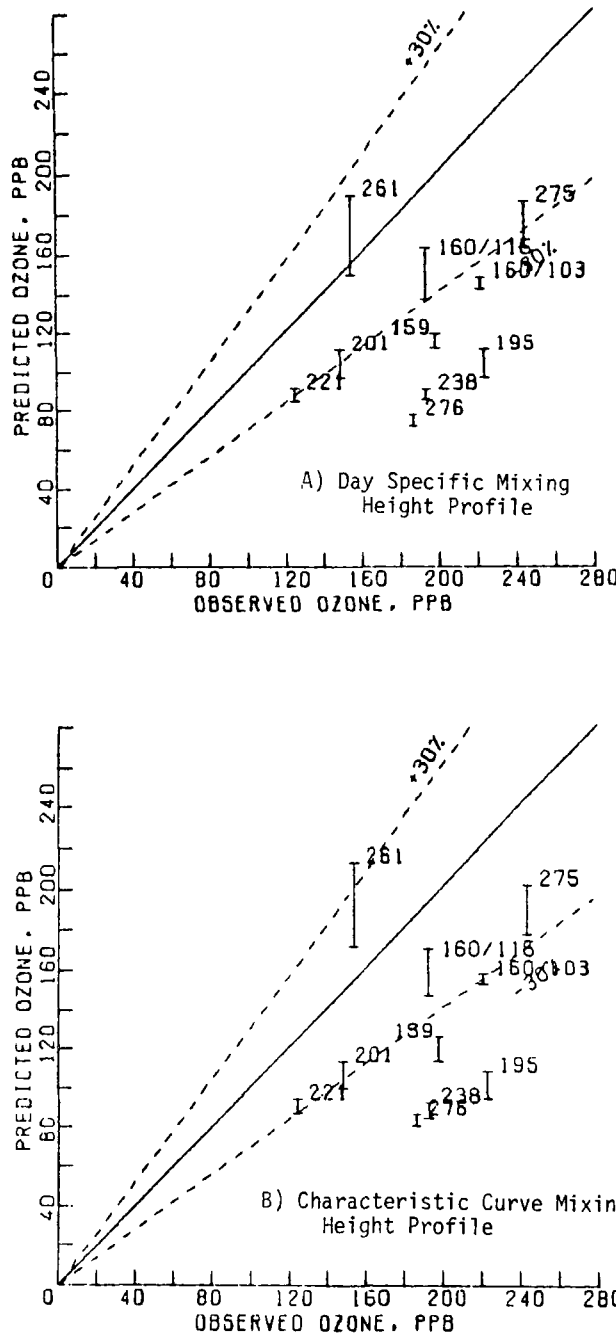

Figure 2-9. Sensitivity of Level II Model Predictions to Emission Inventory Spatial Resolution.

3.0 LEVEL III ANALYSIS

The Level II analysis just described makes use of a comprehensive data base. Such detailed information will not always be available, so alternative procedures for developing model inputs have been formulated (Reference 2). The purpose of this section is to assess the effect of using a less detailed data base on the predictions of peak ozone. The procedures for developing the model inputs are first described, followed by a comparison of the model predictions of peak ozone with those observed. Section 3.3 summarizes the results of a sensitivity analysis designed to test the sensitivity of the model predictions to uncertainty in the input data.

3.1 Model Input Data

The basic differences between the Level II and Level III data bases are in the assumptions about available meteorological and emissions data. For the Level III analysis, it is assumed that only enough wind data are available to ascertain that the peak ozone level is, in fact, downwind of the urban area. Second, only enough radiosonde data are available to estimate the 0800 LDT mixing height and the maximum afternoon height. Finally, the spatial and temporal resolution of the emissions inventory is limited to a seasonal, countywide emissions inventory for VOC and NO_x. The procedures for estimating the model inputs have been described in depth in Reference 2, and the methodologies used here are briefly described below.

Trajectory. With a Level III data base, insufficient information exists to establish an explicit air parcel trajectory. Thus, the column of air is assumed to originate in the center city and begin moving at 0800 LDT towards the site of peak ozone at a uniform speed.

Initial Concentrations. In the Level II analysis, initial concentrations were estimated from the three monitors nearest the trajectory starting point. Because the column of air originates in the urban area in the Level III analysis, the initial concentrations were estimated from the early-morning, urban average levels. The latter were calculated as the mean of the individual 6-9 LDT averages at RAMS sites 101, 102, and 104-107. These six sites were deemed representative of the urban area in general.

Post-0800 Emissions. The technique for calculating post-0800 emissions is similar to that used in the Level II analysis, except that the new assumed trajectory and countywide emissions were used. The VOC and NO_x emissions for each hour were determined by the location of the trajectory segment at each hour and the corresponding countywide emissions density. The emissions fractions were computed with these data in the exact same manner as described in Section 2.2.3.

Boundary Conditions. As in the Level II analysis, only ozone aloft was considered (i.e., precursors aloft were neglected). The same estimates made for the Level II tests were used in this analysis.

Dilution. For the Level III analysis, only the mixing height at 0800 LDT and the maximum afternoon mixing height are estimated, and the characteristic curve defines the rate of the mixed layer's growth. Reference 2 recommends a minimum morning mixing height of 250 meters. The latter accounts for the effects of mixing due to mechanical turbulence caused by increased surface roughness in the urban area, and was used for all the Level III 0800 LDT mixing heights. The maximum afternoon mixing heights were the same as those derived for the Level II analysis.

Chemical Mechanisms. As in the Level II analysis, all tests were conducted with the chemical kinetics mechanism currently incorporated in OZIPP. All default hydrocarbon reactivity factors recommended in Reference 2 were used. Default NO_2/NO_x ratios of 0.25 and .10 were assumed for initial concentrations and post-0800 emissions, respectively.

3.2 Predictions of Peak Ozone

The model inputs derived according to the procedures just described are summarized for each test case in Appendix D. The model results are graphically depicted in Figure 3-1. Once again, model predictions (ordinate) are plotted versus observations (abscissa), with the region between the dashed lines corresponding to predictions within ±30% of observations. Of the ten test cases, nine are within this range, but most are still slightly lower than

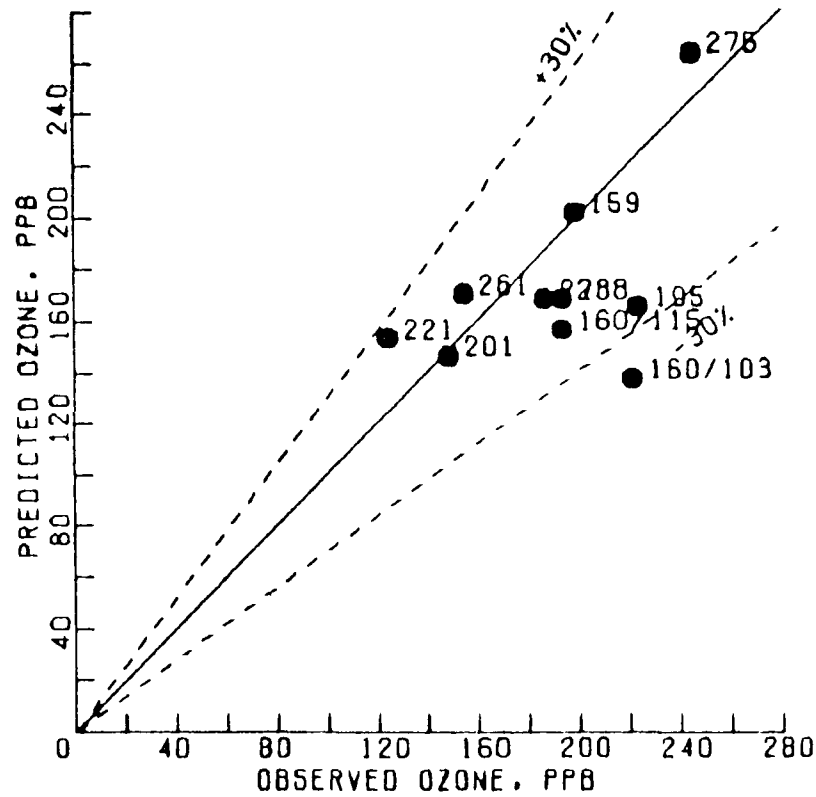

Figure 3-1. Model Predictions Versus Observations of Peak Ozone (Level III).

observations. Nevertheless, the Level III approach shows marked improvement over the Level II analysis.

The rationale underlying the Level III approach rests on two bases. First, it is clear that the Level II approach exhibits several problems. In particular, a consistent wind field is difficult to define, even with a large number of monitors and some measurements aloft. Any trajectory derived from such data will likely have some uncertainty, which in certain cases can critically affect the modeling results (see Section 2.4). Second, the data typically available are of such a limited nature that they preclude a Level II analysis in most instances (i.e., insufficient wind data exist to adequately characterize a trajectory, and emissions data are not sufficiently resolved spatially or temporally to use with a precise trajectory). In the Level III analysis, therefore, the observed peak ozone is assumed to be largely produced from precursors within the city in early morning and emitted subsequently.

A priori, one might expect that the Level III approach would lead to an overestimation of observed ozone since:

(1) the early morning levels of precursors within the urban area are often greater than those in surrounding areas;

(2) the higher levels of early morning precursors might lead to the highest ozone levels in the afternoon;

(3) a sparse network of ozone monitors may not detect the maximum ozone level that actually occurs; and

(4) the model inputs are geared to generate the maximum ozone level.

Because of the dense monitoring network in the RAPS, observations are not as likely to underestimate the true maximum ozone level occurring within or downwind of St. Louis. Thus, the close and only slightly biased predictions summarized in Figure 3-1 are encouraging. However, because of the less rigorous approach used in Level III compared to Level II, there is a greater likelihood that agreement between observations and predictions is fortuitous.

3.3 Sensitivity Analysis

Just as for the Level II analysis, a full factorial design sensitivity analysis was not possible. Rather, attention was focused on the variables most likely to have the greatest impact on predictions of peak ozone, namely dilution, post-0800 emissions, and initial concentrations. The basic approach was to vary a key input variable by ±25%, and then establish the range over which the predicted peak ozone levels might vary, given such an uncertainty in the input. While the choice of a 25% variation is admittedly arbitrary, careful compilation of a Level III data base should yield model inputs within ±25% of the true, or most representative, value.

Dilution. To examine the sensitivity of model predictions to dilution, variations in the 0800 LDT mixing height and then the maximum afternoon mixing height were considered. Simulations were repeated with the morning mixing lowered by 25%, and then increased by 25%. Figure 3-2A summarizes the results. The vertical bars indicate the range over which the predictions varied in each test case, and the circle shows the original prediction described in the previous section. For every test case, model predictions increased when the morning mixing height was increased (i.e., dilution was lowered). Furthermore, the model sensitivities differ according to the test case. For example, predictions differ by 46 PPB for the Day 275 simulation (10/1/76), but by only 5 PPB on Day 195 (7/13/76). Also, nonlinearities are not readily apparent in the model response (i.e., the base case simulation described in the previous section falls at or near the midpoint of the range over which the morning mixing was varied). Finally, except for one test case, model predictions remain within ±30% of the observed level over the entire range of morning mixing heights evaluated.

Figure 3-2B shows the sensitivity of the model predictions to changes in the maximum afternoon mixing height. It should be noted that the ±25% variation in afternoon mixing heights results in a much larger variation, in absolute terms, than the variation in morning mixing height just discussed. Similarly, the model response is also greater, but once again the sensitivity varies according to the test case. In every test case, model predictions were increased when the afternoon mixing height was lowered (i.e., dilution was

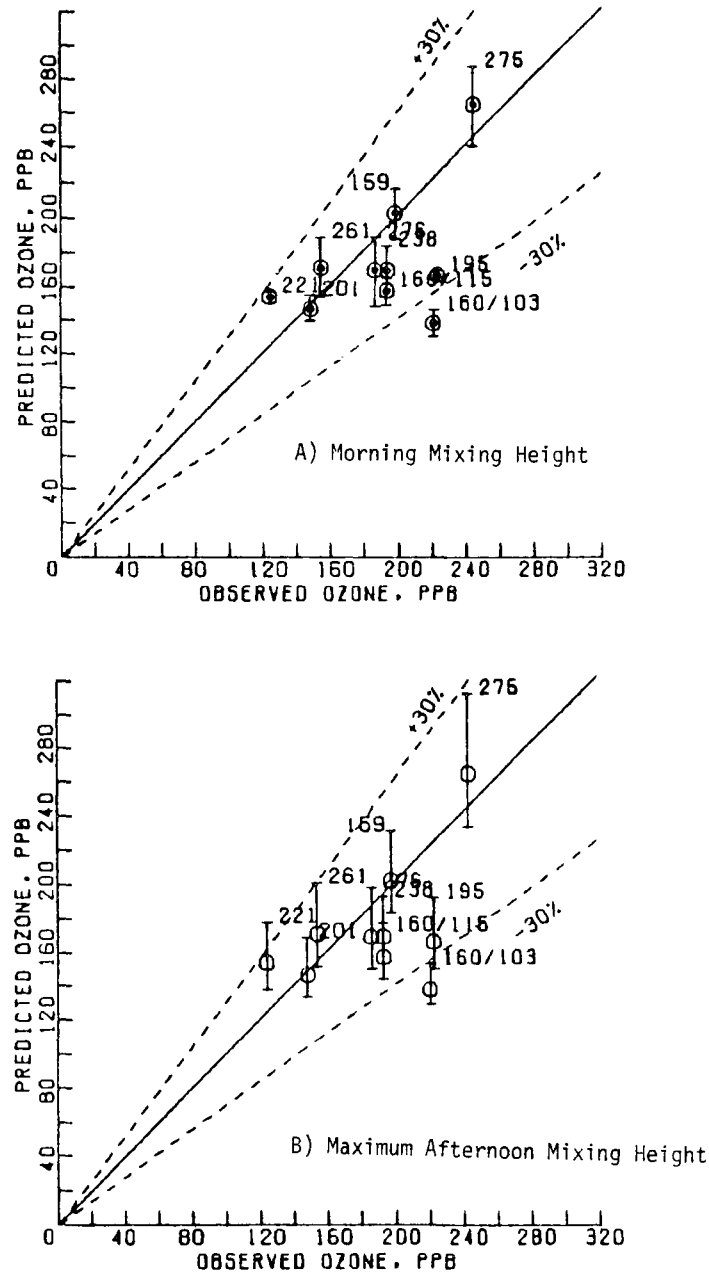

Figure 3-2. Sensitivity of Level III Model Predictions to Mixing Height.

lowered). Note also, that model predictions are increased by a greater amount when dilution is lowered than they are decreased by increasing the dilution rate. However, in most instances, the predictions remain within ±30% of observations over the entire range of variation.

Post-0800 Emissions. Figure 3-3A shows how model predictions vary when both NO_x and VOC emissions are simultaneously changed by ±25%. Again, day to day variations in sensitivity are found, with Days 195 and 221 exhibiting the greatest sensitivity. For most test cases, changing post-0800 emissions by ±25% does not result in model predictions outside the ±30% range of agreement with observations. In every test case, increasing emissions increased ozone. Finally, equally proportional changes in ozone are found when emissions are decreased or increased.

Initial Concentrations. In Figure 3-3B, the sensitivity of model predictions to variations in initial concentrations is shown. Again, both NMOC and NO_x concentrations were simultaneously altered by ±25%. Increasing initial concentrations resulted in increased ozone in every case. The patterns are similar to those found for the previously described sensitivity tests: (1) variations in sensitivity are found from day to day; (2) the base case simulation predictions fall at about the midpoint of the range of predictions; and (3) most predictions remain within ±30% of the observed levels over the range evaluated.

The sensitivity tests have focused on variations in a single variable Simultaneous variations in two or more variables could lead to wider variations in predictions. Furthermore, it is difficult to generalize about model sensitivity to any particular variable. For example, the predictions for Day 195 were more sensitive to post-0800 emissions than to initial concentrations. On the other hand, just the opposite was true for Day 275, suggesting post-0800 emissions are more important in the simulations for Day 195 than they are for Day 275. Even though generalizations are difficult, model predictions are apparently more sensitive to variations in afternoon mixing height than to changes in the others.

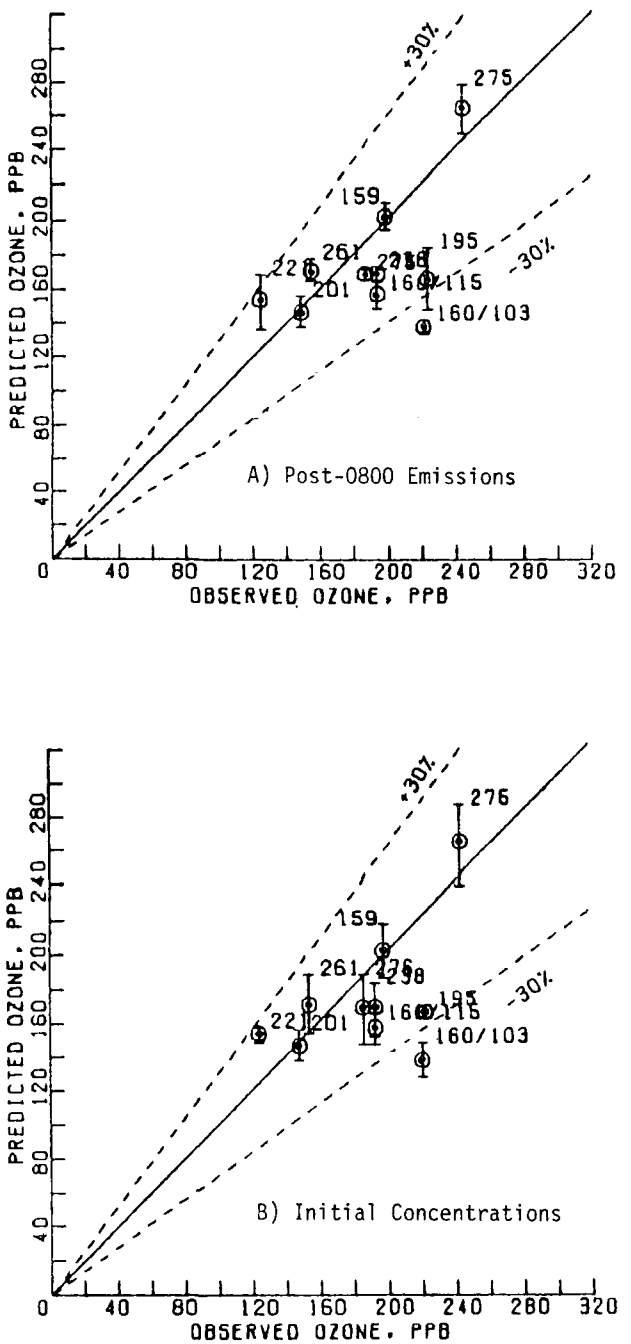

Figure 3-3. Sensitivity of Level III Model Predictions to Post-0800 Emissions and Initial Concentrations.

4.0 COMPARISONS OF EKMA WITH A PAQSM

The final approach for evaluating EKMA consists of comparing the control effectiveness predictions of EKMA with those of a more complex PAQSM. Because PAQSM's are generally perceived as providing the best estimate of the relationship between ozone and its precursors, the results of the PAQSM can serve as one basis for evaluating the performance of the simpler models. However, two major shortcomings exist: (1) the PAQSM simulation of base conditions may not always agree precisely with observations; and (2) no absolute guarantee exists that the more complex PAQSM will accurately simulate changes from base case conditions. A complete validation, as implied by this last limitation, cannot be performed until changes from base conditions are actaully imposed and the observed effects are compared with the PAQSM predictions. Unfortunately, the data base necessary for such complete model validation does not exist. While the second shortcoming cannot be circumvented, the first can be alleviated to some degree by evaluating only those PAQSM results corresponding to cases in which model predictions and observations agree reasonably well in the base case. Even though no absolute validation is possible, the possibility of errors in the input data should be minimized because of the agreement between PAQSM predictions and observations in the base case. As a result, greater confidence is usually placed in the PAQSM predictions of control program effectiveness for those days when the PAQSM simulates base case observations accurately.

As described in Section 1.2, the Urban Airshed Model has been applied to the St. Louis Metropolitan Area for a number of days to simulate ozone formation under conditions encountered during the study period. In addition, a series of detailed sensitivity tests were conducted for three of these days in which VOC emissions were altered from base case conditions. Thus, the principal question addressed in this study is whether or not changes in peak ozone levels accompanying changes in VOC emissions simulated by the Airshed Model are similar to those predicted by EKMA.

The preceding question would, at first, seem straightforward. However, the manner in which these models are applied and the information provided by each complicates the problem to some extent. For example, the Airshed Model predicts pollutant concentrations, resolved both temporally and spatially throughout the modeling region. The regional peak ozone concentration predicted by the Airshed Model may not agree with the observed peak simply because an ozone monitor was not positioned near the location of the predicted peak. The implications of such a disagreement with regard to regulatory applications have not been fully resolved. Also, the Airshed Model prediction at the site of the observed peak may be higher or lower than the measured level. Like the aforementioned problem, procedures for incorporating these potential discrepancies in a regulatory application have not been determined to date. On the other hand, EKMA is by definition an empirical approach, depending on measured levels of ozone. The effects of proposed changes in precursor emissions (i.e., NMOC and NO_x) are evaluated relative to the initial measured ozone level. Thus, the distinct possibility exists that EKMA and the Airshed Model could have significantly different base case conditions in terms of peak ozone.

To circumvent this problem, two separate procedures were followed in comparing the two models. The first entails using Airshed Model results despite any discrepancies between predicted and observed ozone peaks in the base case, and then using EKMA exactly as it would be applied in practice. The basis for comparison with these tests is the relative change in ozone maxima from the base case level. For example, if an Airshed Model simulation were conducted in which hydrocarbon emissions were reduced by 50%, the percent change in the regional peak ozone from the base case is computed, and that relative change is compared to the relative change in peak ozone predicted using EKMA. To some degree, this puts the model predictions on a common basis. The second approach consists of developing the inputs for EKMA on the basis of the Airshed Model simulations (i.e., the Airshed Model peak ozone, rather than the observed peak, would be used as input to the EKMA). For example, if the Airshed Model predicted a peak ozone level of 0.30 ppm, this value would be used to establish the starting point on the EKMA isopleth

diagram, regardless of the observed peak ozone value. In effect, this procedure involves "modeling a model," and also puts the model predictions on a common basis.

Of the two procedures described in the preceding paragraph, the first is the most rigorous test of EKMA's performance. For those situations in which EKMA would be applied, the Airshed Model predictions would not normally be available, and EKMA would have to be relied upon solely. Thus, these tests provide some indication of how closely the models agree when they are applied independently of one another. If the models disagree, the second set of tests may help determine if the causes are due to the differences in model inputs. For example, consider the situation in which the peak predicted by the Airshed Model is at a location with no nearby ozone monitor. The predicted sensitivity of this peak to changes in precursor emissions may be different from that predicted at the location of the measured peak. Thus, even though EKMA may not agree with the Airshed Model in the rigorous test, agreement may exist if the conditions corresponding to the Airshed Model predicted peak are evaluated. Of course, a major limitation of any simpler model is that it does not have the spatial and temporal predictive capabilities of the PAQSMs (i.e., it relies entirely on observations). This is a limitation that cannot be overcome.

The discussion that follows is divided into three parts. In the first portion, the urban Airshed Model is briefly described. This section is followed by a summary of the Airshed Model simulations. Finally, Airshed Model predictions are compared to those obtained with EKMA in the third section

In viewing these comparisons, it must be emphasized that this study is not intended to determine the necessary control level for the St. Louis area, but rather to compare two air quality models. It should be remembered that the RAPS data base covers the 1975-1976 time period. In a regulatory analysis, the use of a more current data base is desirable.

4.1 Description of the Urban Airshed Model

The Airshed Model is a complex PAQSM of the Eulerian (or grid) type.[16] A network of grid cells is overlaid on the region to be modeled and the physical and chemical phenomena leading to ozone formation are mathematically simulated. These processes include emissions of primary pollutants (i.e., VOC and NO_x) into each cell, the advection of pollutants from cell-to-cell, chemical transformations of pollutants into intermediate and secondary species, transport of pollutants into the modeling region from upwind areas, and entrainment of pollutants from aloft due to growth in the mixed layer. The model computes pollutant concentrations within each cell continuously, and thus attempts to reproduce pollutant-concentration time profiles measured at each monitoring site within the modeling region.

In the St. Louis application, the area modeled is 60 km wide in the East-West direction and 80 km in the North-South. The horizontal dimensions of each cell are 4 km x 4 km. Each 4x4 km area is divided into four individual cells in the vertical dimension: the bottom two cells making up the mixed layer, and the two upper cells corresponding to the region above the mixed layer. Pollutant concentrations initially within each cell are estimated from available ambient measurements. Hourly emissions of primary pollutants injected into each cell are input throughout the simulation period which begins at 0500 Central Standard Time (CST) and ends at 1700 CST. The chemical transformations are represented by a detailed chemical mechanism named Carbon Bond II, which describes the NMOC-NO_x-O_3 photochemical interactions. The concentrations of pollutants transported into the modeling region are determined from measurements taken at locations outside, and upwind, of the modeling region. Finally, cell-to-cell advection is fixed by a wind field analysis routine which resolves measured wind data into u (east-west) and v (north-south) components within each cell.

Figure 4-1 illustrates the horizontal grid structure relative to the St. Louis area and the monitoring network. Note that the modeling region encompasses 21 RAPS monitoring sites from which many of the modeling inputs are derived. They also provide the air quality measurements necessary to

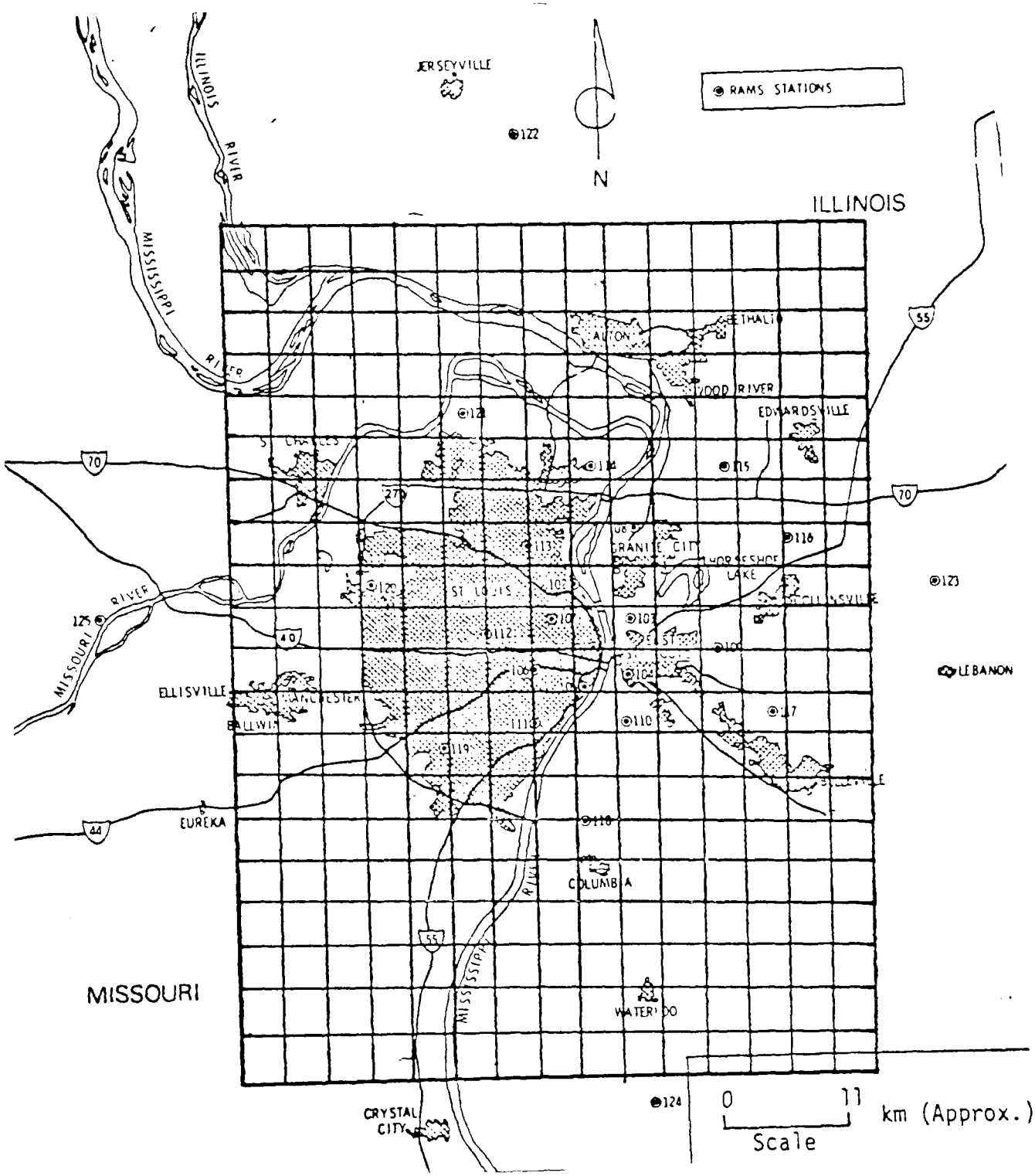

Figure 4-1. St. Louis Modeling Region.

evaluate the model's performance. The outer four sites (i.e., Sites 122-125) are used to determine the boundary concentrations which set pollutant transport into the modeling region. For a more detailed discussion of the Airshed Model application, the reader is referred to Reference 14.

4.2 Summary of Airshed Model Simulations

This section describes the results of applying the Airshed Model to simulate ozone formation on three days in the St. Louis region. Recall from Chapter 1 that the Airshed Model should reproduce observed ozone concentrations reasonably well to serve as the basis for evaluating the performance of simpler models. While a detailed evaluation of the Airshed Model's performance in the base case simulations is beyond the scope of this study, some rudimentary analysis can provide insight into overall model performance. Following this assessment, simulations in which precursors are changed from the base case are described.

4.2.1 Base Case Simulations

The three selected days are June 7, 1976 (Julian Day 159), July 13, 1976 (Day 195) and October 1, 1976 (Day 275). Each of these days is characterized by different meteorological regimes, thus serving to provide a broad basis for model evaluation and for investigating the effectiveness of control programs. On Day 159, the winds are light in early morning, developing into a persistent southeasterly flow by early afternoon. The peak one-hour average ozone concentration was 198 parts per billion (ppb), measured at Site 122, located well to the north of the central urban area. Early morning concentrations of NMOC and NO_x within the urban core were relatively high, and the estimated ozone concentration above the early morning mixed layer was the highest of the three days. On Day 195, winds were also out of the southeast but somewhat stronger in early morning than on Day 159. The measured NMOC and NO_x concentrations in the urban core on this day were much lower than those of the other two days, while a moderate level of ozone aloft was estimated. Nevertheless, the measured one-hour average peak ozone was the second highest of the three days - 223 ppb at Site 114, slightly north of the urban core. Day 275 had the highest measured ozone concentration of the three days -

244 ppb at Site 102 in the northern portion of the urban core. On this day the winds were light and variable throughout the day, which is typical of a stagnating air mass. Elevated early morning precursor levels were measured within the urban core and the estimated level of ozone aloft was the lowest of the three days. Some of the key measurements and Airshed Model inputs characterizing the three days are summarized in Table 4-1.

Of principal interest (although not necessarily the best indicator of model performance) is the Airshed Model's prediction of regional peak ozone concentration. Figure 4-2 was constructed to compare the model's predictions with observations in terms of magnitude, location, and timing of the ozone peaks. In this figure, the large rectangle indicates the modeling region while the smaller one shows the relative location of the urban core. The location of the Airshed's prediction of peak ozone is denoted by a "□" while the location of the observed peak is marked by an "O." The magnitude and time of the corresponding peaks are shown to the right of each diagram, along with the percent difference between observed and predicted peaks. The figure clearly indicates significant differences between predicted and observed peaks in terms of magnitude and location. However, these differences are not necessarily indicative of model accuracy. For example, the Airshed regional peak on Day 159 is at a location with no nearby monitor, while the actual observed peak was outside the modeling region. On the other hand, the predicted regional peak for Day 195 is somewhat lower than the observed peak, indicating a model underprediction. For Day 275, the magnitude of the peaks is similar, although the locations are somewhat different.

To provide a better indication of overall model performance, the Airshed Model predictions of ozone at each of the 21 monitoring locations within the modeling region were compared to the measured peaks.* The most rigorous test

---

* Actually, the Airshed Model predicts cell-wide average concentrations, not point concentrations necessary for direct comparison with monitored pollutant concentrations. In the discussions that follow, the average concentrations in the ground level cell corresponding to each monitor are compared to the measured levels.

Table 4-1. Summary of Miscellaneous Measurements and Airshed Model Inputs.

	Julian Day		
	159	195	275
Measured O_3 peak, ppb	198	223	244
Site of measured O_3 peak	122	114	102
Time of observed peak, CDT*	1600-1700	1600-1700	1500-1600
Measured 6-9 a.m. CDT urban average** NMOC, ppmC	1.8	0.2	1.9
Measured 6-9 a.m. CDT urban average** NO_x, ppm	.205	.048	.236
Measured 6-9 a.m. CDT urban average NMOC/NO_x ratio	7.6:1	7.0:1	8.1:1
O_3 level aloft input to Airshed Model, ppb	114	78	63
0800-1500 CDT network average wind speed, m/sec***	1.0	2.3	0.6
Maximum afternoon mixing height input to Airshed Model, meters	1972	1853	529

---

* CDT, Central Daylight Time

** Urban averages computed from the 6-7, 7-8 and 8-9 a.m. average at Sites 101, 102, 104, 105, 106, and 107. The reported NMOC/NO_x ratios are the averages of the six site-ratios, and thus do not necessarily equal the ratio of the urban average concentrations.

*** From Reference 14

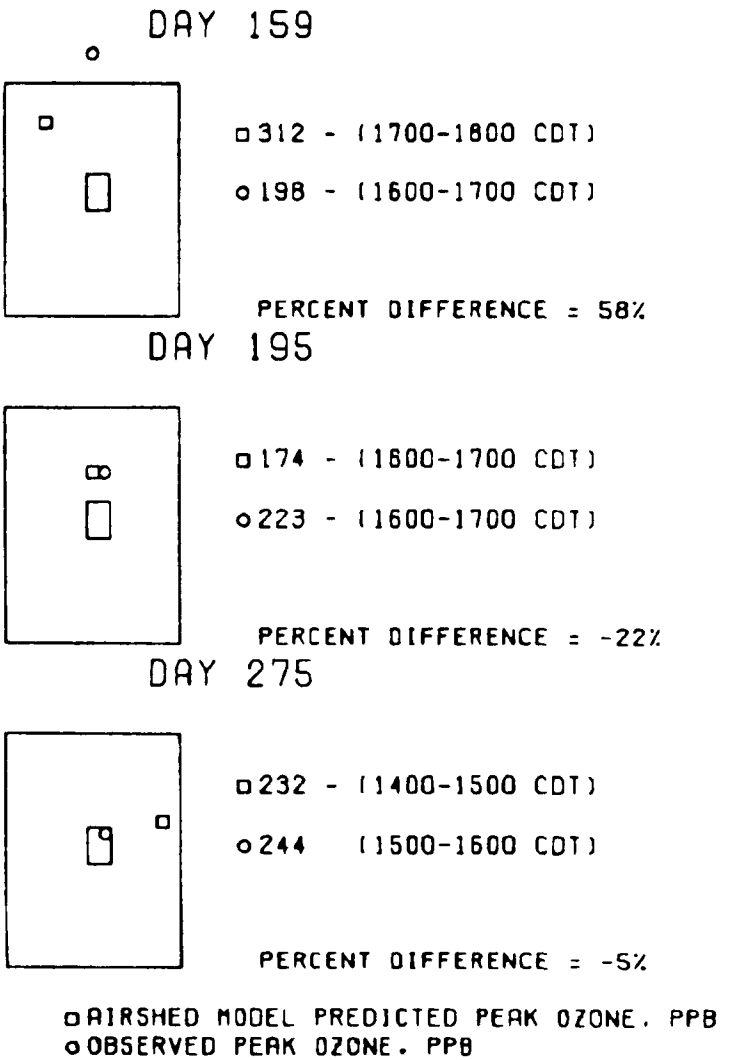

Figure 4-2. Airshed Predictions Versus Observations of Regional Peak Ozone.

involves comparing the observed ozone peak at each site with the ozone level predicted by the Airshed Model precisely at the time of the observed peak. The results of this test are illustrated graphically in the left hand portion of Figure 4-3. When the timing criterion is relaxed, the Airshed peaks predicted at each monitoring site are compared to the observations, regardless of the time of the peak. These results are shown in the right hand portion of the same figure. In each of the individual graphs in Figure 4-3, the predicted ozone (y-axis) is plotted versus observed ozone (x-axis). For reference, the 45 degree line (solid) indicates perfect agreement between predictions and observations, while the other two dashed lines indicate over-and underpredictions of ±30%. The results for Day 159 indicate that most predictions are within ±30% of the observed level, with or without the timing criterion. However, a tendency does exist for the model to overpredict ozone levels, especially at those sites with higher measured levels. On the other hand, the Airshed Model tends to underpredict ozone levels on Day 195, even though most predictions are within 30% of the observed levels. On Day 275, the most rigorous test indicates a tendency to overpredict at the observed low ozone levels, and underpredict at the higher levels. When the timing criterion is relaxed, the agreement is improved somewhat, but underpredictions at locations with high measured ozone still persist.

A detailed evaluation of model performance should, to the extent possible, address how well the model reproduces concentrations of precursor patterns as well as ozone patterns. While such an analysis is beyond the scope of this study, particular attention was focused on the Airshed Model's predictions of early-morning, urban core concentrations of NMOC and NO_x because of the implications for applying EKMA. Airshed Model predictions of these precursors are compared to observed levels in Table 4-2. General patterns of precursor levels were reproduced by the Airshed Model (e.g., high precursor levels on Days 159 and 275, low levels on Day 195), although a tendency for underprediction was found. (Note that in every case, NO_x is underpredicted, ranging from 14% to 42%, while on two of the days, NMOC levels were underestimated.) The urban core, 6-9 a.m. NMOC/NO_x ratios predicted by the Airshed Model agree reasonably well with the ratios derived from ambient measurements.

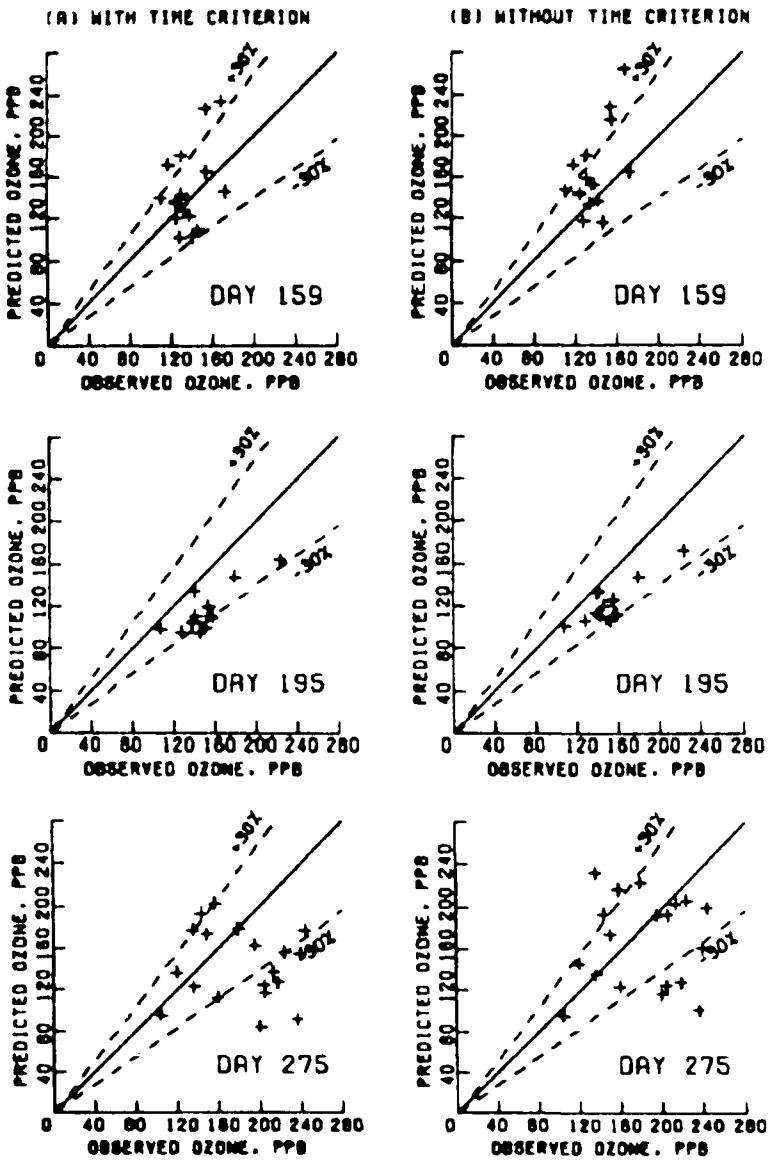

Figure 4-3. Airshed Predictions Versus Observations of Peak Ozone.

Table 4-2. 6-9 a.m. Urban Core Precursor Predictions Versus Observations.*

	Predicted	Observed
Day 159		
6-9 a.m. CDT urban average NMOC, ppm	1.2	1.8
6-9 a.m. CDT urban average NO_x, ppm	.152	.205
6-9 a.m. CDT urban average NMOC/NO_x	8.1:1	7.6:1
Day 195		
6-9 a.m. CDT urban average NMOC, ppm	0.2	0.2
6-9 a.m. CDT urban average NO_x, ppm	.028	.048
6-9 a.m. CDT urban average NMOC/NO_x	8.9:1	7.0:1
Day 275		
6-9 a.m. CDT urban average NMOC, ppm	1.5	1.9
6-9 a.m. CDT urban average NO_x, ppm	.203	.236
6-9 a.m. CDT urban average NMOC/NO_x	7.7:1	8.1:1

* Urban average NMOC and NO_x levels are computed from the 6-7, 7-8, and 8-9 a.m. averages at Sites 101, 102, 104, 105, 106, and 107 and the cells corresponding to those sites. The NMOC/NO_x ratios are the average of 6-9 a.m. ratios at the individual sites (cells), thus, they do not necessarily equal the ratio of the urban average concentrations.

The elementary analyses just described were not intended to assess conclusively the accuracy of the model, nor do they provide a complete picture of model performance. However, they do give some insight into how well the model is reproducing observed ozone levels. In most instances, predicted ozone levels at the locations of monitoring sites are within ±30% of the observations. Except for Day 159, the model tends to underpredict the higher ozone levels. On Day 159, the model is biased towards overprediction at most monitoring sites. Finally, a tendency exists for the model to underpredict the early-morning precursor levels within the urban core.

4.2.2 Simulations of Changes in VOC Emissions

A number of sensitivity tests were conducted to assess how the Airshed Model predictions of ozone respond to changes in VOC emissions. These tests were designed primarily to indicate the potential effectiveness of emission reduction programs. To establish this sensitivity over a wide range, reductions in VOC of 17%, 42% and 75% (from base levels) were tested. These reductions were applied uniformly to area and point source hydrocarbon emissions, as well as to initial NMOC concentrations.* Boundary conditions were held constant in all simulations.

Figure 4-4 summarizes the sensitivity results with respect to changes in the predicted peak ozone levels. The large boxes represent the modeling region, with the inner ones indicating the urban core. One diagram is included for each simulation. On each, the location, time and magnitude of the predicted peak ozone are shown. The first apparent result is that ozone levels are lowered by reductions in VOC emissions, although the relative changes are different. For example, a 75% reduction in VOC gives ozone reductions between 41 and 64%, depending on the particular day. Secondly, the results indicate that, as VOC's are reduced, the peak ozone level is likely to

---

* Clearly, a realistic control program would not produce uniform emission reductions. However, the uniformity assumption makes the task manageable and eliminates the need to make some arbitrary assumptions regarding point versus area reductions.

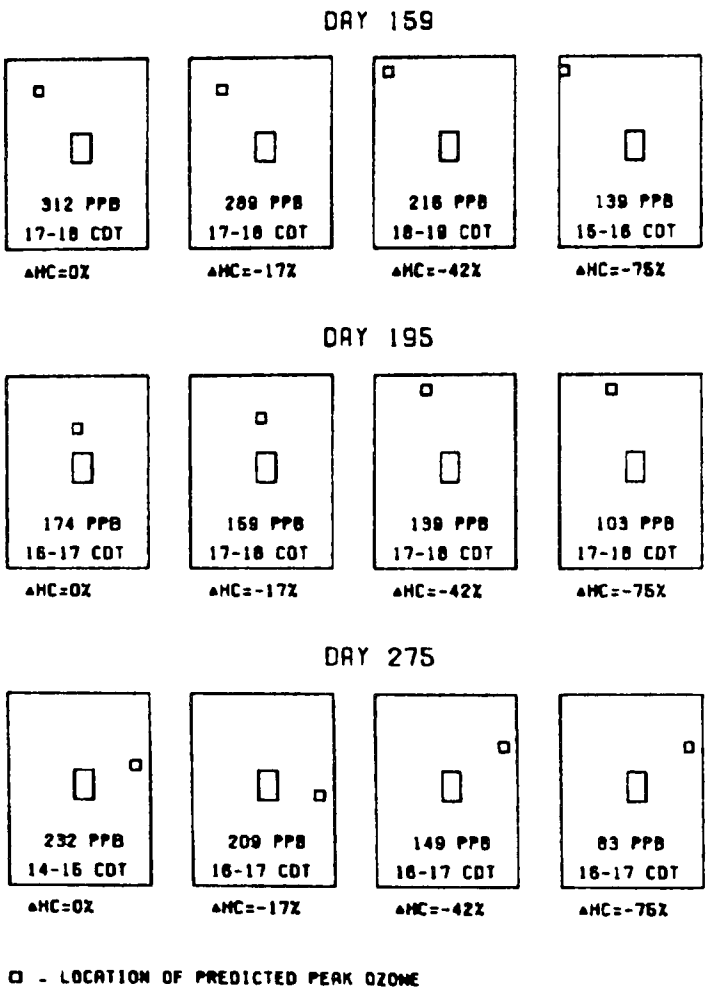

Figure 4-4. Summary of Airshed Model Simulations.

occur slightly farther from the city (i.e., farther downwind). Although not universally true, the peak often occurs later in the day under an emission reduction scenario.

Figure 4-5 illustrates the simulation results in another way. First, regional peak ozone concentrations are graphed against VOC reductions, followed by a graph showing the relative change (i.e, percent change) in ozone accompanying the reductions. In this last figure, a line of unit slope is included as reference to indicate equally proportional changes between VOC and ozone. The figure clearly indicates that the O_3 response to changes in VOC is different for each day. The Airshed Model predicts the largest incremental changes in O_3 on Day 275, while Day 195 exhibits the least response. In all cases, the percent change in ozone is less than the change in VOC input to the model. These findings are not entirely surprising since boundary conditions remained unchanged in all simulations, and one might expect the importance of boundary conditions to vary from day to day.

In examining Figure 4-5, one may be tempted to estimate the emission reduction necessary to achieve the National Ambient Air Quality Standard (NAAQS) for ozone. Several caveats are in order. Recall that in the base case simulations, the Airshed Model predictions of regional peak ozone did not agree precisely with measured peaks. In fact, a large difference existed on Day 159. Whether or not the Airshed Model's predicted peak would be accepted as the basis for a regulatory application has not been resolved. Secondly, as described above, boundary conditions were not changed in any simulation. In a regulatory application, some estimate of future boundary conditions might be factored into the model applications (e.g., the level of ozone aloft might be altered to reflect the implementation of upwind control programs in the future).[2] Finally, the modeling results provide information on how the O_3 levels change on particular days. To establish the control needed to meet the ozone standard, this information must be related to the statistical form of standard. The latter allows, on average, one maximum daily value to be greater than 0.12 ppm at each site during a year.[17] Procedures for relating the model output to the form of the standard are being explored, but have not

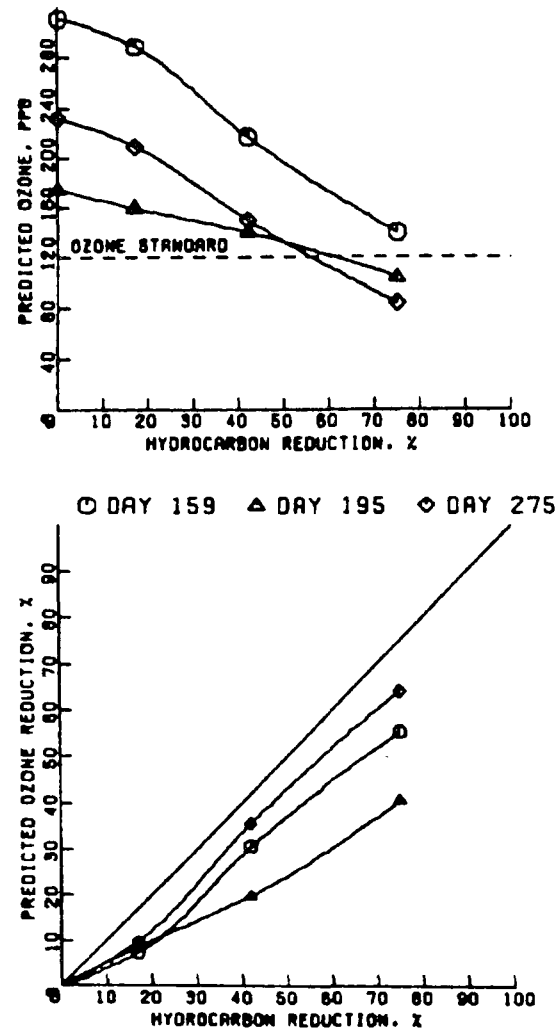

Figure 4-5. Airshed Model Sensitivity of Regional Peak Ozone to Hydrocarbon Reductions.

yet been prescribed. Thus, the information presented in Figure 4-5 could not necessarily be used to estimate the reduction in VOC emissions needed to achieve the ambient ozone standard.

4.3 Comparison of EKMA with Airshed

The previous section described the results of the Airshed Model simulations in which VOCs were reduced uniformly from base conditions. These simulations have been replicated, to the extent possible, with Level III EKMA. Two different sets of comparisons, along the lines described in Section 4.2, are made. The first involves comparing the models exactly as they would be applied, in practice, without trying to compensate for known model differences. For example, the base case ozone peaks used in EKMA are measured levels, while base case peaks used with the Airshed Model are the regional peaks predicted by Airshed. Other known differences in model inputs exist between Airshed and EKMA also (e.g., NMOC/NO_x ratio, dilution rate, etc.). This is a very severe test and provides information on the model predictions obtained under independent applications.

The second set of comparisons entails resolving known differences in model inputs to eliminate these differences as potential sources of discrepancy between models. In effect, EKMA was made to replicate, as closely as possible, the conditions in the Airshed Model. Another way of looking at the second set of comparisons is that EKMA is being used to model the more complex Airshed Model. Such tests may provide some information regarding potential discrepancies found in the first set of comparisons.

4.3.1 Independent Model Tests

Figure 4-6 shows the models' sensitivity to changes in hydrocarbons for each day. The first apparent result is that relationships between model responses differ according to the day being modeled. First, consider Day 159. EKMA is less sensitive over the entire range of emission reductions than the Airshed Model (i.e., EKMA predicts a smaller reduction in ozone for a given hydrocarbon reduction). On Day 195, Airshed and EKMA agree reasonably well up to a 40% reduction in emissions. At reductions greater than 40%, EKMA becomes

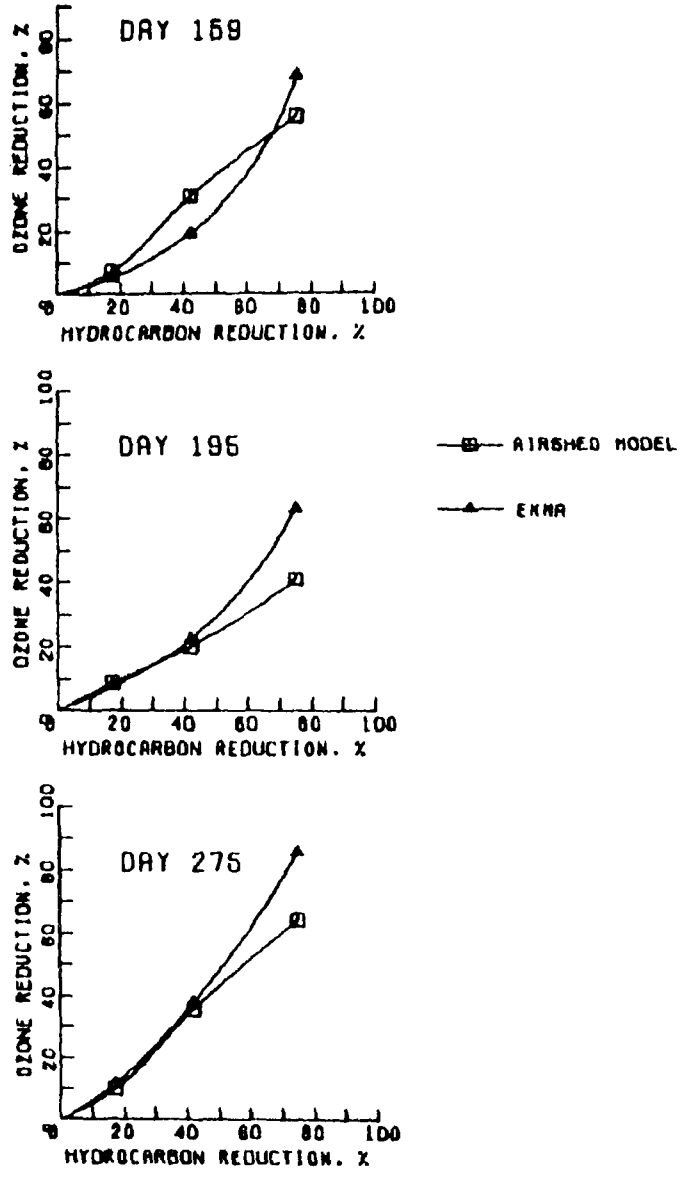

Figure 4-6. Comparison of Airshed and EKMA (Independent Tests).

substantially more sensitive than Airshed to incremental changes in VOCs. On Day 275, the agreement between Airshed and EKMA is reasonably good up to a reduction of about 40%; but again, EKMA exhibits a greater sensitivity to HC changes at higher reductions. These findings demonstrate that EKMA and the Airshed Model do not agree under all conditions.

While the overall model responses are an important consideration, a major function of any of these models is to determine how much control is needed to achieve the NAAQS for ozone. As discussed earlier, this question cannot be directly answered here. However, it is possible to estimate for each day the VOC emission reduction needed to lower a daily peak to 120 ppb. Presumably, data such as these would be used in determining the precise degree of control needed to achieve the ozone NAAQS.*

Table 4-3 summarizes the results, assuming an independent application of models. Two sets of Airshed Model predictions are presented in the table. In the first set, the Airshed Model results are used as is, with the base case peak corresponding to the model predicted peak (not the observed). In this case, EKMA predictions, when compared to those of the Airshed Model, are lower, about the same, and lower on Days 159, 195 and 275, respectively. For those days in which EKMA yielded lower controls than Airshed, the differences are on the order of 10%.** The second set of predictions corresponds to a simplistic method for calibrating the Airshed Model to base case measurements.

---

* It should be emphasized that in all simulations in which VOC emissions were reduced, boundary conditions were kept at the base levels. In a true regulatory application, some consideration may be given to altering boundary conditions to reflect the impact of upwind control programs. This is most important with respect to ozone aloft. Furthermore, the form of the ozone NAAQS complicates the process of using the Airshed Model results to estimate the level of control needed to achieve the NAAQS. The NAAQS allows for one maximum daily one-hour level to be above 0.12 ppm per year, per site. The three days that have been modeled correspond to peaks observed at three different sites. Thus, the number of site/days that have been modeled is insufficient to estimate the lowest level of control that is just needed to achieve the NAAQS.

** On Day 159, the control needed to reduce the Airshed predicted peak of 120 ppb is outside the range of tests, and thus the difference could be somewhat greater.

Table 4-3. Emission Reductions Needed to Reduce Peak O_3 to 120 ppb.

Day		Airshed*	EKMA
159	Base case peak O_3, ppb	312	198
	O_3 reduction necessary to lower peak to 120 ppb	62% (39%)	39%
	HC reduction necessary to lower peak to 120 ppb	>75% (52%)	66%
195	Base case peak O_3, ppb	174	223
	O_3 reduction necessary to lower peak to 120 ppb	31% (46%)	46%
	HC reduction necessary to lower peak to 120 ppb	60% (>75%)	62%
275	Base case peak O_3, ppb	232	244
	O_3 reduction necessary to lower peak to 120 ppb	48% (51%)	51%
	HC reduction necessary to lower peak to 120 ppb	57% (59%)	47%

* The HC reductions in parenthesis refer to the control needed to lower ozone by the same <u>percent</u> as the other two models.

Here, the Airshed Model response curve (Figure 4-6) is used to estimate the hydrocarbon reduction that will give the percent change in ozone that is necessary to lower the measured peak to 120 ppb. For this simplistic calibration of the Airshed Model to base conditions, the comparisons lead to somewhat different results. In this case, EKMA estimates of control are higher, lower, and lower than those of the Airshed Model. Once again, the differences between Airshed predicted controls and those of EKMA are on the order of 10%, or less.

The results just described are similar to the findings regarding the comparisons of overall model response, i.e., the comparisons reveal day-to-day variations in results. However, differences between EKMA and the Airshed Model were usually on the order of ±10%. EKMA gave moderately higher estimates of emission reductions in only one case (14% higher). Thus, based on the Airshed Model results, EKMA would not appear to consistently overestimate the VOC emission reduction necessary to lower peak ozone to the level of the standard.

4.3.2 Common Basis Tests

As described above, the comparisons of Section 4.3.1 were made on the basis of independent applications of two models. In this section, comparisons of the models are made using the Airshed Model simulations as the basis, i.e., the EKMA simulation is made to replicate the Airshed base case simulation as closely as possible. In these tests, the 6-9 a.m. NMOC/NO_x ratio predicted by Airshed for the "urban core" (see Table 2-1) and the Airshed Model predicted peak ozone are both used to establish the EKMA starting point. Additionally, the OZIPP program was modified to reflect more precisely the growth in mixing height as treated in the Airshed Model, and NMOC and NO_x concentrations aloft corresponding to Airshed Model inputs were used in the EKMA modeling.* Presumably, these modifications put the models on

---

* The mixing height growth in Airshed is based on a piecewise linear fit to measured mixing heights. NMOC and NO_x levels aloft were on the order of .05 ppmC and .003 ppm, respectively.

a more common basis and allow for a more direct comparison of model results by removing possible discrepancies in model inputs.

Figure 4-7 depicts the relative changes in peak ozone as a function of changes in hydrocarbons. The results are somewhat similar to those in the preceding section. However, the overall agreement between Airshed and EKMA is slightly improved. In most cases, EKMA appears to be more sensitive to changes in VOC emissions than the Airshed Model over the entire range of evaluation. On Day 159, however, EKMA's sensitivity is less than Airshed's, up to a control level of about 75%.

Table 4-4 summarizes the individual emission reductions predicted by each model to be necessary to lower the Airshed Model's base case peak ozone to 120 ppb. EKMA gives lower control estimates than Airshed in all three cases. The largest difference is 9%, although the possibility exists for a larger difference on Day 159. Once again, the comparisons suggest that EKMA does not consistently overestimate the controls needed to reduce peak ozone levels to 120 ppb.

These findings suggest that the model differences found in the previous sections are not entirely due to discrepancies in model input. Even when the models are put on a common basis, differences do occur. EKMA cannot exactly reproduce the Airshed Model predictions over all conditions considered, but it does not consistently overestimate the VOC reductions necessary to reduce peak ozone levels to 120 ppb.

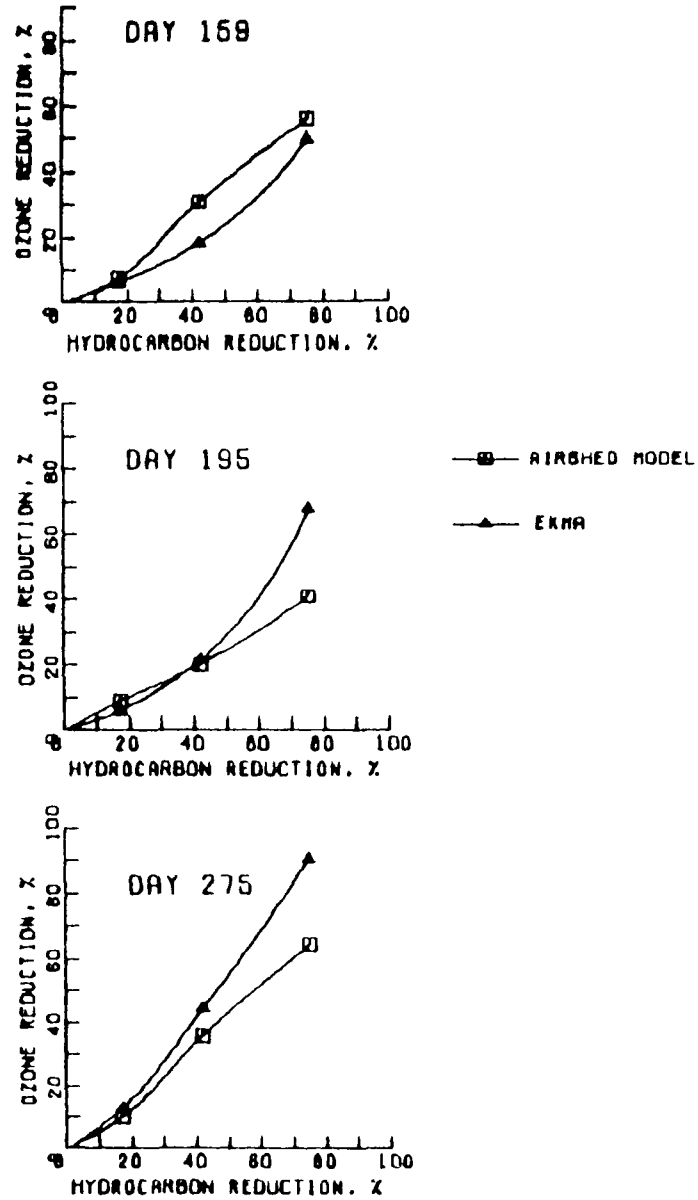

Figure 4-7. Comparison of Airshed and EKMA (Common Basis Tests).

Table 4-4. Emission Reductions Needed to Lower Peak O_3 to 120 ppb.

Day		Airshed	EKMA
159	Base case peak O_3, ppb	312	312
	O_3 reduction necessary to lower peak to 120 ppb	62%	62%
	HC reduction necessary to lower peak to 120 ppb	>75%	72%
195	Base case peak O_3, ppb	174	174
	O_3 reduction necessary to lower peak to 120 ppb	31%	31%
	HC reduction necessary to lower peak to 120 ppb	60%	51%
275	Base case peak O_3, ppb	232	232
	Reduction in O_3 necessary to lower peak to 120 ppb	48%	48%
	HC reduction necessary to lower peak to 120 ppb	57%	50%

5.0 CONCLUSIONS AND RECOMMENDATIONS

Three methods for evaluating EKMA have been considered. The first two consist of comparing absolute model predictions of peak ozone with observations. The major differences between these two methods are in the complexity of the data base, and the assumptions used in deriving the model inputs. Again, these two methods do not address the key questions of how well EKMA predicts changes in peak ozone due to changes in precursor emissions. However, the first two approaches do provide some indication of how well the model simulates the ozone formation processes. The third approach more directly addresses the major question of interest. Here EKMA predictions of changes in ozone are compared to those of a state-of-the-art photochemical air quality simulation model. The major findings of each phase of the study are summarized below, followed by recommendations for additional study.

The predictions of peak ozone using OZIPP/EKMA in a Level II mode are not good. Substantial underpredictions of ozone resulted in almost every case. A detailed evaluation of each simulation revealed that ambient NMOC levels may also have been underpredicted. The same pattern was also found with the relatively inert pollutant CO, suggesting a problem with the emissions/ambient precursor relationship. However, the findings of the sensitivity analysis suggest that the lack of agreement between predictions and observations could possibly be explained for some days. Of critical importance is the definition of the air parcel trajectory. Using different mathematical techniques to calculate a trajectory will often lead to different trajectories, and sometimes these differences can result in significantly different model predictions.

The foregoing findings indicate that a Level II approach used in a regulatory framework may have some serious problems. Model predictions of peak ozone appear to be critically sensitive to particular model inputs that are difficult to estimate, even with a comprehensive data base. How the predictions of changes in ozone resulting from changes in precursors would be affected by poor absolute predictions of ozone is not fully understood, but one study has suggested that estimates of controls needed to meet the ozone NAAQS would be underpredicted for a case in which base case peak ozone

concentrations are underpredicted.[9] While some tests could have been conducted to address this problem, it is clear that using different techniques to derive the model inputs will lead to different results. It is beyond the scope of this study to examine several various alternatives that could be employed. In summary, then, the model does not replicate peak ozone levels in a reasonable manner, but it is not clear whether this is a failure of the model itself or comes about from problems in developing model inputs. In either case, the poor model performance does not lead to confidence in using the Level II approach to make estimates of changes in ozone that would result from changes in precursors.

Somewhat surprisingly, when the data base complexity is reduced to that commensurate with a Level III analysis, model performance in predicting peak ozone is markedly improved. Clearly, this improvement is the result of starting the trajectory in an area with the highest precursor initial loading. Because of the assumed trajectory, the agreement between predictions and observations may be somewhat fortuitous. Nevertheless, one would expect that the high initial loading would eventually lead to an ozone peak, although the timing and location of the peak may not correspond precisely with an ozone monitoring site. Furthermore, the general pattern of the Level II trajectories correspond to the assumed Level III trajectory in many instances, although differences in timing and location occur (i.e., most Level II trajectories pass near the urban area by the late morning). Thus, a distinct possibility exists that the "smoothing" of the data attendant with a Level III analyses may remove some data anomalies inherent in the development of the Level II inputs. While the Level III approach is less intuitively appealing from a technical point of view than the Level II analysis, peak ozone predictions do agree reasonably well with observations. Furthermore, the model predictions were found to be relatively insensitive to model inputs as compared to the Level II approach. Because of these two factors, greater confidence would normally be placed in the Level III predictions of changes in ozone than in those found from a Level II approach.

The most direct means investigated for evaluating the accuracy of EKMA in predicting changes in ozone accompanying changes in precursors was to compare EKMA's predictions with those of a complex PAQSM. Even though no absolute guarantee exists that the PAQSM predictions are accurate, these complex models represent the state-of-the-art in modeling ozone formation, and as such, should provide the best available estimate. Comparisons of EKMA wth the PAQSM were complicated by differences in their mode of application. Considering all of the tests, EKMA did not reproduce the PAQSM results precisely. However, when estimates of the degree of control needed to reduce peak ozone to the level of the standard were made for each of three days with the two models, differences in the estimated VOC emission reductions were less than 10%. EKMA was not found to over or underestimate the required reduction, as compared to the PAQSM reduction. One apparent finding of the study was that the VOC emission reductions needed to reduce peak ozone to the level of the standard is dependent on the day being modeled. For example, the PAQSM predicted that the level of control needed to reduce peak ozone to 120 ppb was greater for Day 195 than for Day 275, even though the latter had the higher ozone peak (both predicted by the PAQSM and observed). The extent to which this is a result of meteorological effects or background conditions is not known at this time, but the fact that EKMA replicated these results is encouraging.

The above findings lead to the following recommendations for future study.

- The approaches for estimating Level II model inputs need more detailed study. In particular, techniques for estimating air parcel trajectories need further investigation. Techniques for considering surface level winds in conjunction with the winds measured higher in the mixed layer should be evaluated.

- The trajectory model underlying EKMA should be compared to a more complex photochemical trajectory model. Differences in the treatment of specific physical phenomena should be identified, and their effects should be isolated to identify possible limitations and potential improvements in the trajectory model underlying EKMA.

- Further studies are needed to identify potential differences that may result from the use of different chemical mechanisms. In particular, EKMA should be compared to the PAQSM using the same chemistry.

- Comparisons should be made in which boundary conditions to the PAQSM and EKMA are altered in accordance with current regulatory guidelines.[2]

6.0 REFERENCES

1. Uses, Limitations and Technical Basis of Procedures for Quantifying Relationships Between Photochemical Oxidants and Precursors, EPA-450/2-77-021a, U.S. Environmental Protection Agency, Research Triangle Park, North Carolina, November 1977.

2. G. L. Gipson, W. P. Freas, R. F. Kelly, and E. L. Meyer, Guideline for Use of City-specific EKMA in Preparing Ozone SIP's, EPA-450/4-80-027, U.S. Environmental Protection Agency, Research Triangle Park, North Carolina, March 1981.

3. J. Trijonis, Verification of the Isopleth Method for Relating Photochemical Oxidant to Precursors, EPA-600/3-78-019, U.S. Environmental Protection Agency, Research Triangle Park, North Carolina, February 1978.

4. J. Trijonis and Marilyn Marians, "Historical Emission and Ozone Trends in the Houston Area," Proceedings, Ozone/Oxidants Interaction with the Total Environment II, Specialty Conference, Air Pollution Control Association, October 1976.

5. "Data Collection for 1982 Ozone Implementation Plan Submittals," Federal Register, November 14, 1979, 44 (221) 65669-65670.

6. F. A. Schiermeir, Air Monitoring Milestones: RAPS' Field Measurements, Environmental Science and Technology, 12, 1978.

7. Ozone Isopleth Plotting Package (OZIPP), EPA-600/8-78-014b, U.S. Environmental Protection Agency, Research Triangle Park, North Carolina, July 1978.

8. G. Z. Whitten and H. Hugo, User's Manual for Kinetics Model and Ozone Isopleth Plotting Package, EPA-600/8-78-014a, U.S. Environmental Protection Agency, Research Triangle Park, North Carolina, July 1978.

9. H. E. Jeffries, et al., Effects of Chemistry and Meteorology on Ozone Control Calculations Using Simple Trajectory Models and the EKMA Procedure, EPA-450/4-81-034, U.S. Environmental Protection Agency, Research Triangle Park, North Carolina, November 1981 (in press).

10. M. W. Chan, D. W. Allard and I. Tombach, Ozone and Precursor Transport Into an Urban Area - Evaluation of Approaches, EPA-450/4-79-039, U.S. Environmental Protection Agency, Research Triangle Park, North Carolina, December 1979.

11. Procedures for Quantifying Relationships Between Photochemical Oxidants and Precursors: Supporting Documentation, EPA-450/2-77-021b, U.S. Environmental Protection Agency, Research Triangle Park, North Carolina, February 1978.

12. F. L. Ludwig, Assessment of Vertical Distributions of Photochemical Pollutants and Meteorological Variables in the Vicinity of Urban Areas, EPA-450/4-79-017, U.S. Environmental Protection Agency, Research Triangle Park, North Carolina, August 1979.

13. R. Haws and R. Paddock, The Regional Air Pollution Study (RAPS) Grid System, EPA-450/3-76-021, U.S. Environmental Protection Agency, Research Triangle Park, North Carolina, December 1975.

14. K. L. Schere, "Evaluation of the Urban Airshed Model Using Data of the Regional Air Pollution Study," presented at Symposium on RAPS Results, St. Louis, Missouri, October 1980.

15. K. L. Schere and K. L. Demerjian, "A Photochemical Box Model for Urban Air Quality Simulation," Proceedings, 4th Joint Conference on Sensing of Environmental Pollutants, American Chemical Society, November 1977.

16. S. D. Reynolds and L. E. Reid, An Introduction to the SAI Airshed Model and Its Usage, SAI Publication EF 78-53R, Systems Applications, Incorporated, 101 Lucas Valley Road, San Rafael, California, May 1978.

17. Code of Federal Regulations, "National Primary and Secondary Ambient Air Quality Standards," Title 40, Part 50.9.

APPENDIX A

The following figures and tables summarize the Level II inputs for each test case that was modeled. Three items are included for each day:

(1) a data sheet summarizing the model inputs;

(2) a map showing the derived air parcel trajectory;

(3) a figure showing the day-specific mixing height profile and the associated dilution rate.

MODLL INPUT DATA

DATE: 10/1/76 JULIAN DAY: 275 SITE: 102

Simulation Start Time: 0800 LDT

Simulation End Time: 1800 LDT

Initial Concentrations:

NMHC 0.73 ppmC; NO_x .127 ppm; O_3 .005 ppm; NO_2/NO_x .36

O_3 Aloft: 0.06 ppm

Post 8 a.m. Emissions:

Hour	NMOC Emission Density, kg-moles/km^2 hr	NMOC Emission Fraction	NO_x Emission Density, kg-moles/km^2 hr	NO_x Emission Fraction
1	1.954	0.653	.295	0.567
2	4.727	1.579	.764	1.467
3	1.715	0.573	.265	0.509
4	1.781	0.595	.277	0.532
5	1.816	0.607	.287	0.551
6	1.793	0.599	.280	0.538
7	1.865	0.623	.298	0.572
8	2.029	0.678	.335	0.643

10/1/76
Day 275

Peak Ozone = .24 ppm
Time of Peak = 1500-1600 LDT

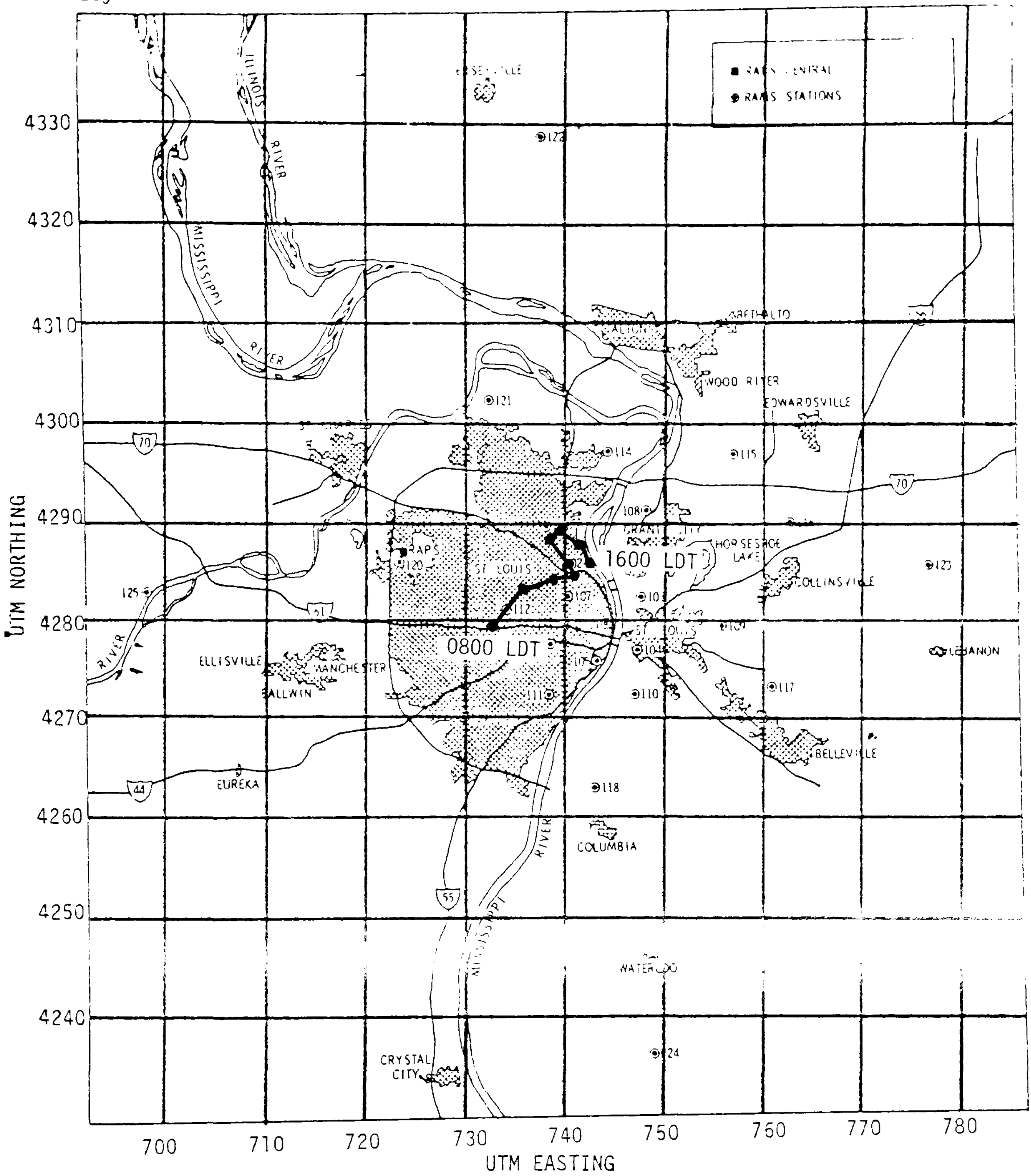

October 1, 1976
Day 275

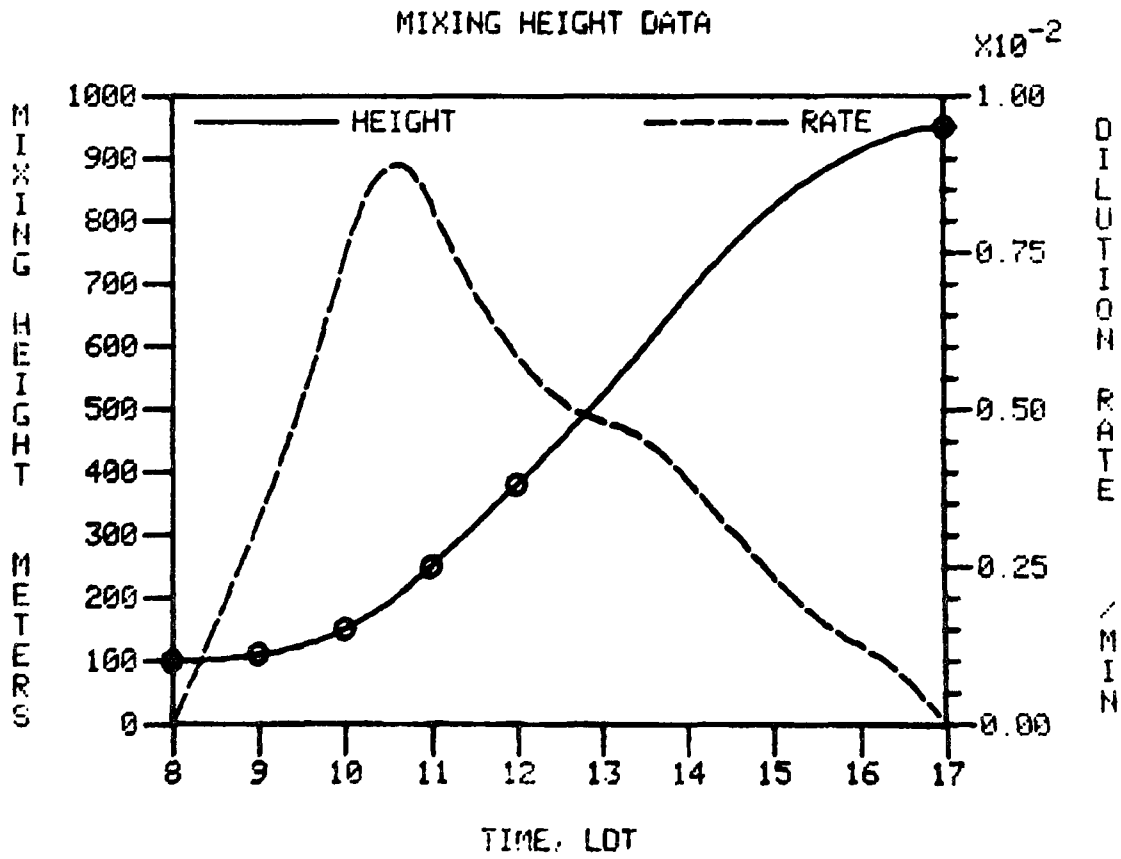

MODEL INPUT DATA

DATE: 7/13/76 JULIAN DAY: 195 SITE: 114

Simulation Start Time: 0800 LDT

Simulation End Time: 1800 LDT

Initial Concentrations:

NMHC 0.10 ppmC; NO_x 0.005 ppm; O_3 0.035 ppm; NO_2/NO_x 0.52

O_3 Aloft: 0.08 ppm

Post 8 a.m. Emissions:

Hour	NMOC Emission Density, kg-moles/km^2 hr	NMOC Emission Fraction	NO_x Emission Density, kg-moles/km^2 hr	NO_x Emission Fraction
1	0.098	0.085	0.017	0.296
2	0.091	0.079	0.015	0.261
3	0.091	0.079	0.014	0.244
4	0.615	0.536	0.046	0.801
5	1.322	1.152	0.424	7.387
6	3.101	2.701	0.648	11.289
7	1.943	1.693	0.299	5.209
8	2.107	1.835	0.336	5.854
9	1.455	1.267	0.206	3.589

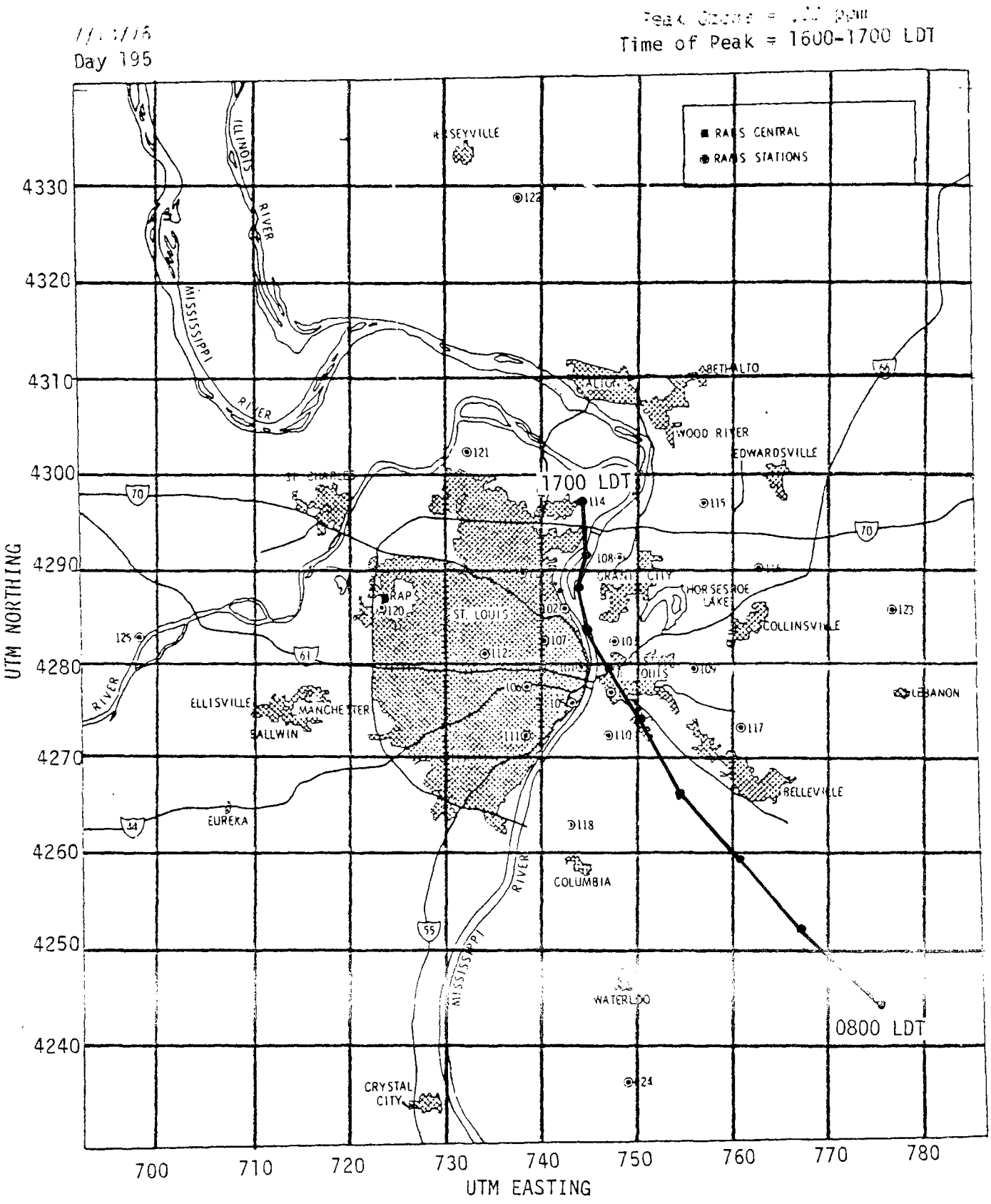
Peak Ozone = [illegible] ppm
Time of Peak = 1600-1700 LDT
Day 195
RAMS CENTRAL
RAMS STATIONS
1700 LDT
0800 LDT
ST. LOUIS
EAST ST. LOUIS
GRANITE CITY
EDWARDSVILLE
WOOD RIVER
BETHALTO
COLLINSVILLE
BELLEVILLE
LEBANON
HORSESHOE LAKE
ELLISVILLE
MANCHESTER
BALLWIN
EUREKA
COLUMBIA
WATERLOO
CRYSTAL CITY
ILLINOIS RIVER
MISSISSIPPI RIVER
UTM NORTHING
UTM EASTING
4330
4320
4310
4300
4290
4280
4270
4260
4250
4240
700
710
720
730
740
750
760
770
780

July 13, 1976
Day 195

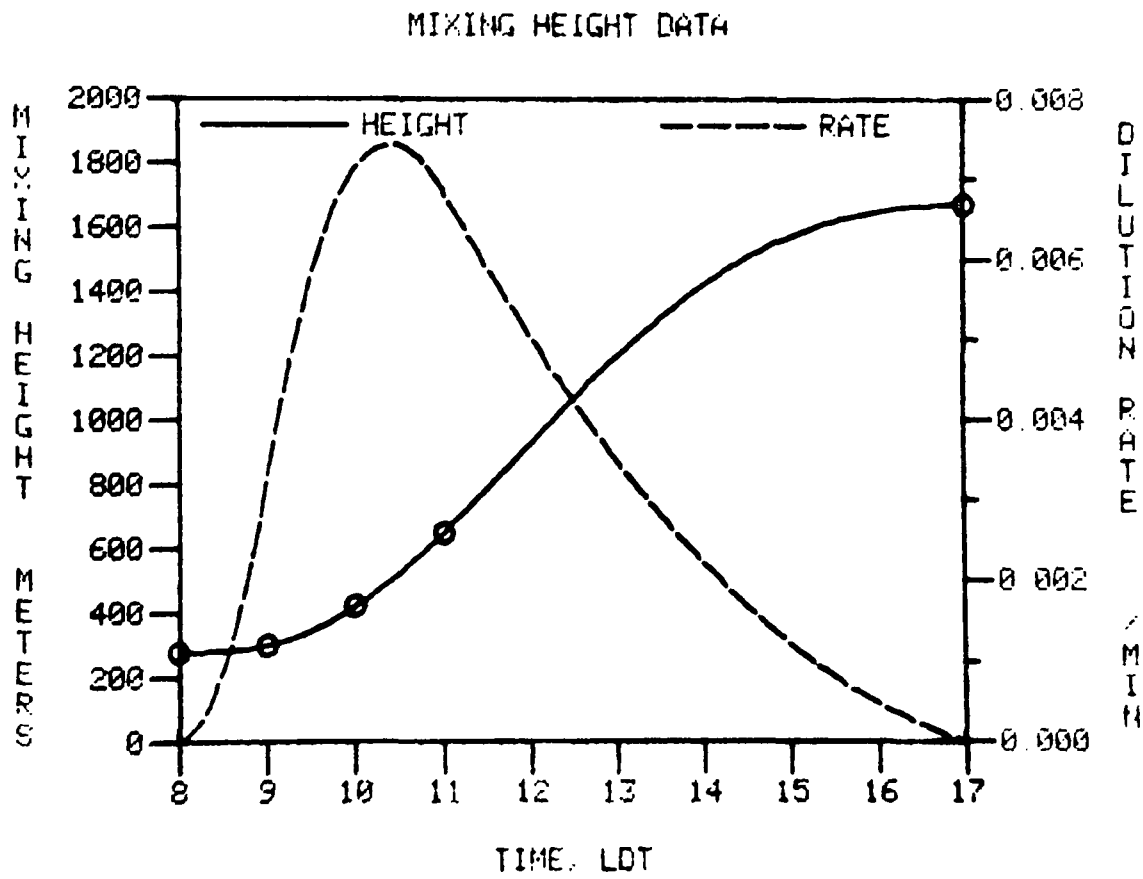

MODEL INPUT DATA

DATE: 6/8/76 JULIAN DAY: 160 SITE: 115

Simulation Start Time: 0800 LDT

Simulation End Time: 1800 LDT

Initial Concentrations:

NMHC 0.65 ppmC; NO_x 0.046 ppm; O_3 0.023 ppm; NO_2/NO_x 0.65

O_3 Aloft: 0.10 ppm

Post 8 a.m. Emissions:

Hour	NMOC Emission Density, kg-moles/km^2 hr	NMOC Emission Fraction	NO_x Emission Density, kg-moles/km^2 hr	NO_x Emission Fraction
1	0.431	0.108	0.114	0.403
2	2.633	0.659	0.229	0.809
3	2.363	0.591	0.241	0.852
4	1.895	0.474	0.290	1.025
5	3.464	0.867	0.554	1.958
6	1.908	0.477	0.293	1.036
7	1.559	0.390	0.261	0.923
8	0.746	0.186	0.170	0.601
9	0.762	0.191	0.174	0.615
10	0.874	0.219	0.097	0.343

5/2/16
Day 160

Peak Ozone ... ppm
Time of Peak = 1700-1800 LDT

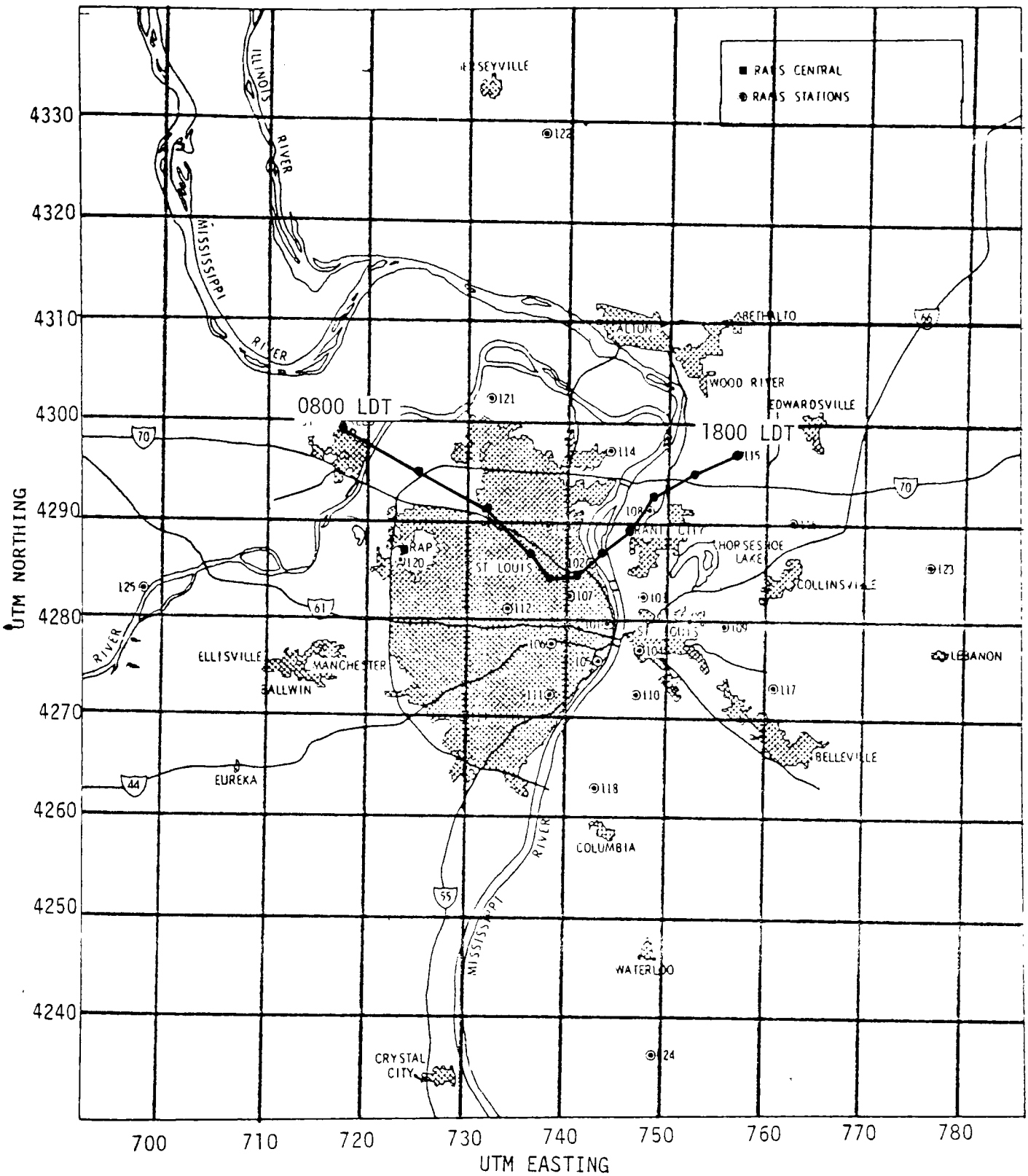

June 8, 1976
Day 160

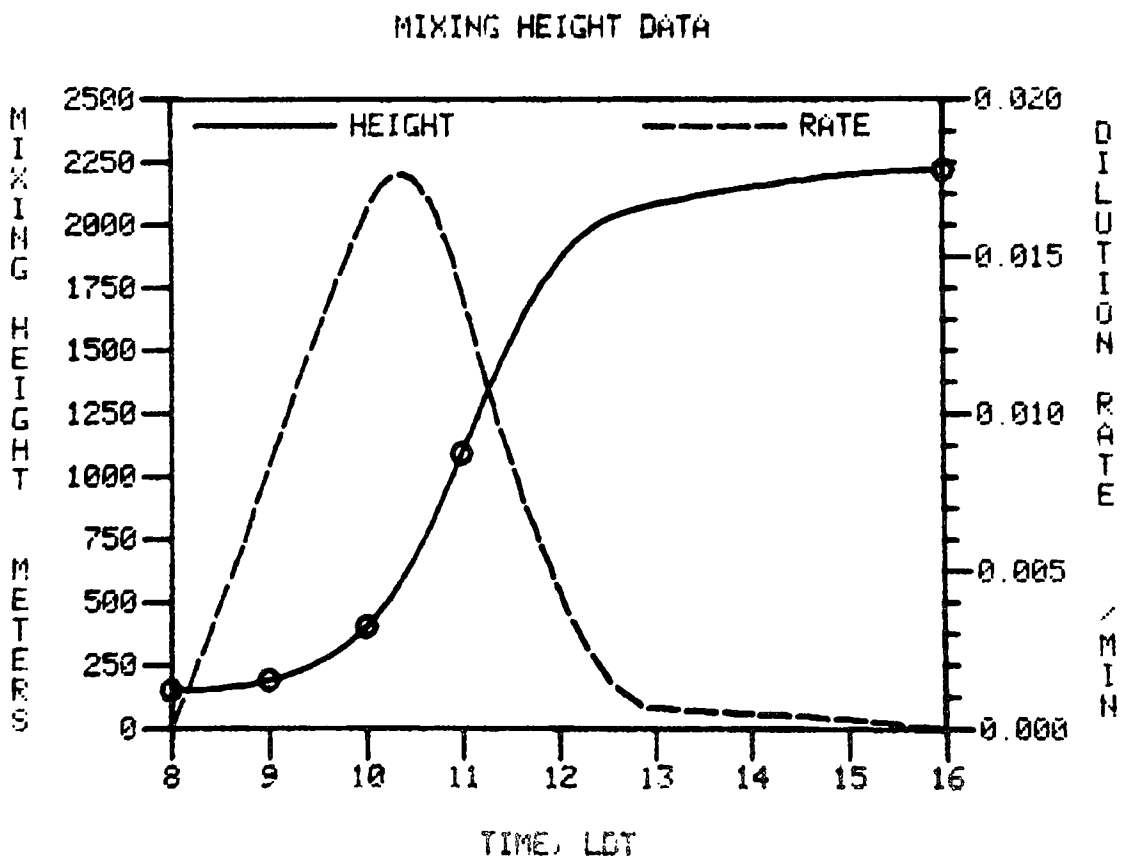

MODEL INPUT DATA

DATE: 6/7/76 JULIAN DAY: 159 SITE: 122

Simulation Start Time: 0800 LDT

Simulation End Time: 1800 LDT

Initial Concentrations:

NMHC 0.39 ppmC; NO_x 0.036 ppm; O_3 0.039 ppm; NO_2/NO_x 0.81

O_3 Aloft: 0.11 ppm

Post 8 a.m. Emissions:

Hour	NMOC Emission Density, kg-moles/km^2 hr	NMOC Emission Fraction	NO_x Emission Density, kg-moles/km^2 hr	NO_x Emission Fraction
1	0.174	0.064	0.019	0.076
2	0.160	0.059	0.016	0.064
3	0.207	0.076	0.019	0.076
4	0.261	0.096	0.023	0.092
5	0.216	0.079	0.021	0.084
6	0.424	0.156	0.177	
7	0.430	0.158	0.175	0.697
8	0.172	0.063	0.008	0.032
9	0.073	0.027	0.009	0.036

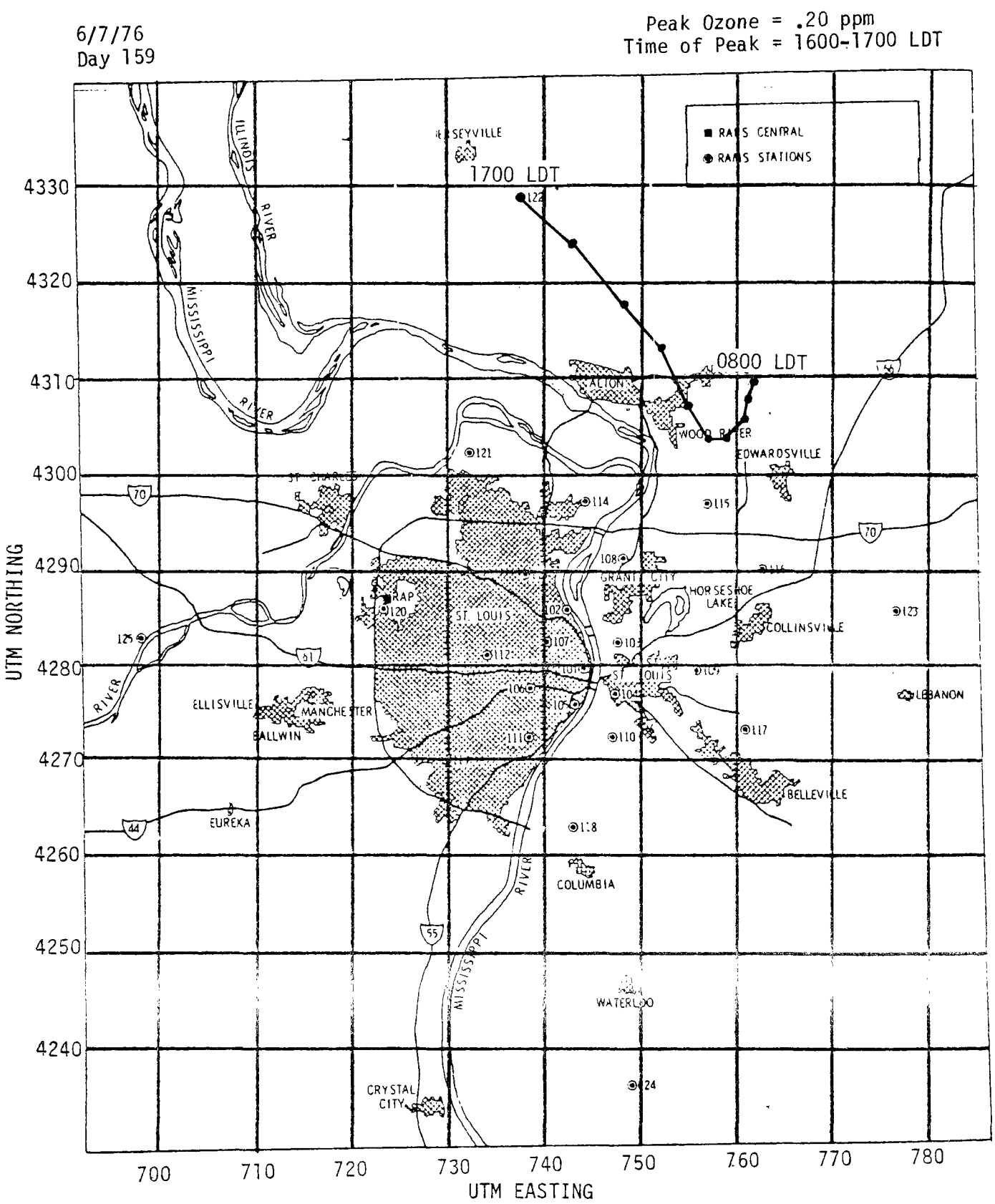
6/7/76
Day 159
Peak Ozone = .20 ppm
Time of Peak = 1600-1700 LDT
RAMS CENTRAL
RAMS STATIONS
1700 LDT
0800 LDT
ILLINOIS RIVER
MISSISSIPPI RIVER
ALTON
WOOD RIVER
EDWARDSVILLE
ST. CHARLES
ST. LOUIS
GRANT CITY
HORSESHOE LAKE
COLLINSVILLE
LEBANON
BELLEVILLE
ELLISVILLE
MANCHESTER
BALLWIN
EUREKA
COLUMBIA
WATERLOO
CRYSTAL CITY
UTM NORTHING
UTM EASTING
4330
4320
4310
4300
4290
4280
4270
4260
4250
4240
700
710
720
730
740
750
760
770
780

June 7, 1976
Day 159

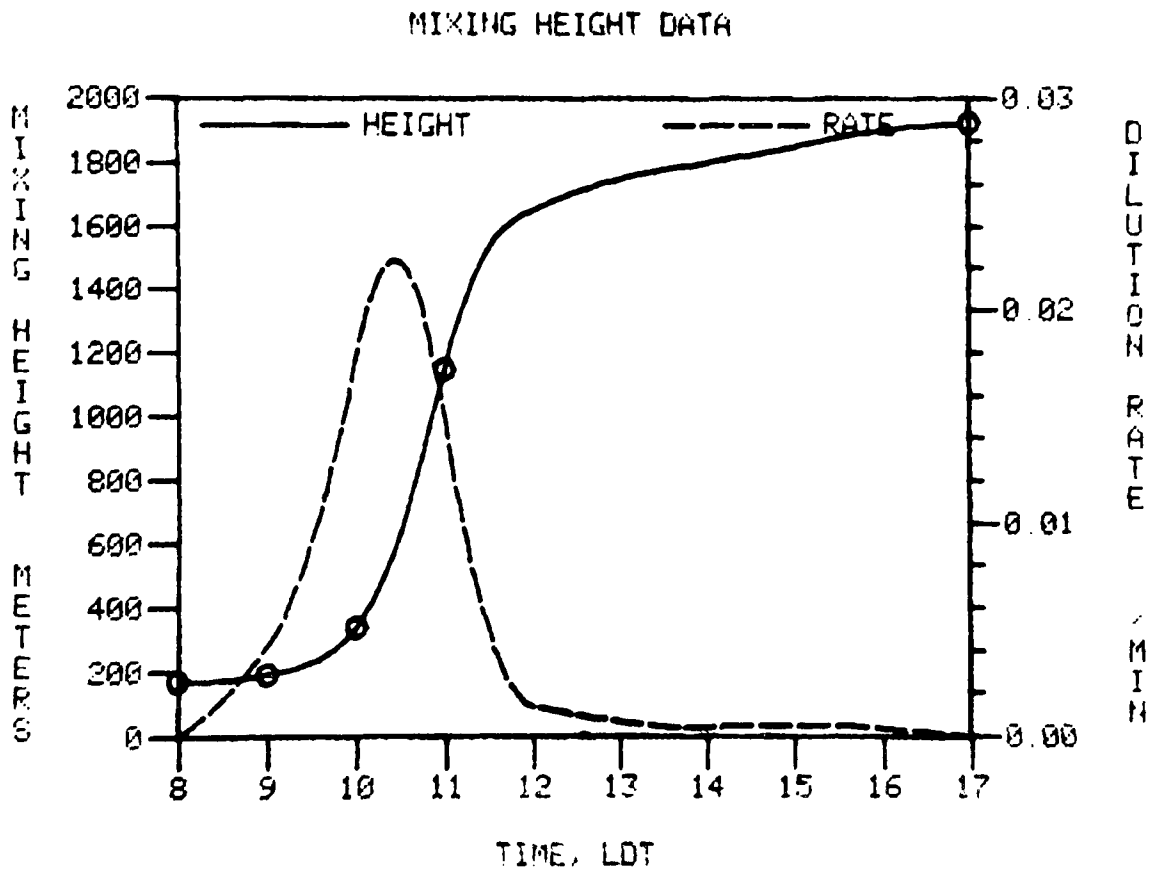

MODEL INPUT DATA

DATE: 6/8/76 JULIAN DAY: 160 SITE: 103

Simulation Start Time: 0800 LDT

Simulation End Time: 1800 LDT

Initial Concentrations:

NMHC 0.34 ppmC; NO_x 0.064 ppm; O_3 0.023 ppm; NO_2/NO_x 0.77

O_3 Aloft: 0.10 ppm

Post 8 a.m. Emissions:

Hour	NMOC Emission Density, kg-moles/km^2 hr	NMOC Emission Fraction	NO_x Emission Density, kg-moles/km^2 hr	NO_x Emission Fraction
1	1.193	0.571	0.235	0.597
2	1.757	0.840	0.234	0.595
3	2.741	1.311	0.415	1.054
4	1.710	0.818	0.259	0.658
5	4.995	2.389	0.809	2.055
6	4.951	2.368	0.797	2.025
7	1.367	0.654	0.337	0.856

6/8/76
Day 160

Peak Ozone = .19 ppm
Time of Peak = 1400-1500 LDT

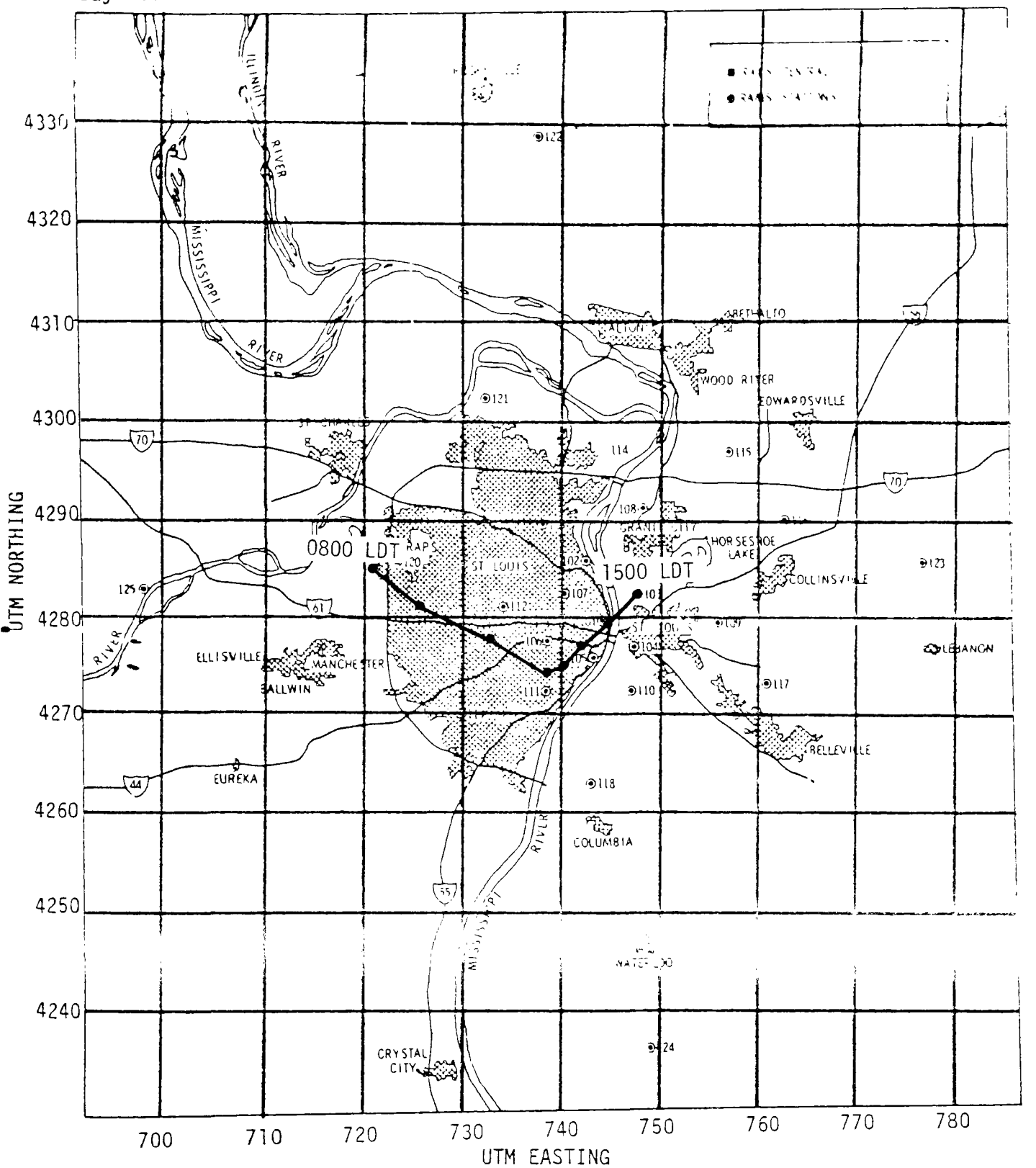

June 8, 1976
Day 160

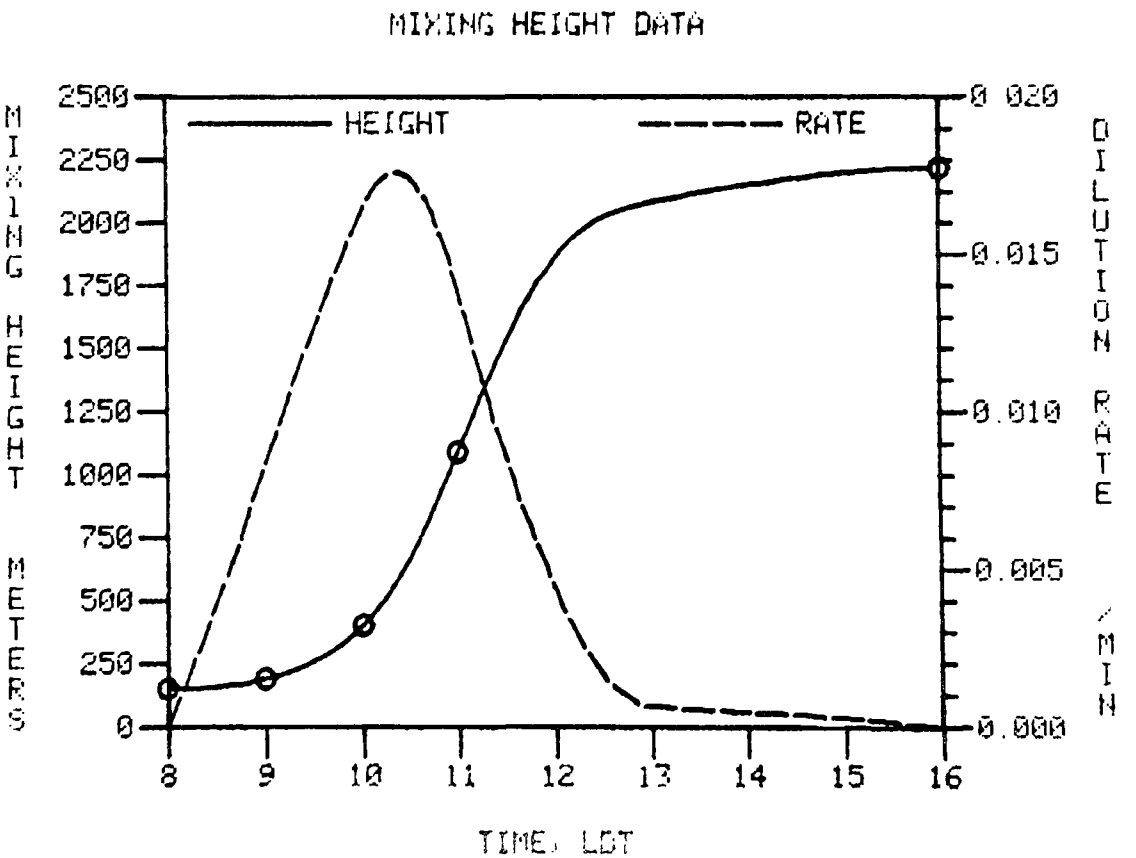

MODEL INPUT DATA

DATE: 8/25/76 JULIAN DAY: 238 SITE: 115

Simulation Start Time: 0800 LDT

Simulation End Time: 1800 LDT

Initial Concentrations:

NMHC 0.18 ppmC; NO_x 0.025 ppm; O_3 0.013 ppm; NO_2/NO_x 0.37

O_3 Aloft: 0.09 ppm

Post 8 a.m. Emissions:

Hour	NMOC Emission Density, kg-moles/km^2 hr	NMOC Emission Fraction	NO_x Emission Density, kg-moles/km^2 hr	NO_x Emission Fraction
1	0.058	0.074	0.012	0.117
2	0.055	0.075	0.011	0.107
3	0.055	0.075	0.011	0.107
4	0.366	0.496	0.047	0.459
5	0.279	0.378	0.043	0.420
6	0.275	0.373	0.042	0.410
7	0.265	0.359	0.024	0.234

8/25/76
Day 238

Peak Ozone = .19 ppm
Time of Peak = 1400-1500 LDT

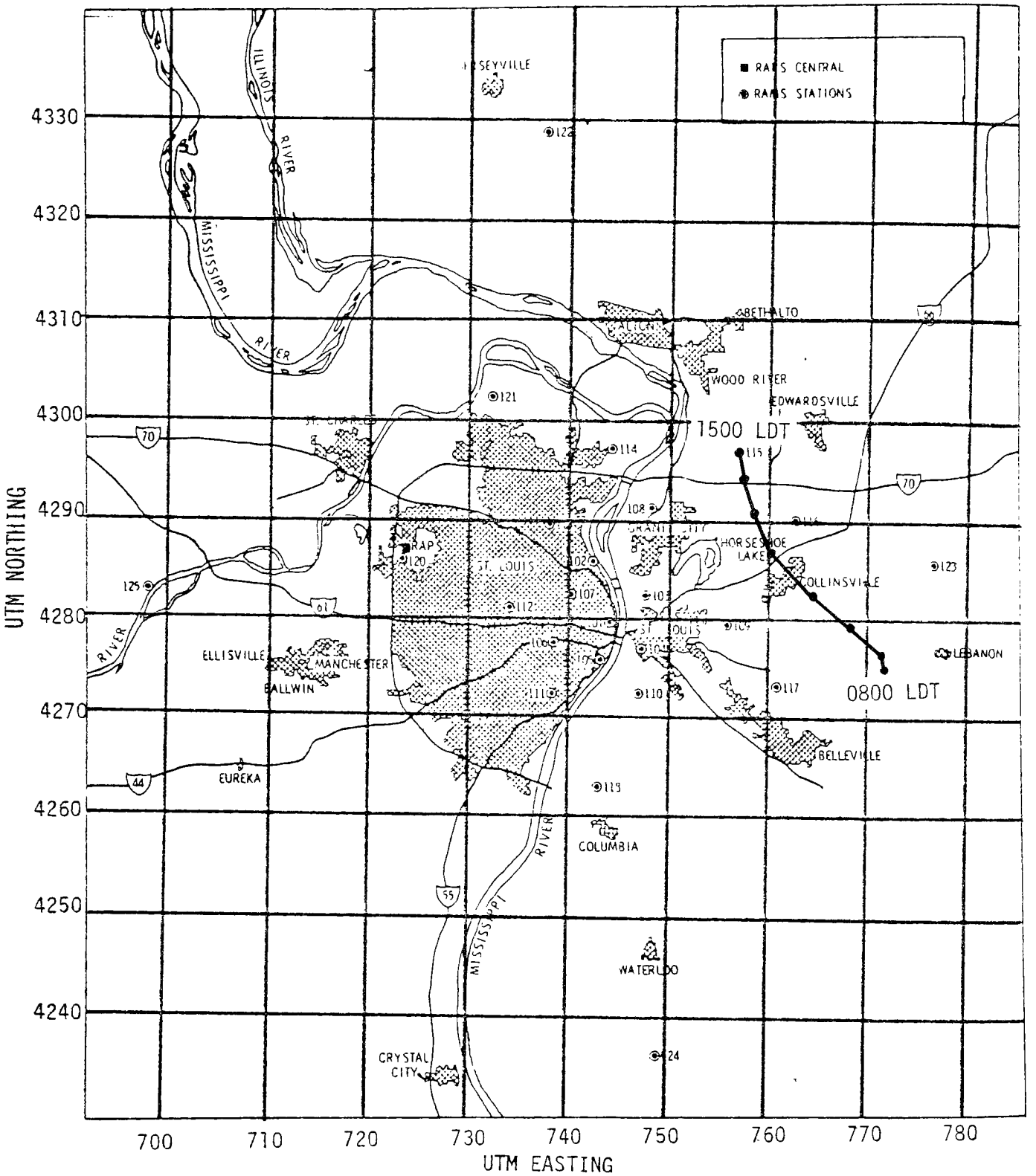

August 25, 1976
Day 238

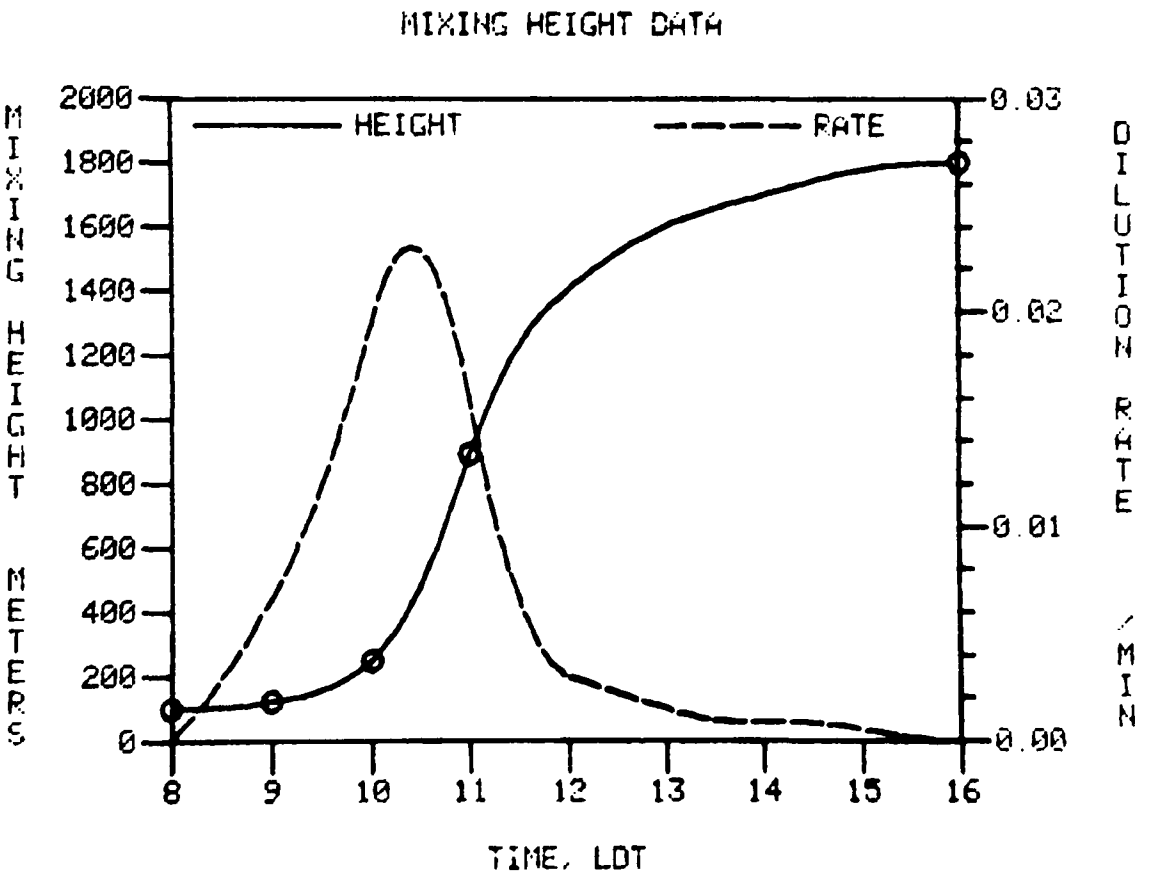

MODEL INPUT DATA

DATE: 10/02/76 JULIAN DAY: 275 SITE: 115

Simulation Start Time: 0800 LDT

Simulation End Time: 1800 LDT

Initial Concentrations:

NMHC 0.94 ppmC; NO_x 0.296 ppm; O_3 0.005 ppm; NO_2/NO_x 0.23

O_3 Aloft: 0.06 ppm

Post 8 a.m. Emissions:

Hour	NMOC Emission Density, kg-moles/km^2 hr	NMOC Emission Fraction	NO_x Emission Density, kg-moles/km^2 hr	NO_x Emission Fraction
1	0.378	0.098	0.170	0.154
2	0.412	0.107	0.132	0.120
3	0.431	0.112	0.135	0.122
4	0.445	0.115	0.138	0.125
5	0.716	0.186	0.081	0.073
6	0.166	0.043	0.021	0.019
7	0.167	0.043	0.021	0.019
8	0.168	0.044	0.021	0.019
9	0.165	0.043	0.021	0.019
10	0.165	0.043	0.020	0.018

10/2/76
Day 276

Peak Ozone = .19 ppm
Time of Peak = 1700-1800 LDT

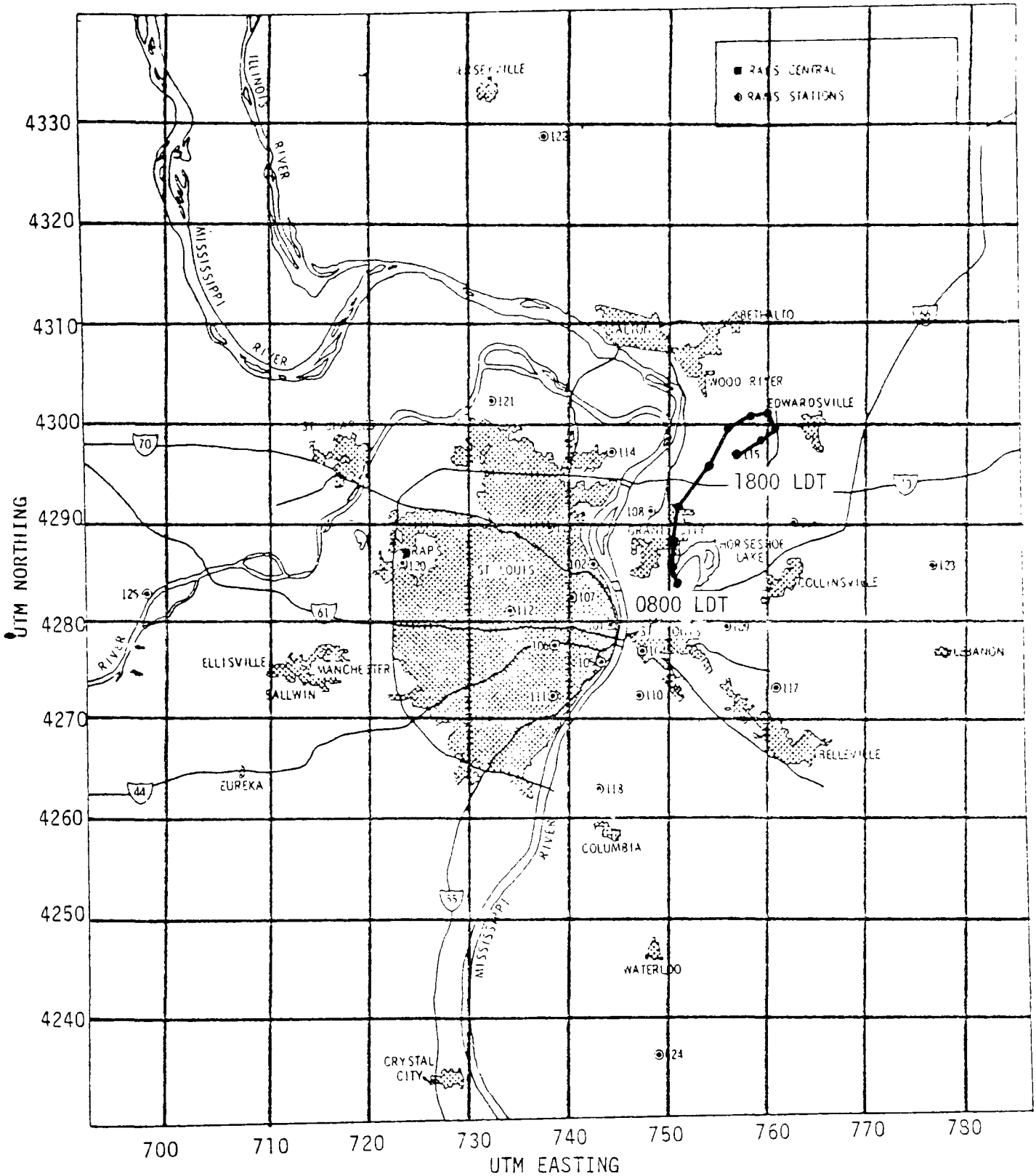

October 2, 1976
Day 276

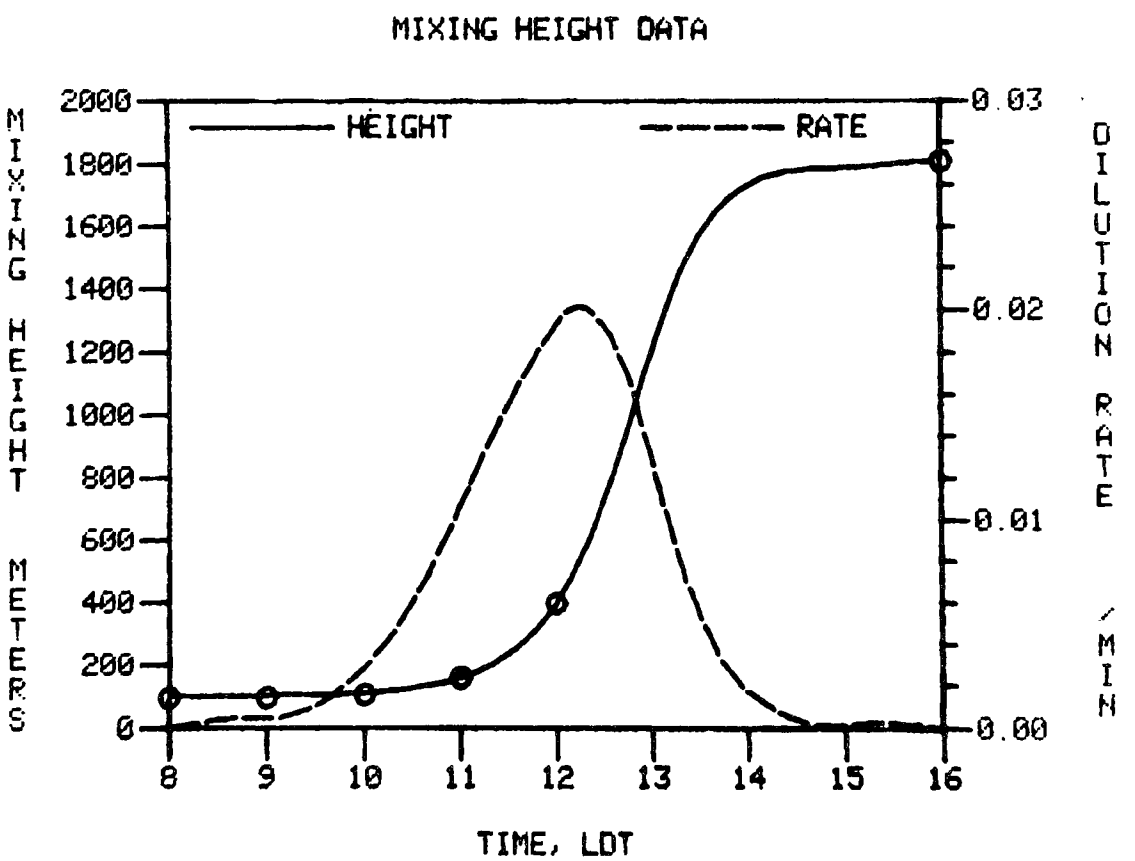

MODEL INPUT DATA

DATE: 9/17/76 JULIAN DAY: 261 SITE: 118

Simulation Start Time: 0800 LDT

Simulation End Time: 1800 LDT

Initial Concentrations:

NMHC 1.73 ppmC; NO_x 0.157 ppm; O_3 0.005 ppm; NO_2/NO_x 0.30

O_3 Aloft: 0.06 ppm

Post 8 a.m. Emissions:

Hour	NMOC Emission Density, kg-moles/km^2 hr	NMOC Emission Fraction	NO_x Emission Density, kg-moles/km^2 hr	NO_x Emission Fraction
1	5.074	0.650	0.867	1.224
2	4.741	0.608	0.763	1.078
3	4.717	0.605	0.743	1.049
4	4.824	0.618	0.756	1.068
5	1.695	0.217	0.258	0.364
6	1.203	0.154	0.184	0.260

9/17/76
Day 261

Peak Ozone = .15 ppm
Time of Peak = 1300-1400 LDT

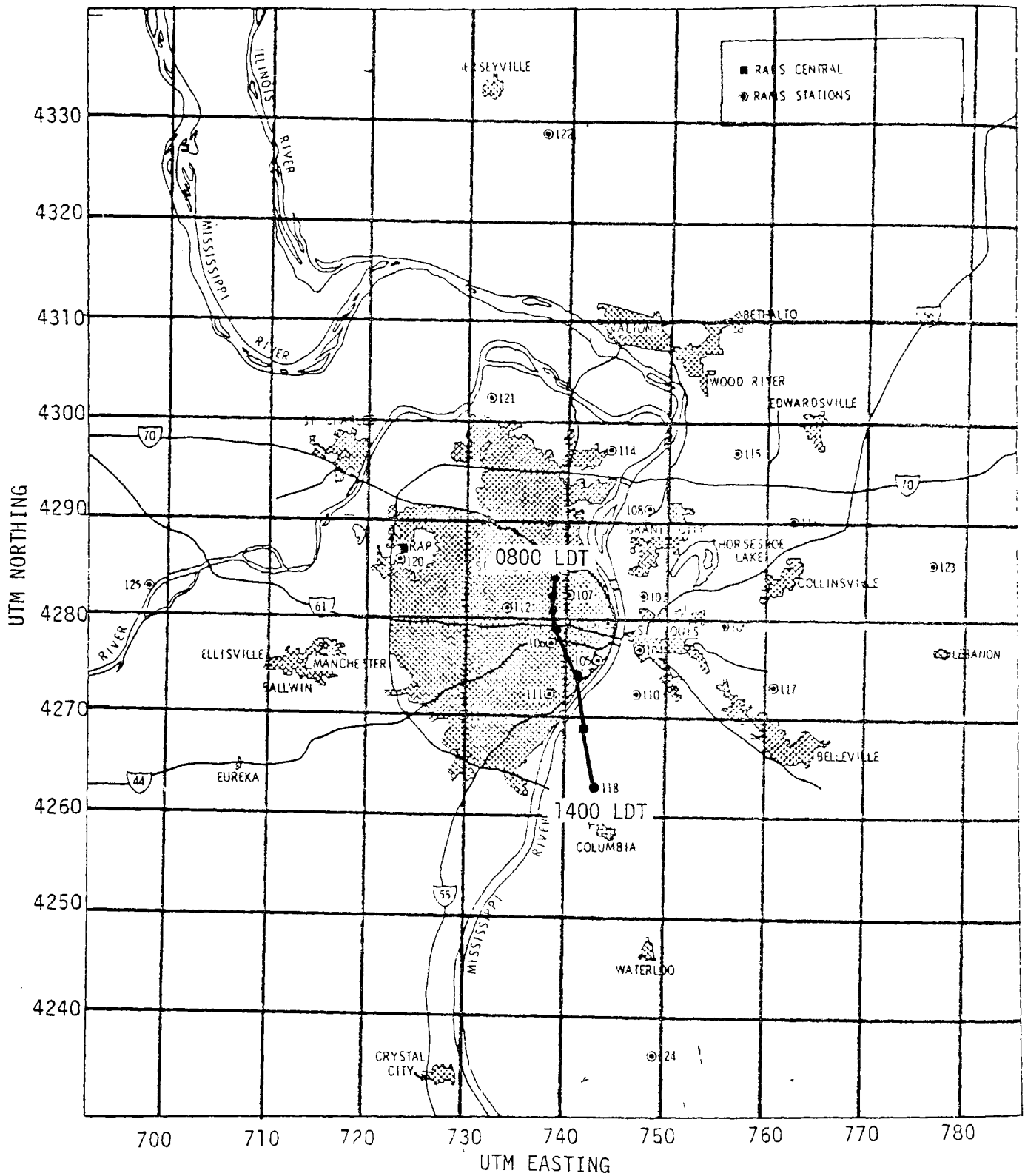

September 17, 1976
Day 261

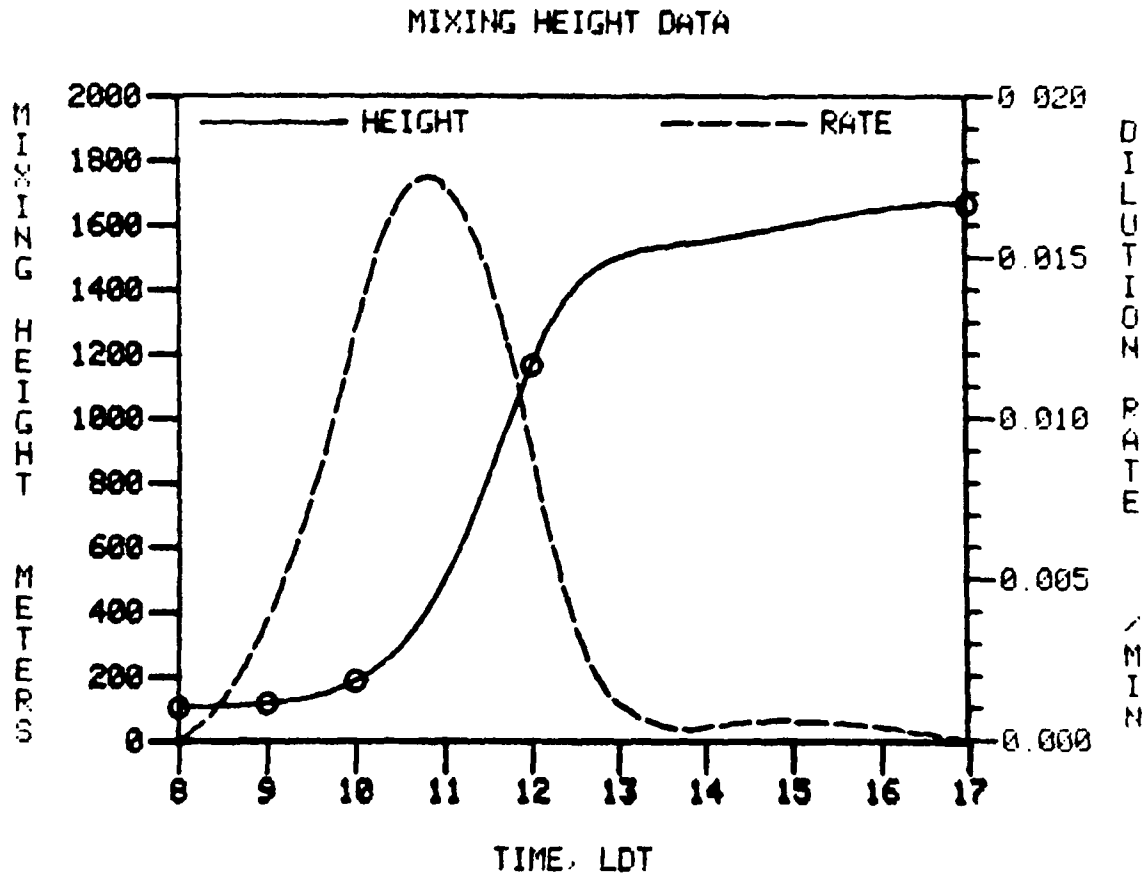

MODEL INPUT DATA

DATE: 7/19/76 JULIAN DAY: 201 SITE: 122

Simulation Start Time: 0800 LDT

Simulation End Time: 1800 LDT

Initial Concentrations:

NMHC 0.10 ppmC; NO_x 0.009 ppm; O_3 0.063 ppm; NO_2/NO_x 0.70

O_3 Aloft: 0.08 ppm

Post 8 a.m. Emissions:

Hour	NMOC Emission Density, kg-moles/km^2 hr	NMOC Emission Fraction	NO_x Emission Density, kg-moles/km^2 hr	NO_x Emission Fraction
1	0.114	0.278	0.027	0.732
2	1.660	4.049	0.248	6.721
3	3.773	9.202	0.578	15.664
4	1.054	2.571	0.122	3.306
5	0.343	0.837	0.031	0.840
6	0.039	0.095	0.009	0.244

7/19/76
Day 201

Peak Ozone = .15 ppm
Time of Peak = 1300-1400 LDT

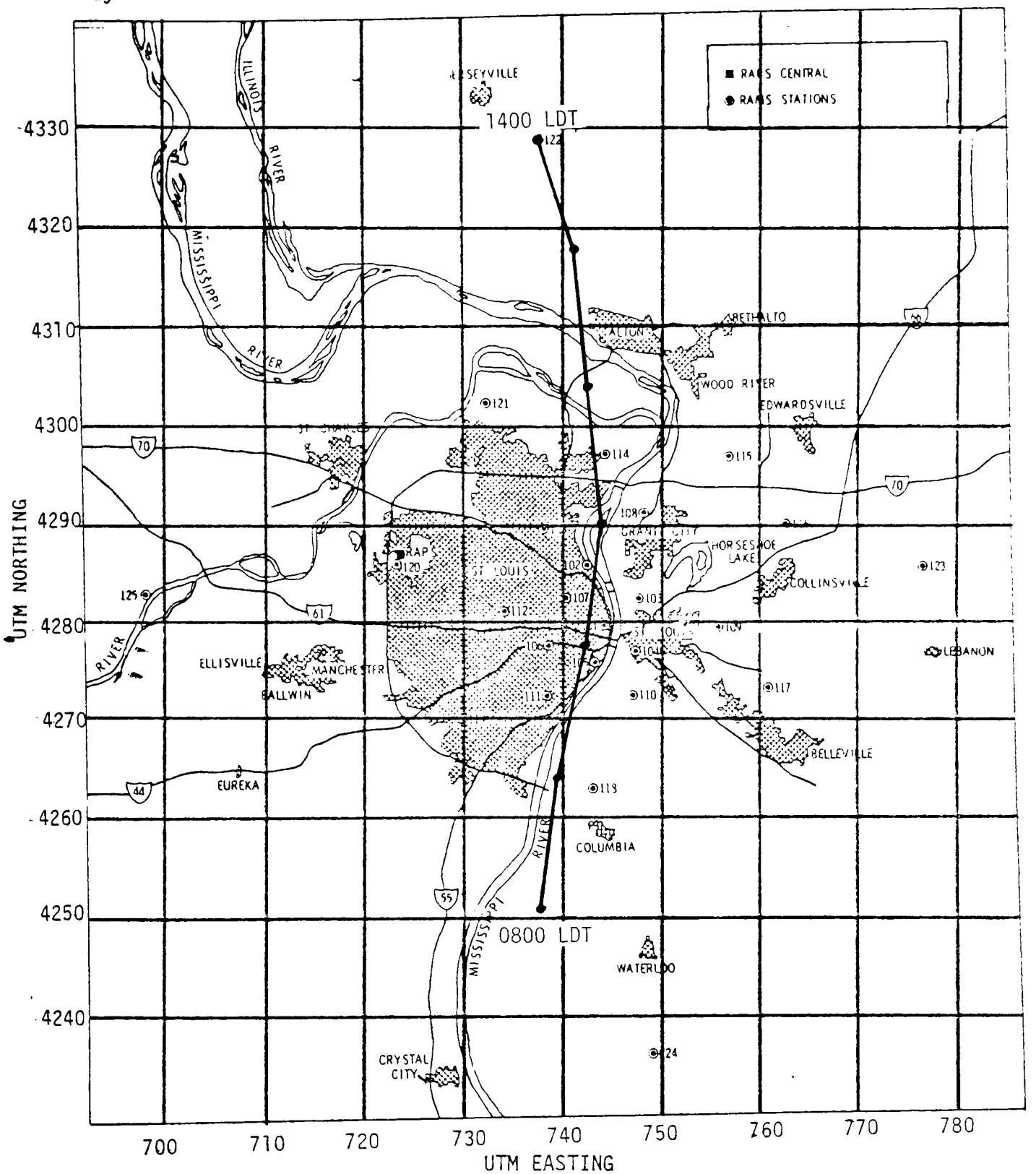

July 19, 1976
Day 201

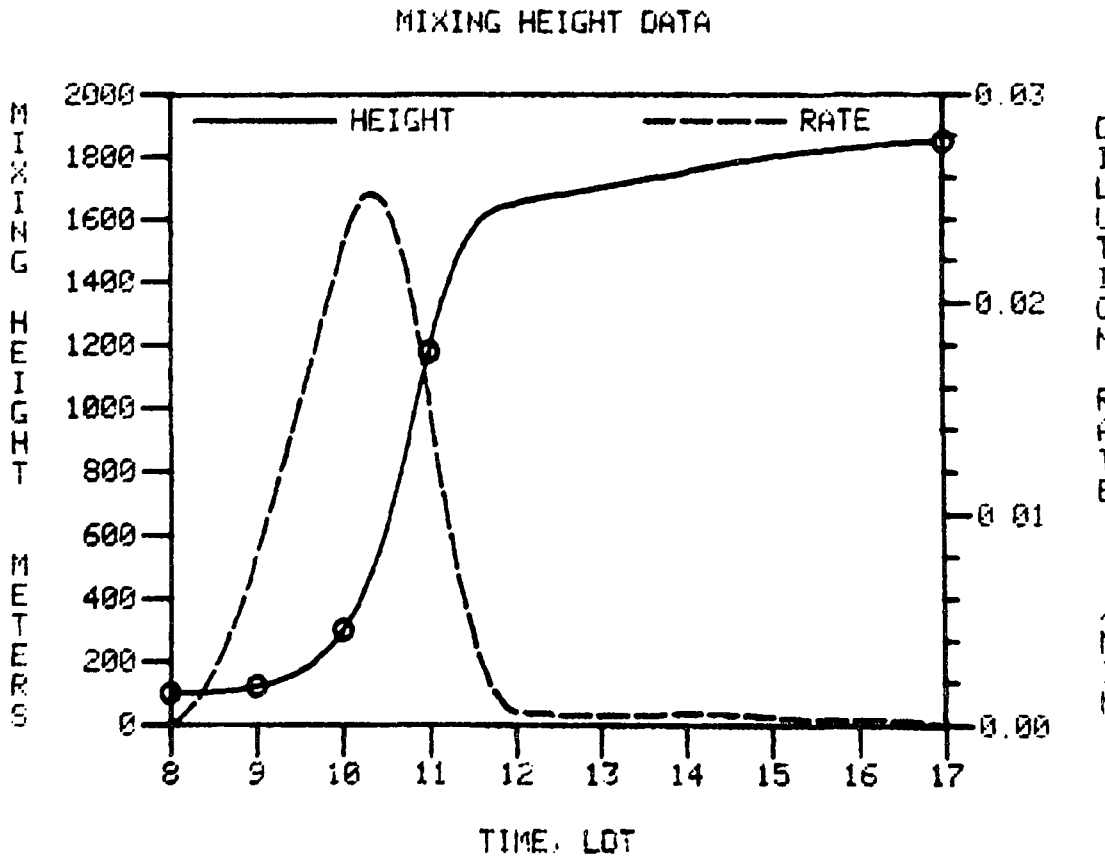

MODEL INPUT DATA

DATE: 8/8/76 JULIAN DAY: 221 SITE: 125

Simulation Start Time: 0800 LDT

Simulation End Time: 1800 LDT

Initial Concentrations:

NMHC 0.12 ppmC; NO_x 0.008 ppm; O_3 0.023 ppm; NO_2/NO_x 0.62

O_3 Aloft: 0.07 ppm

Post 8 a.m. Emissions:

Hour	NMOC Emission Density, kg-moles/km^2 hr	NMOC Emission Fraction	NO_x Emission Density, kg-moles/km^2 hr	NO_x Emission Fraction
1	0.188	0.382	0.069	2.104
2	0.438	0.890	0.132	4.024
3	1.434	2.915	0.504	15.366
4	0.708	1.439	0.177	5.396
5	0.798	1.622	0.201	6.128
6	0.383	0.778	0.170	5.183
7	0.401	0.815	0.176	5.366
8	0.383	0.778	0.170	5.183
9	0.172	0.350	0.132	4.024
10	0.169	0.343	0.131	3.994

8/8/76
Day 221

Peak Ozone = .12 ppm
Time of Peak = 1800-1900 LDT

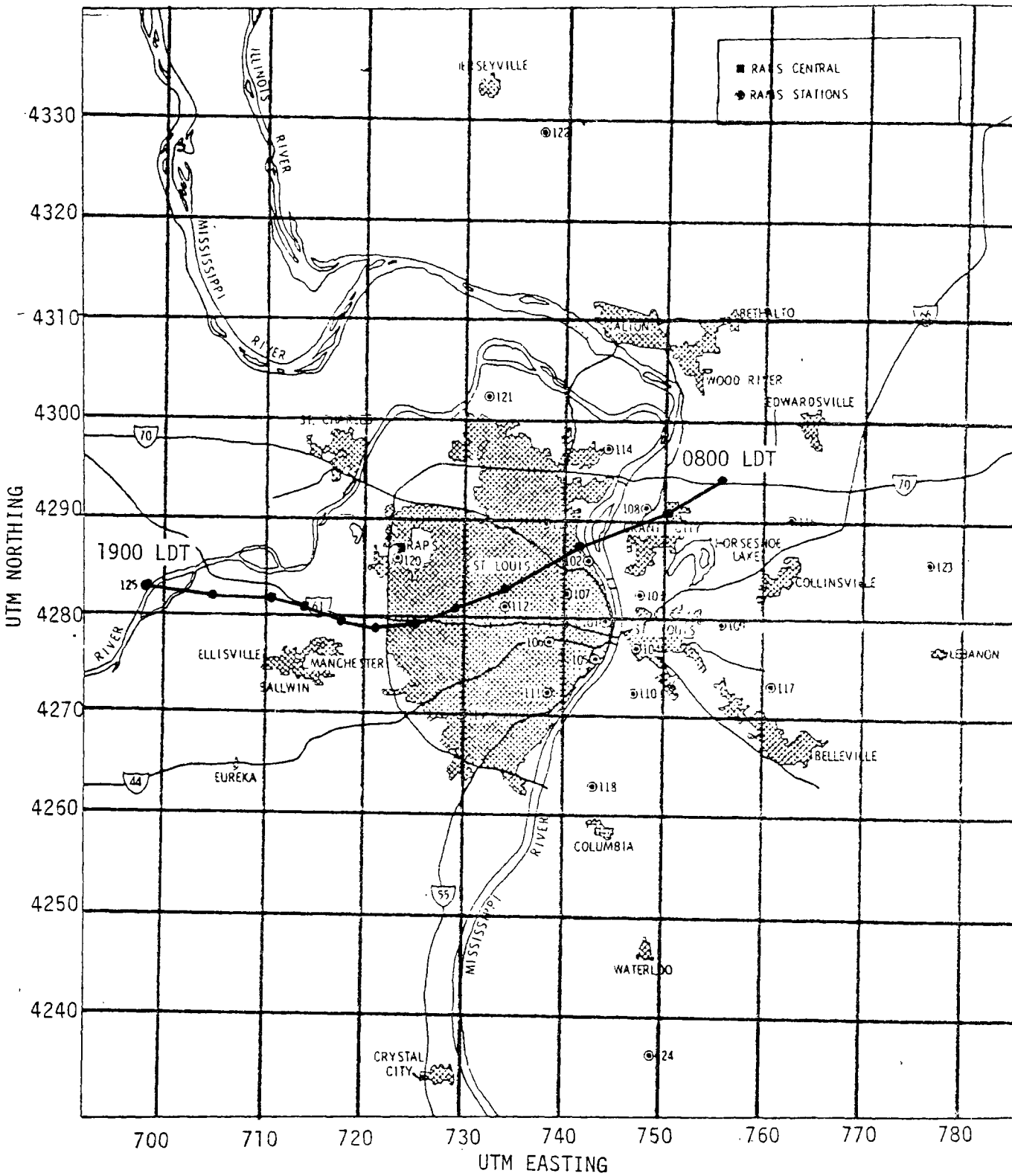

August 8, 1976
Day 221

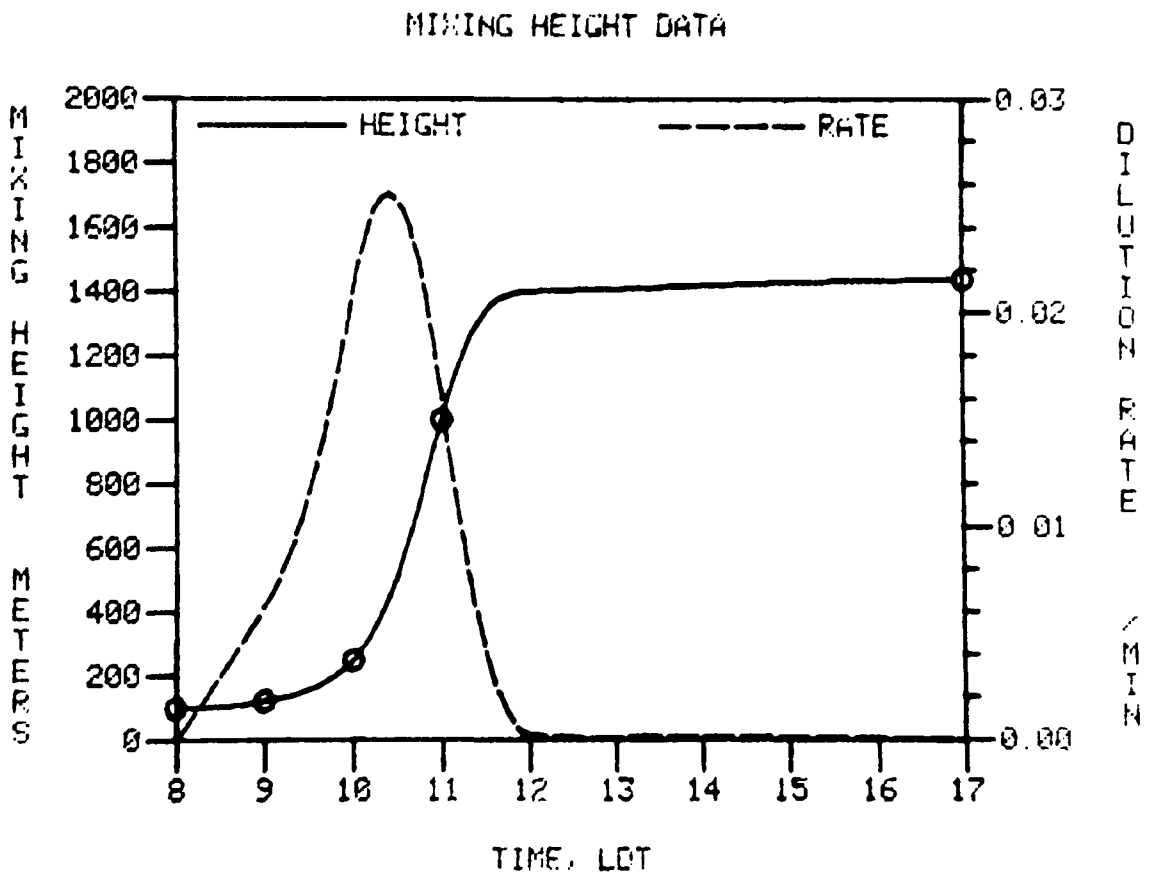

APPENDIX B

The following figures compare Level II predicted with observed temporal patterns of ozone, CO, NO_x, NMHC, NO, NO_2, NMOC/NO_x, and NO_2/NO_x. All pollutant concentrations are in points of ppm (ppmC for NMOC), and the time is Local Daylight Time starting at 8 a.m.

October 1, 1976
Day 275

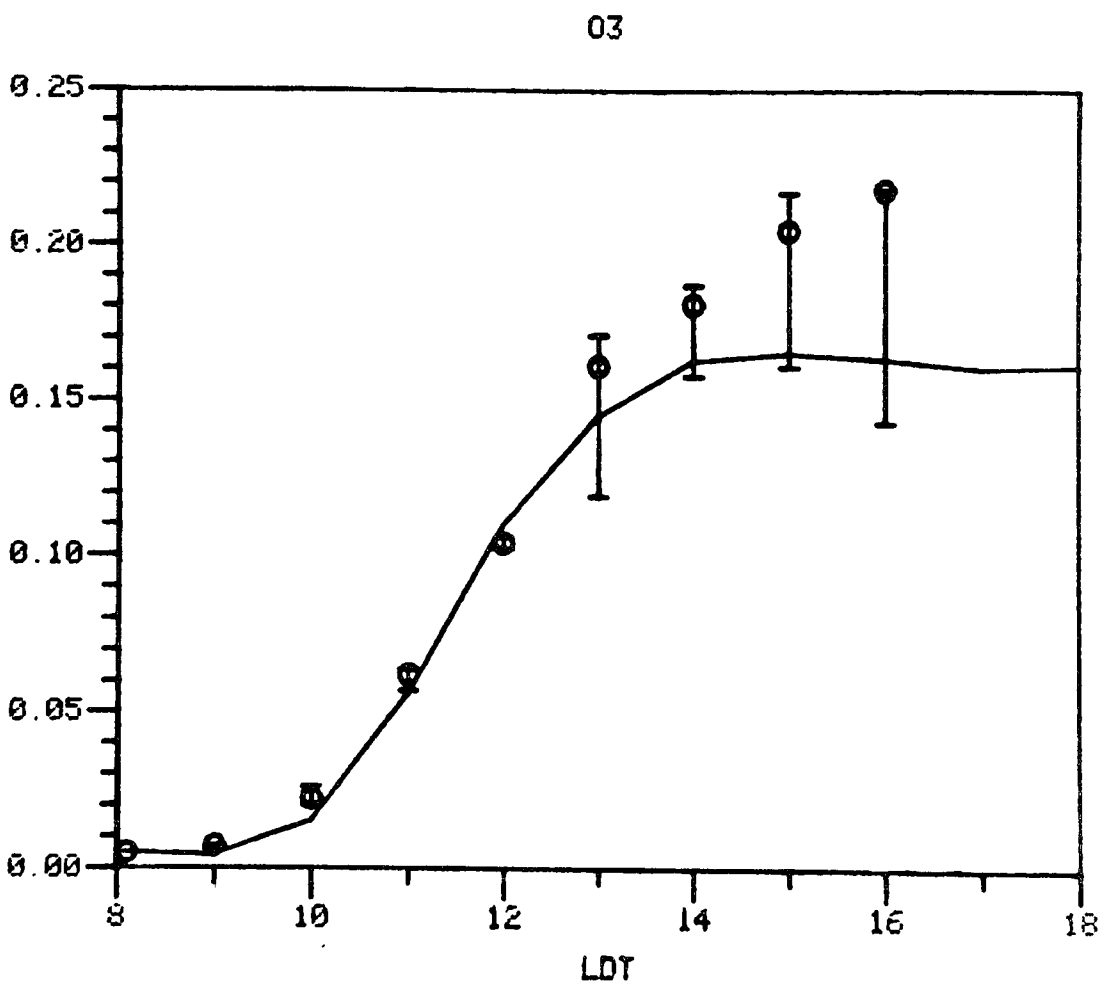

October 1, 1976
Day 275

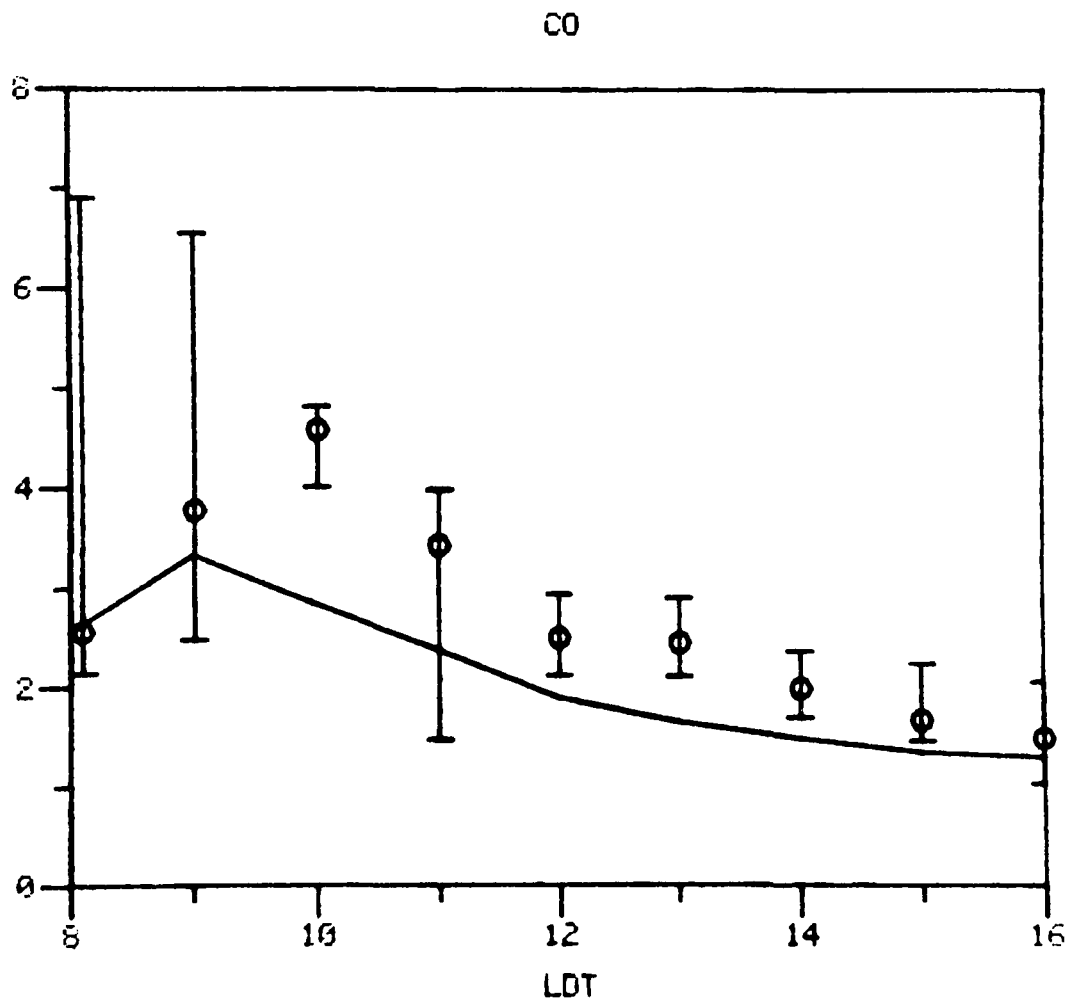

October 1, 1976
Day 275

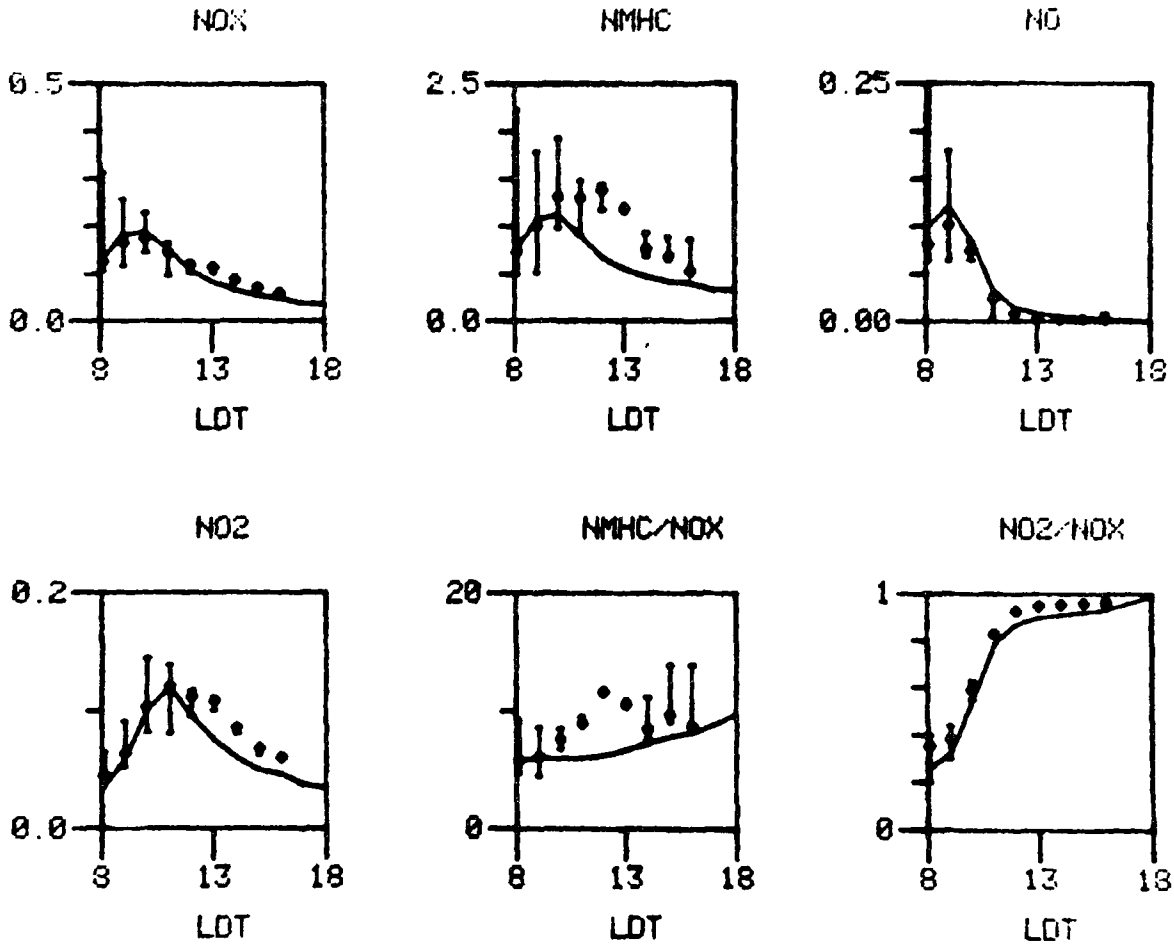

July 13, 1976
Day 195

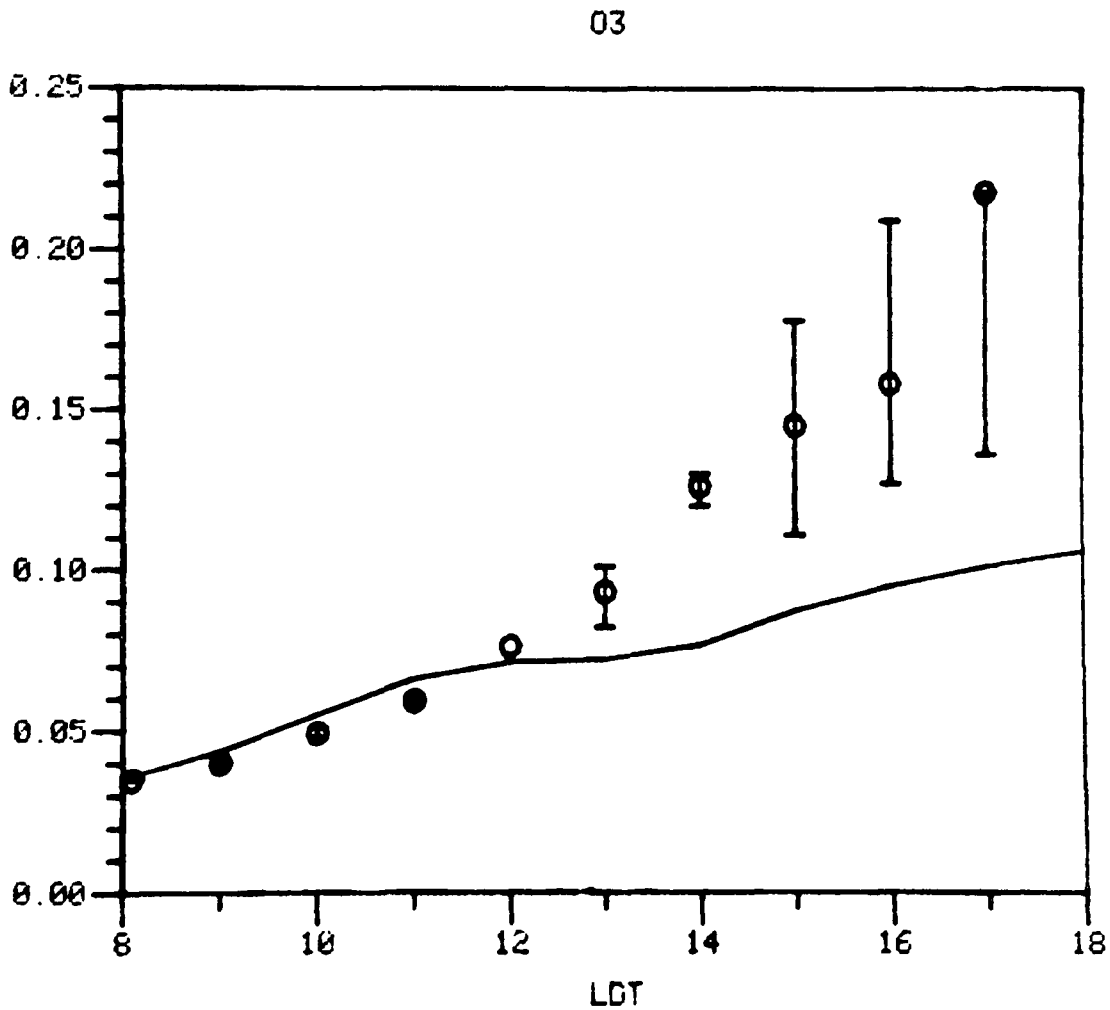

July 13, 1976
Day 195

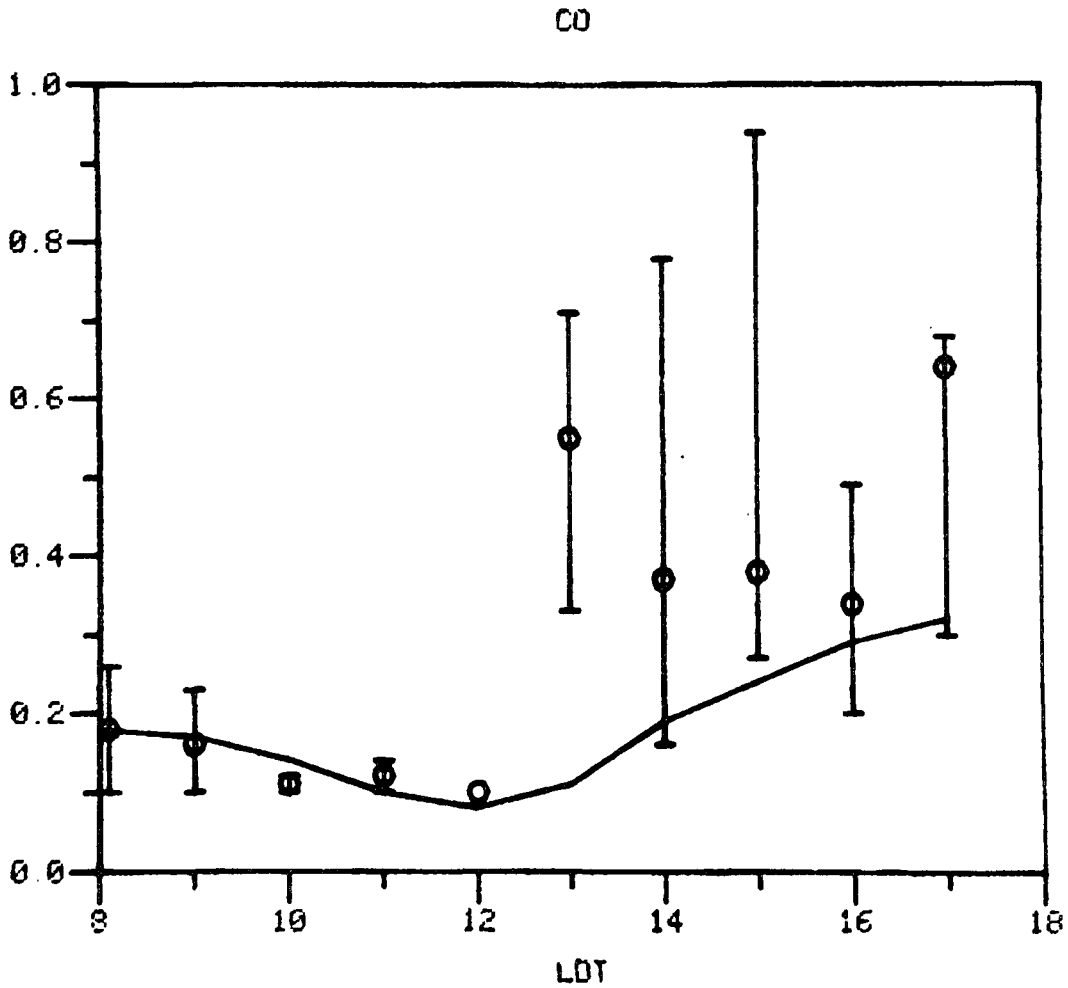

July 13, 1976
Day 195

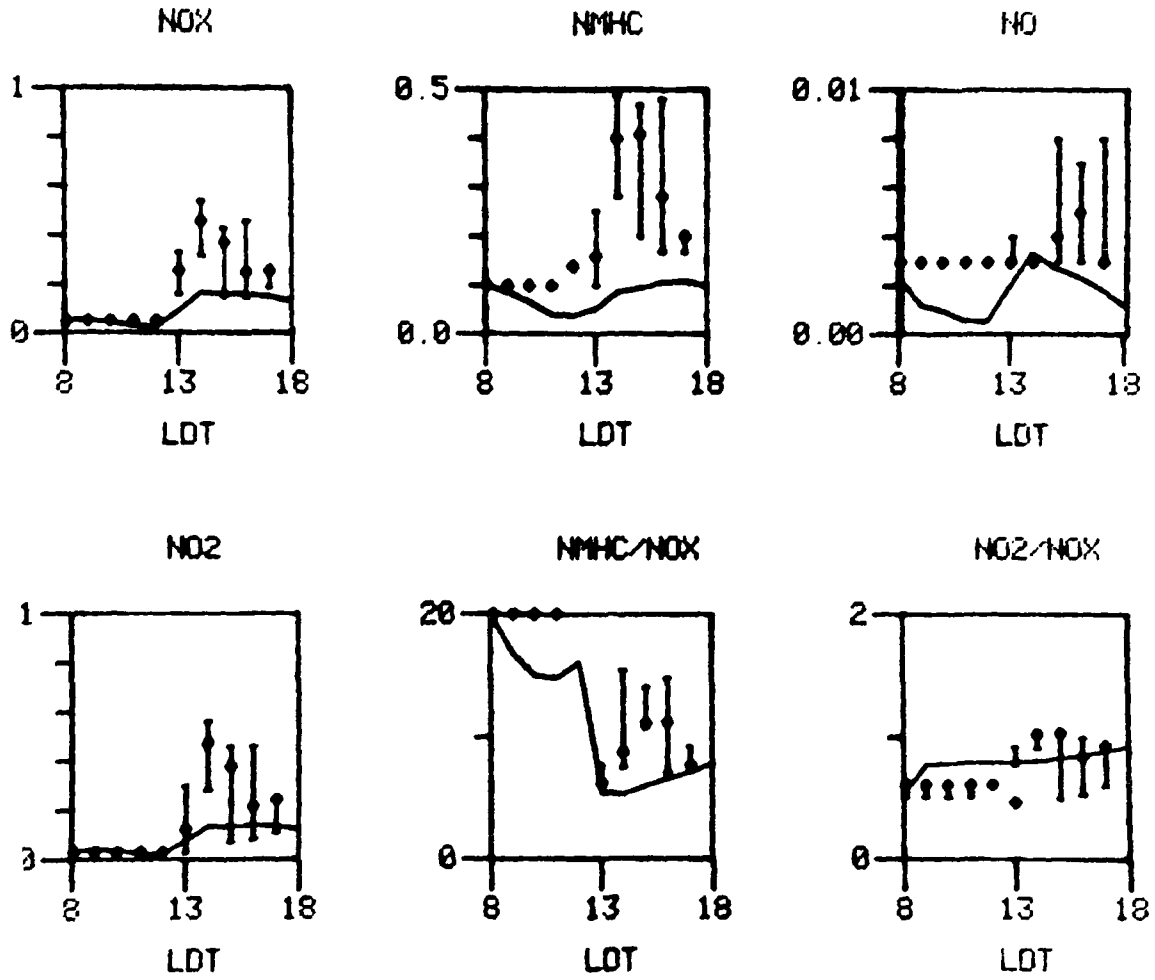

June 8, 1976
Day 160

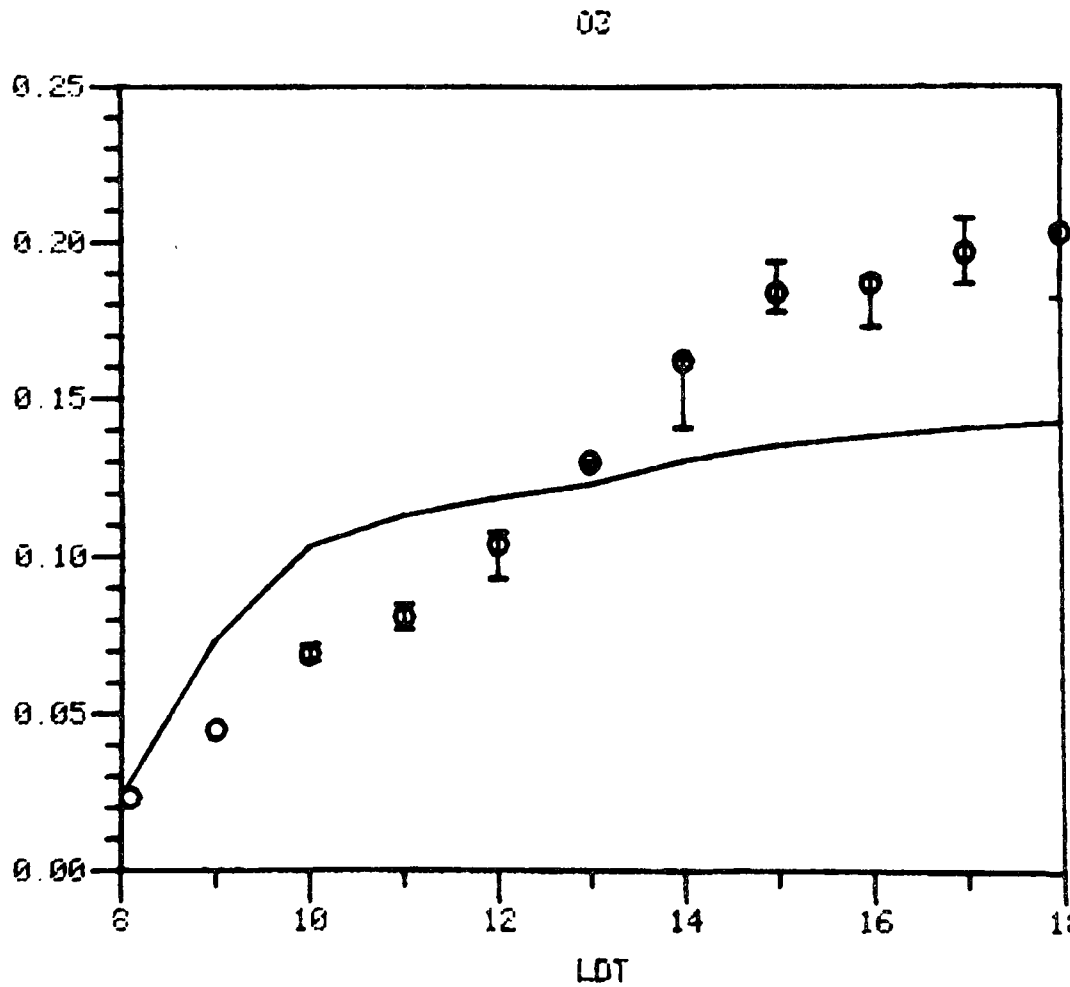

June 8, 1976
Day 160

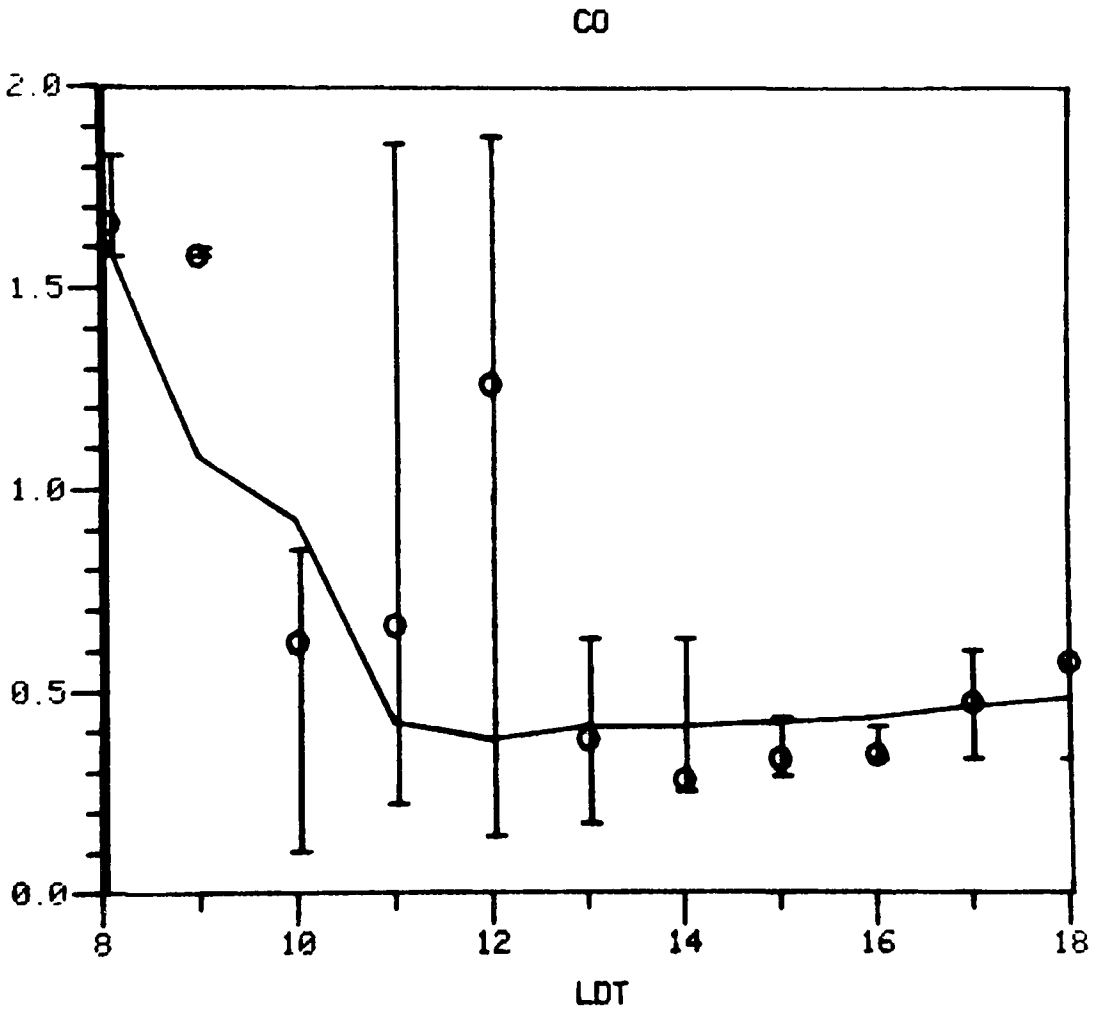

June 8, 1976
Day 160

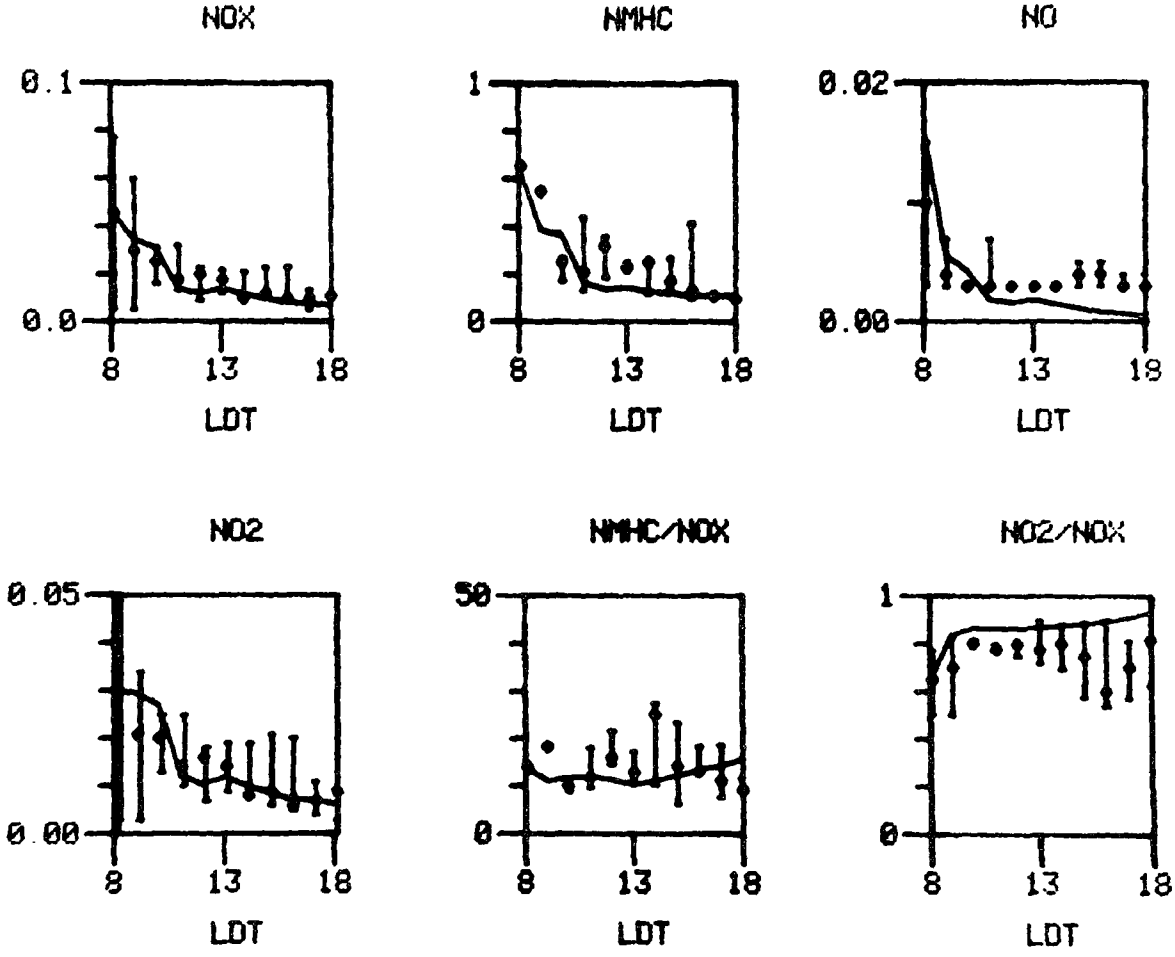

June 7, 1976
Day 159

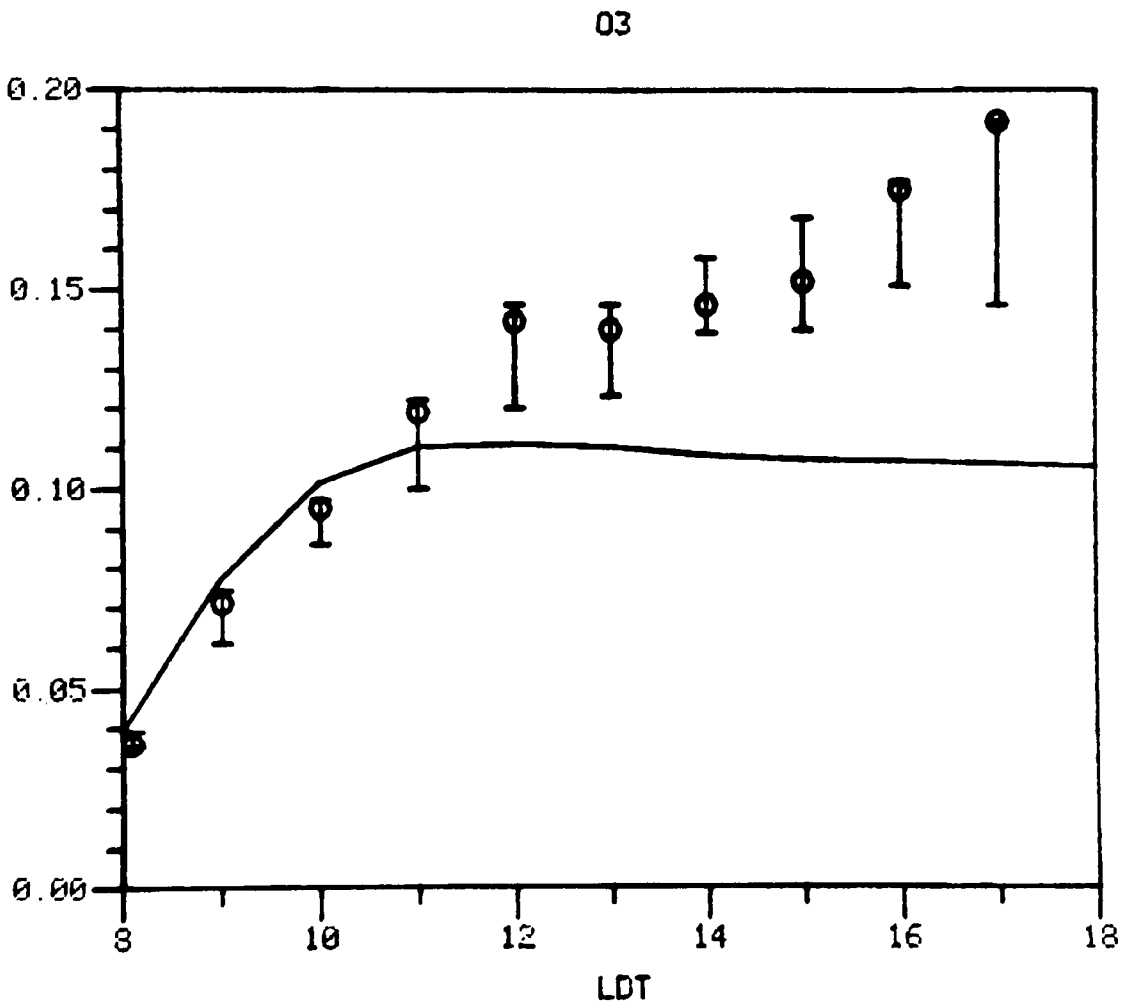

June 7, 1976
Day 159

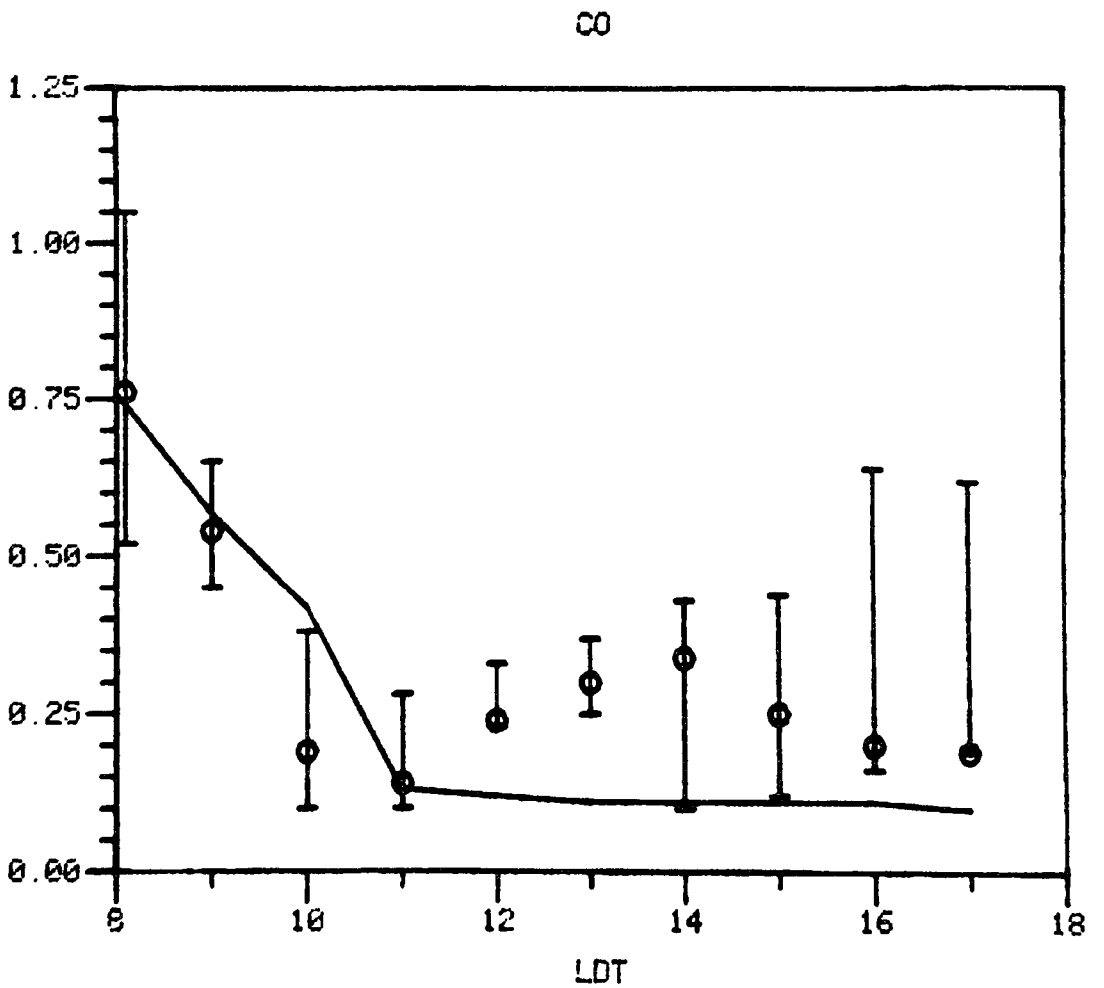

June 7, 1976
Day 159

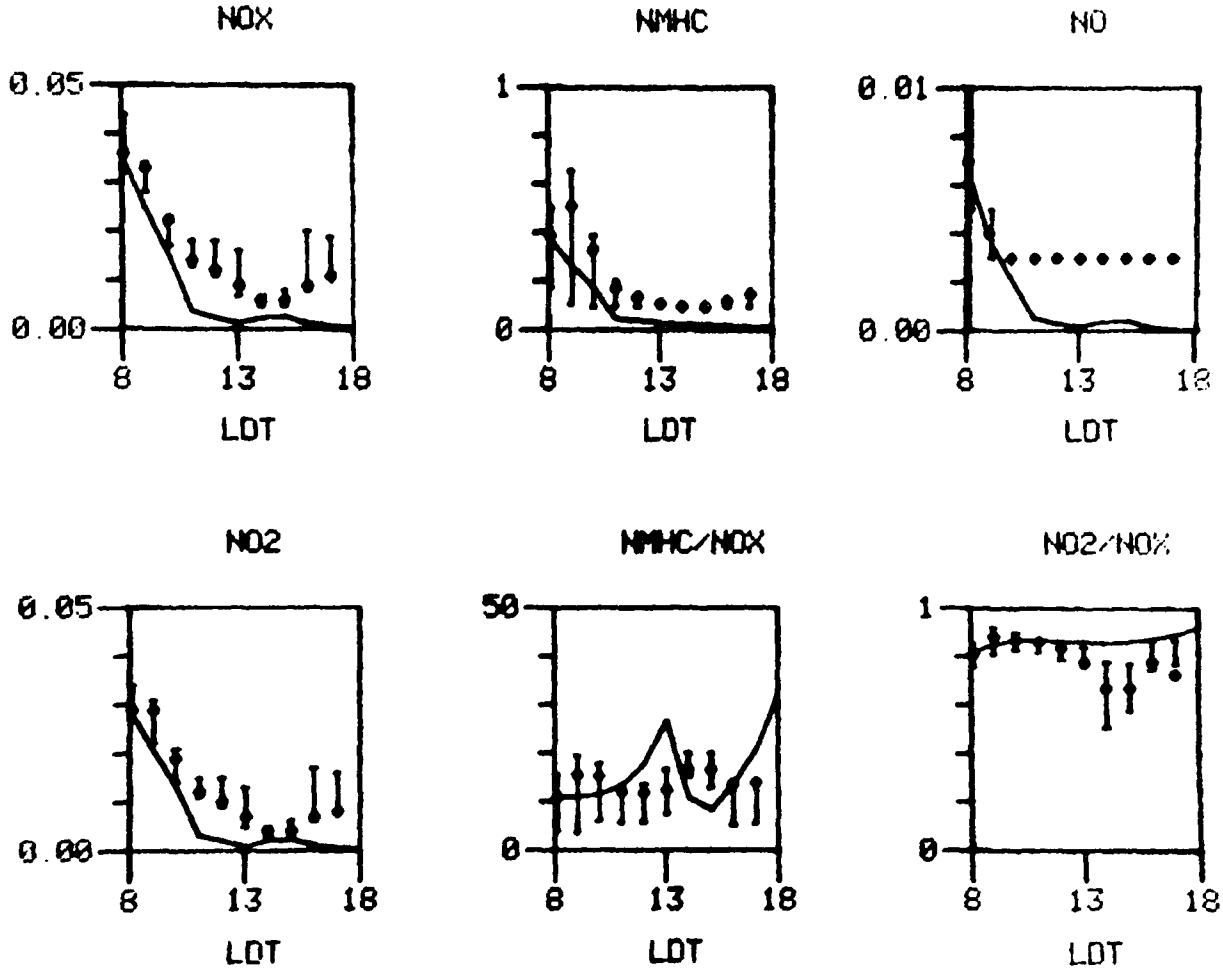

June 8, 1976
Day 160

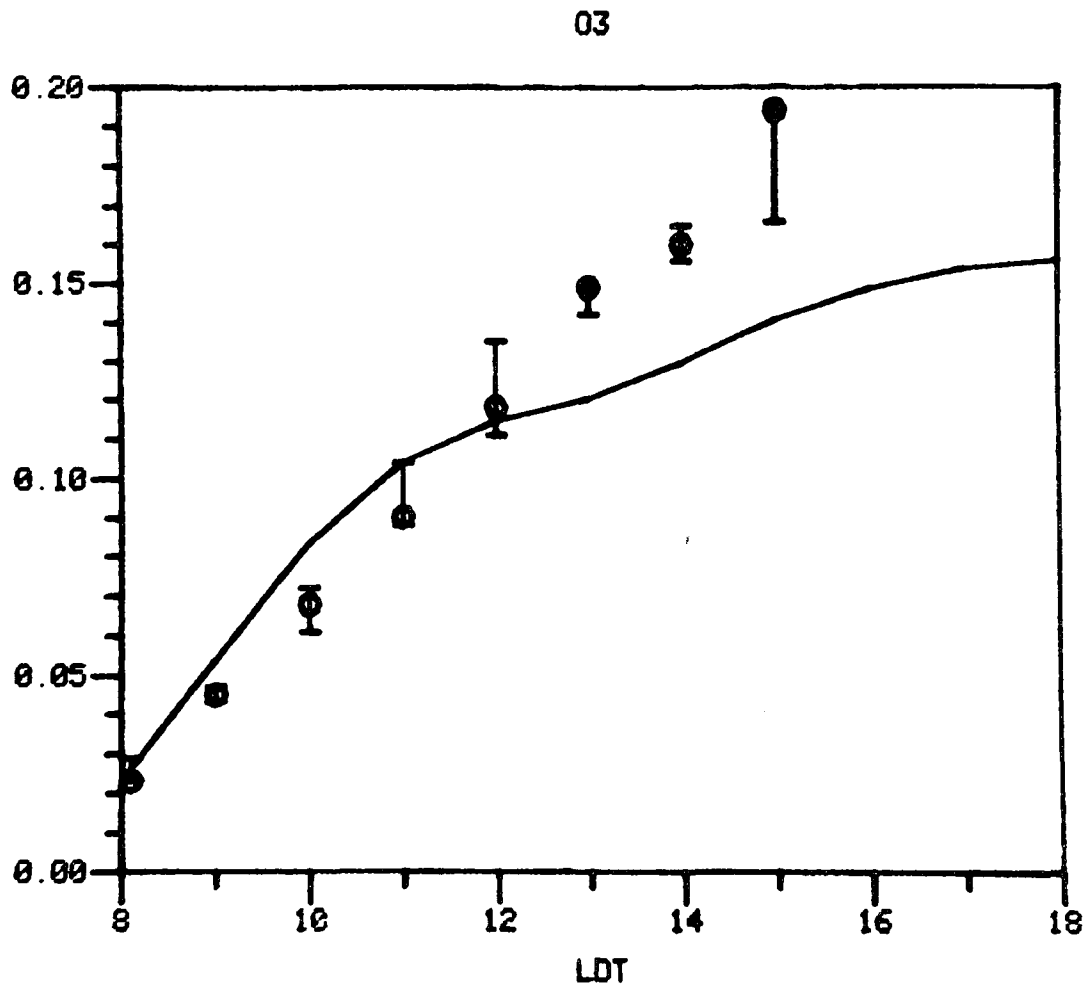

June 8, 1976
Day 160

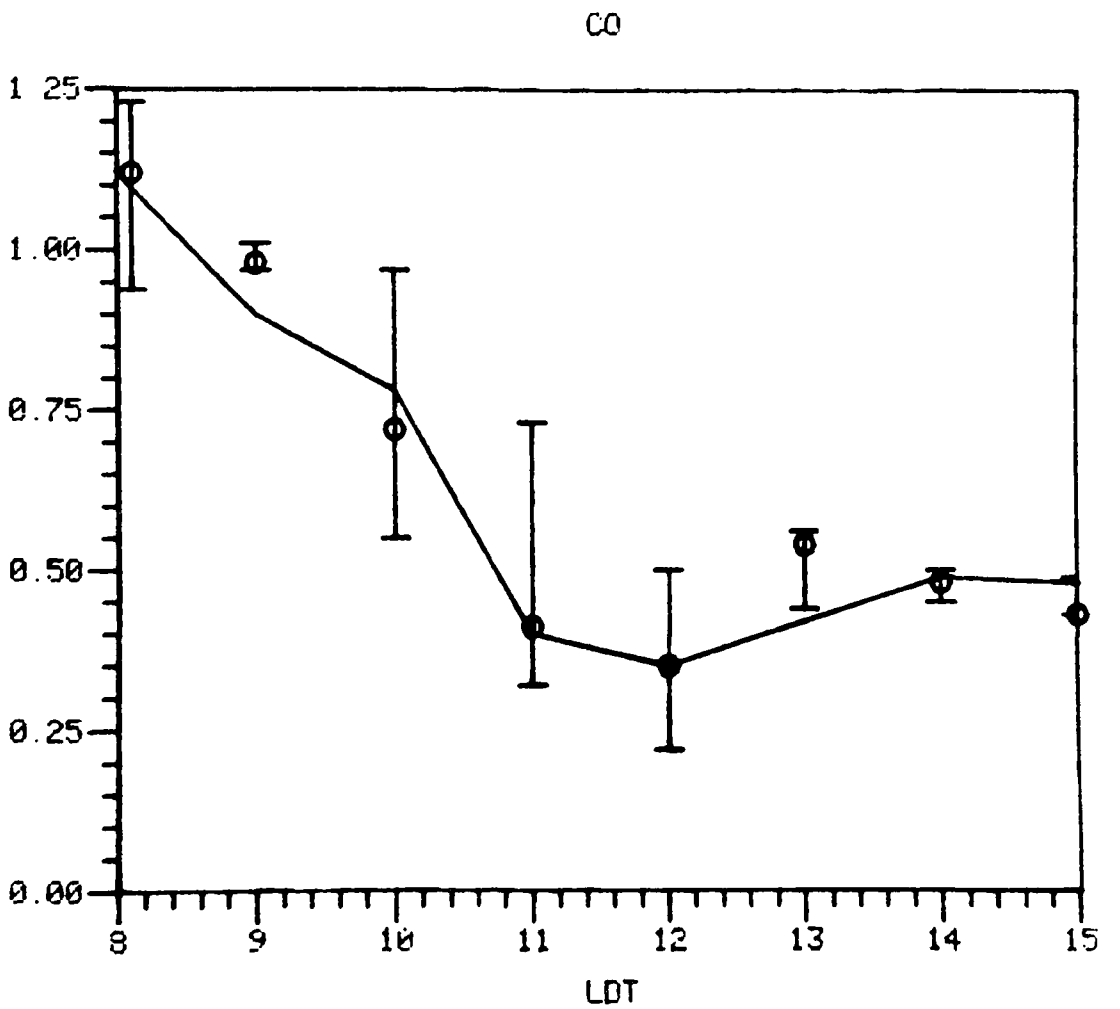

June 8, 1976
Day 160

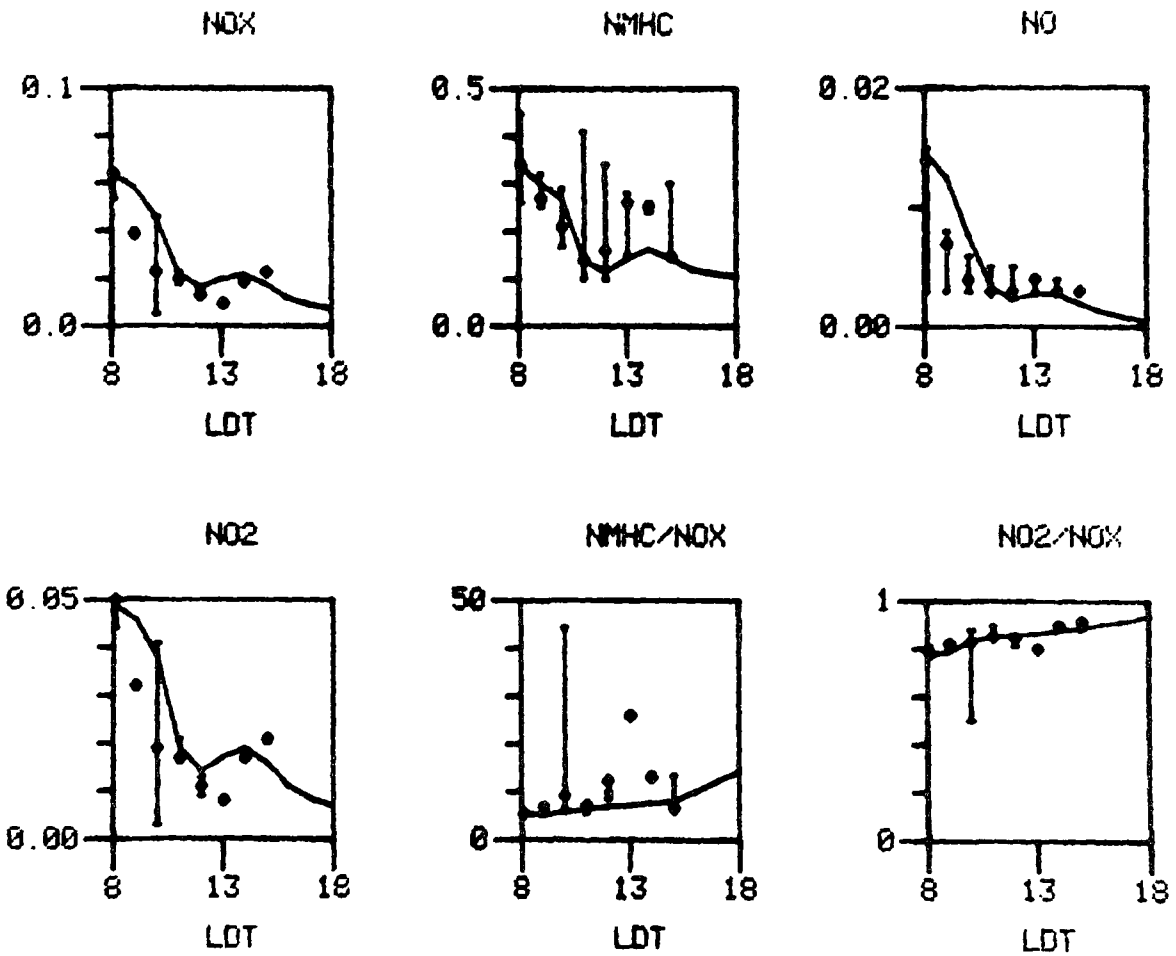

August 25, 1976
Day 238

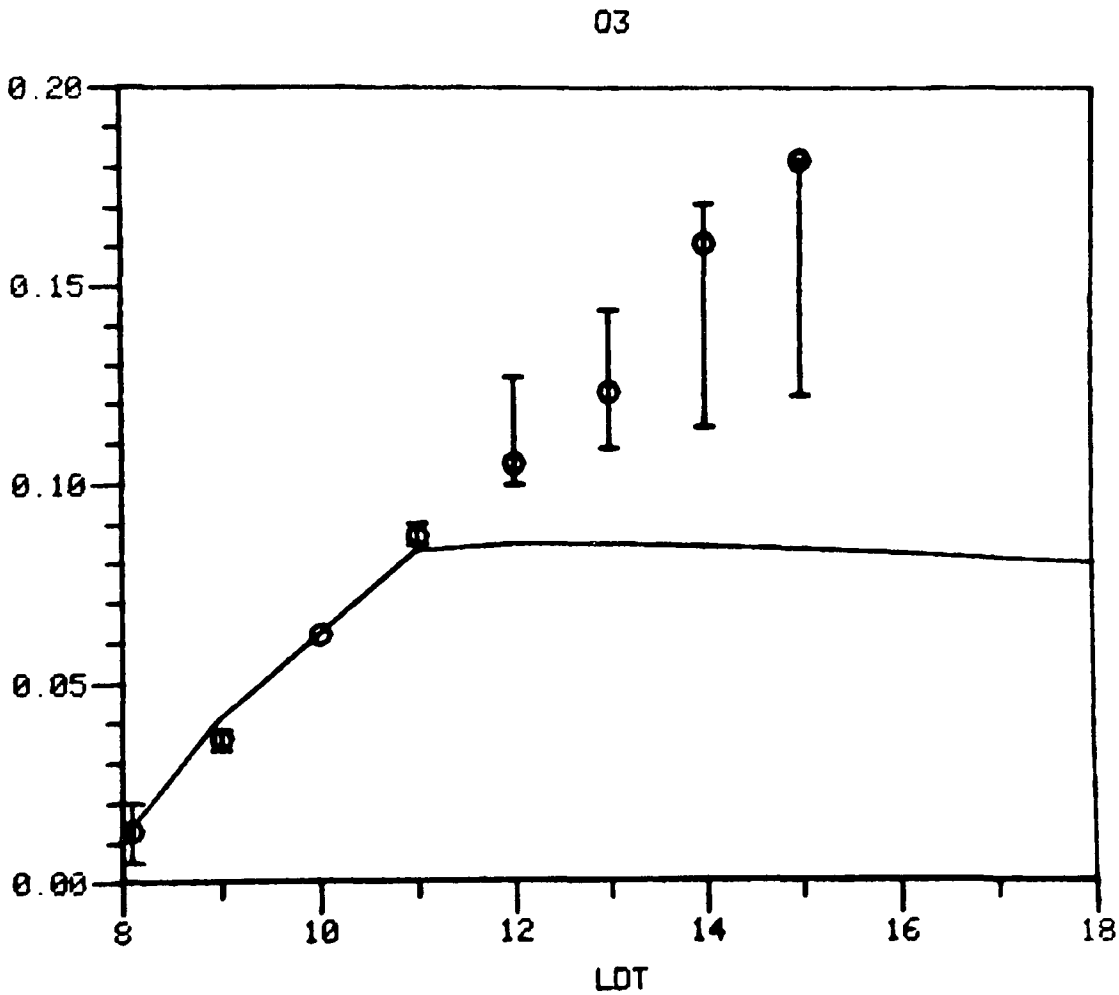

August 25, 1976
Day 238

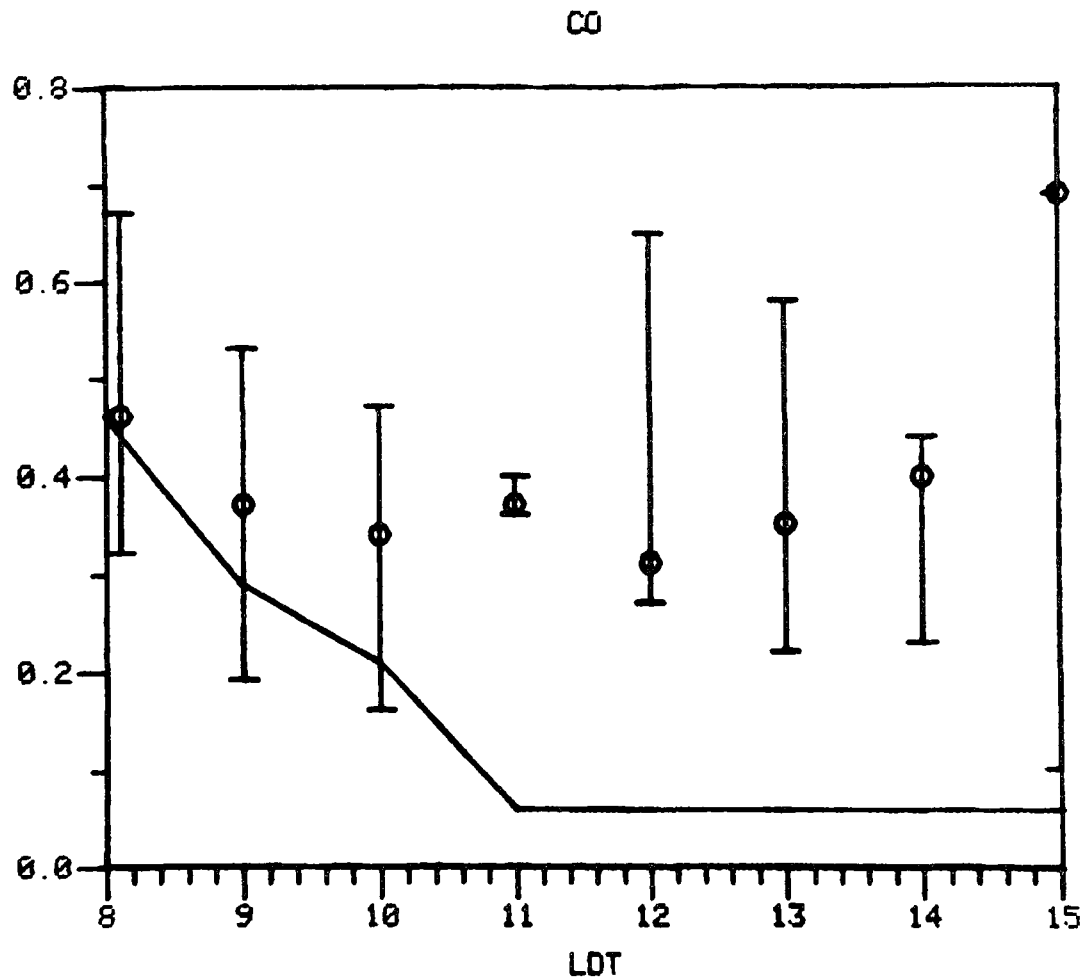

August 25, 1976
Day 238

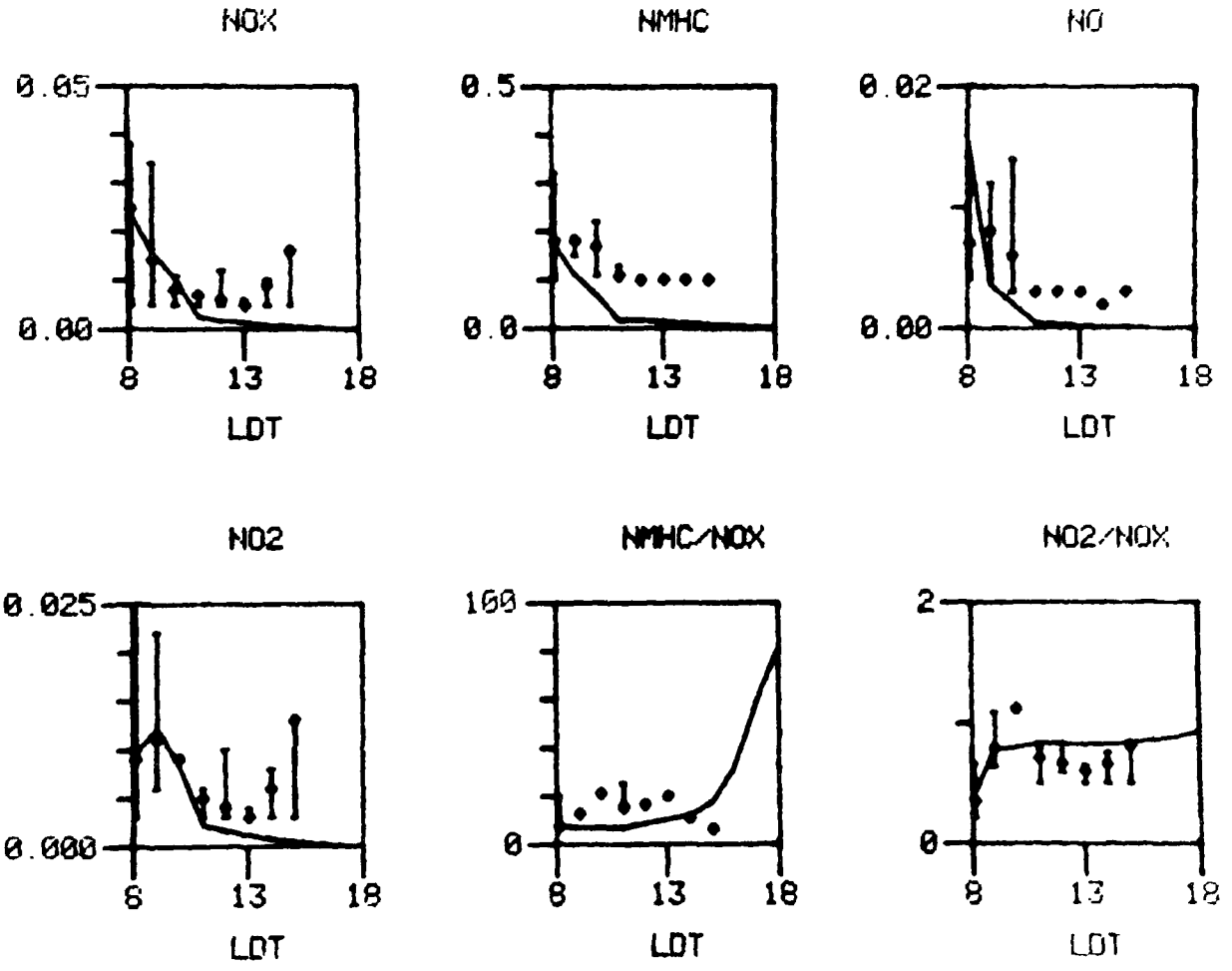

October 2, 1976
Day 276

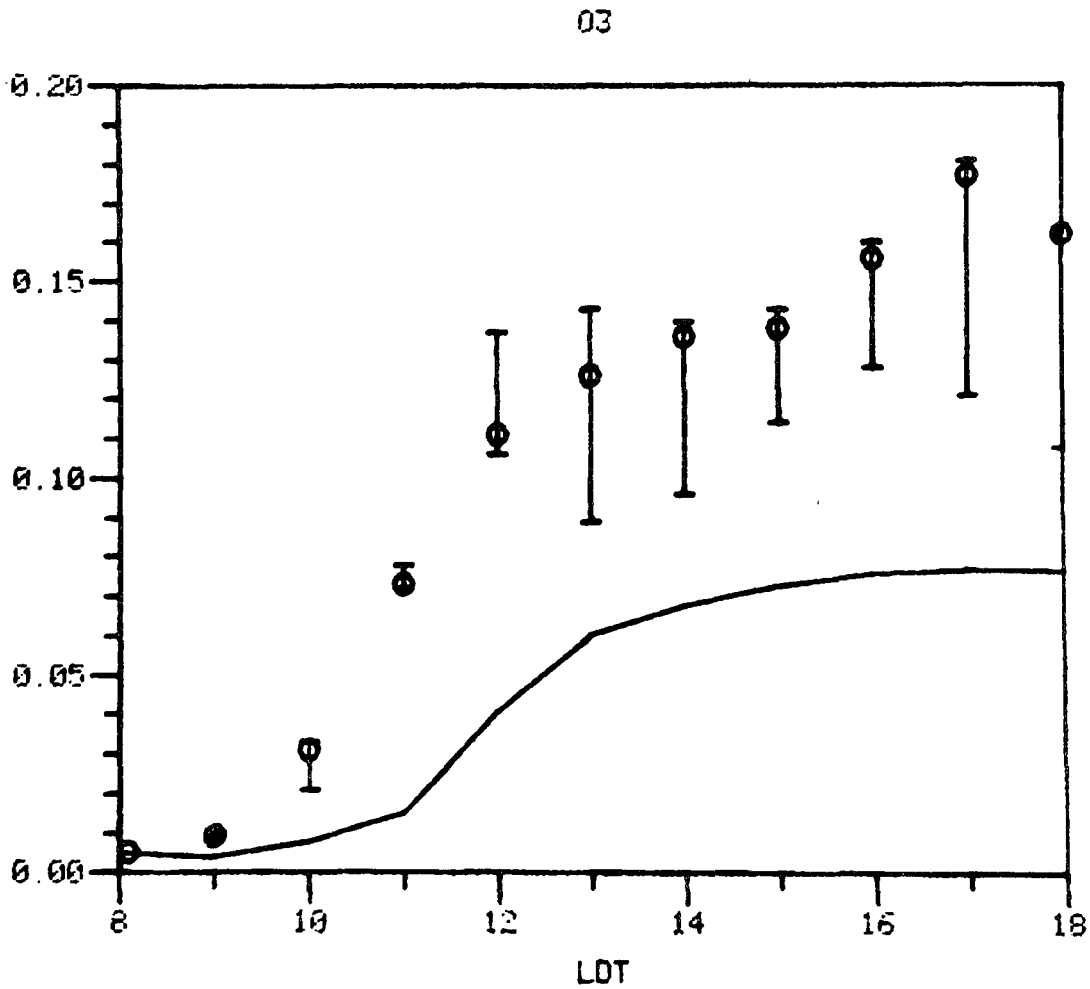

October 2, 1976
Day 276

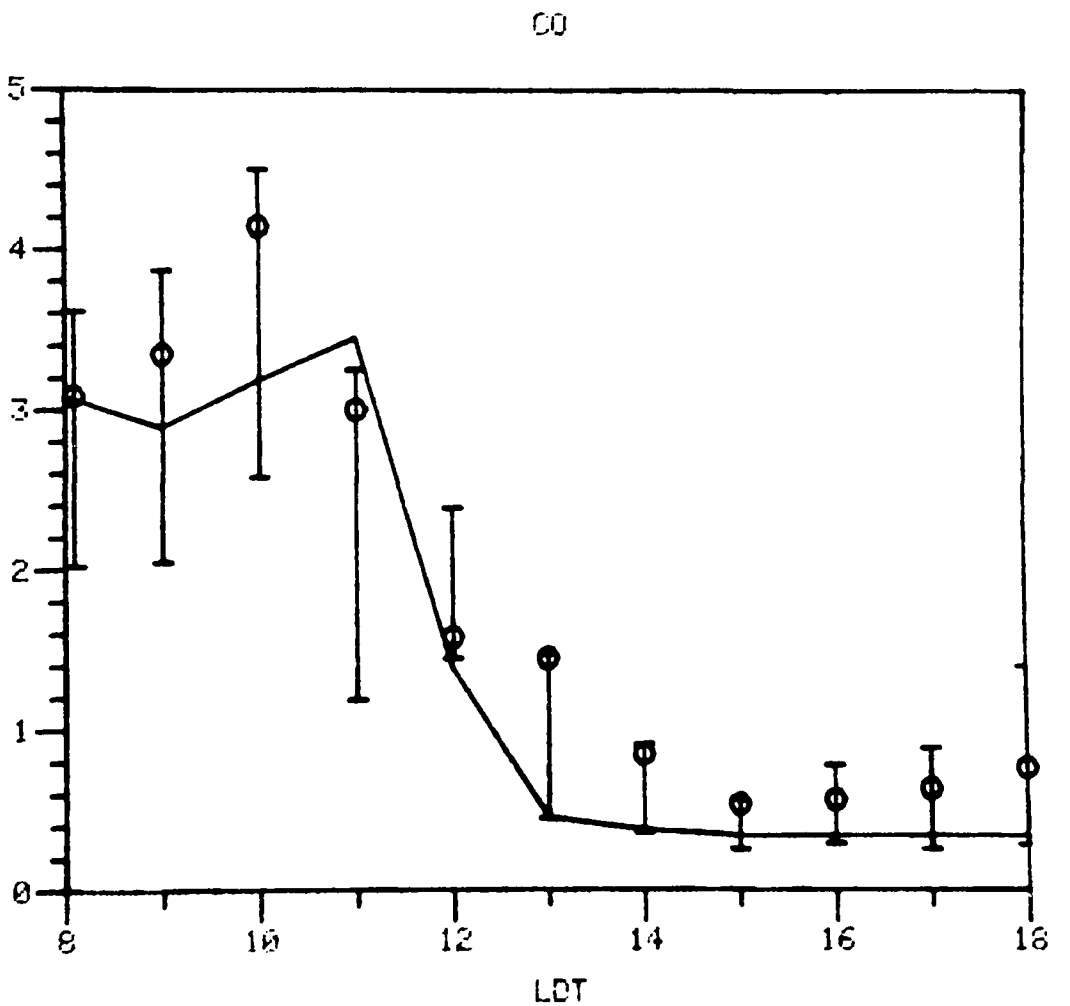

October 2, 1976
Day 276

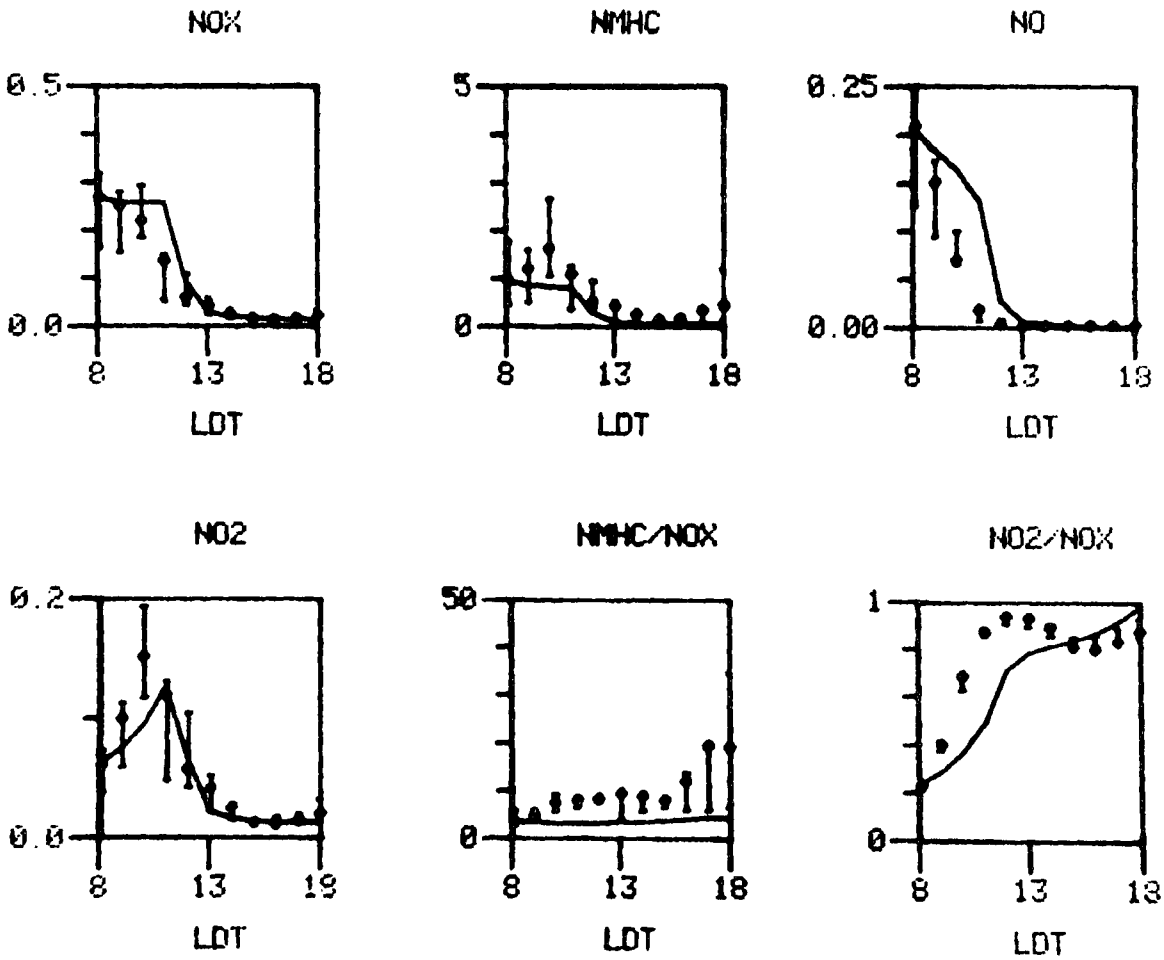

September 17, 1976
Day 261

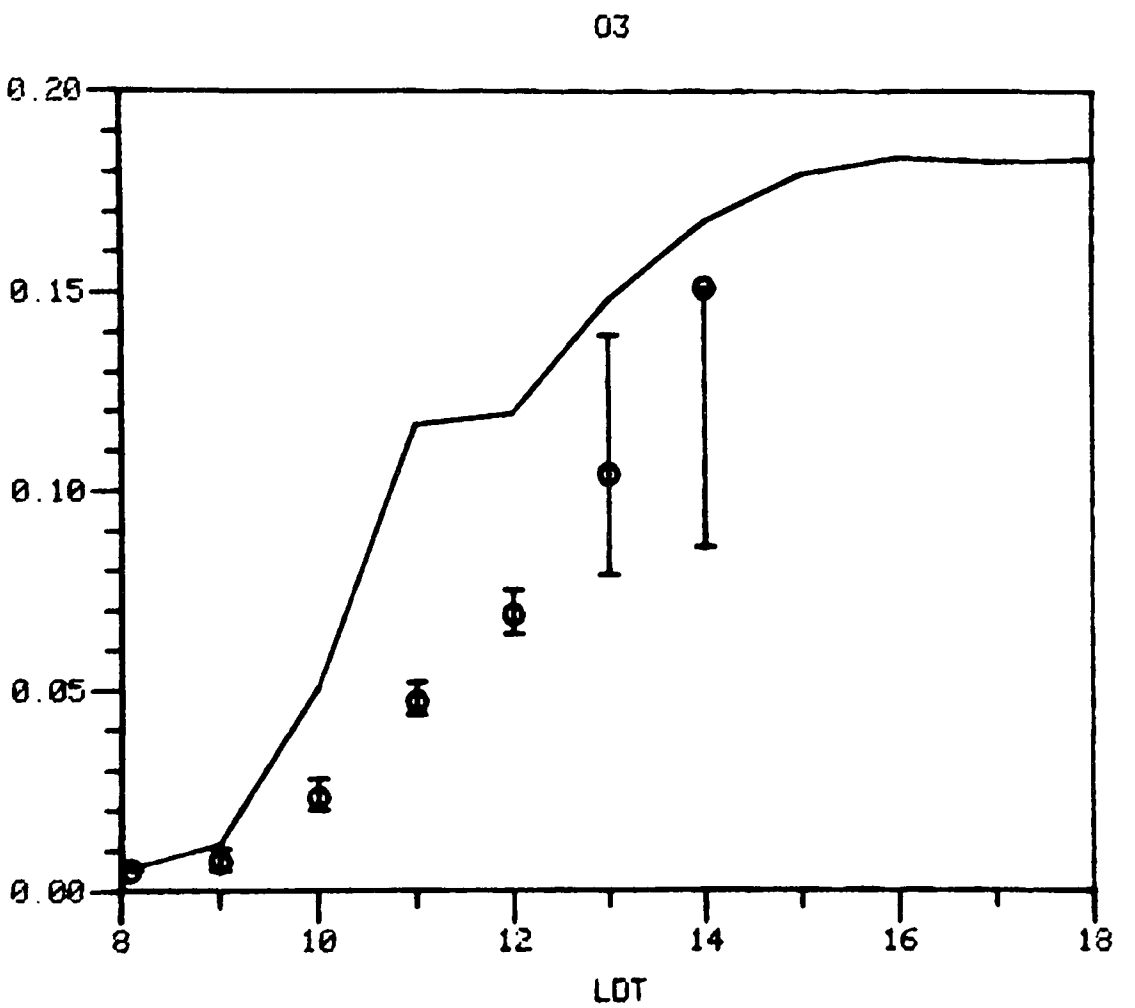

September 17, 1976
Day 261

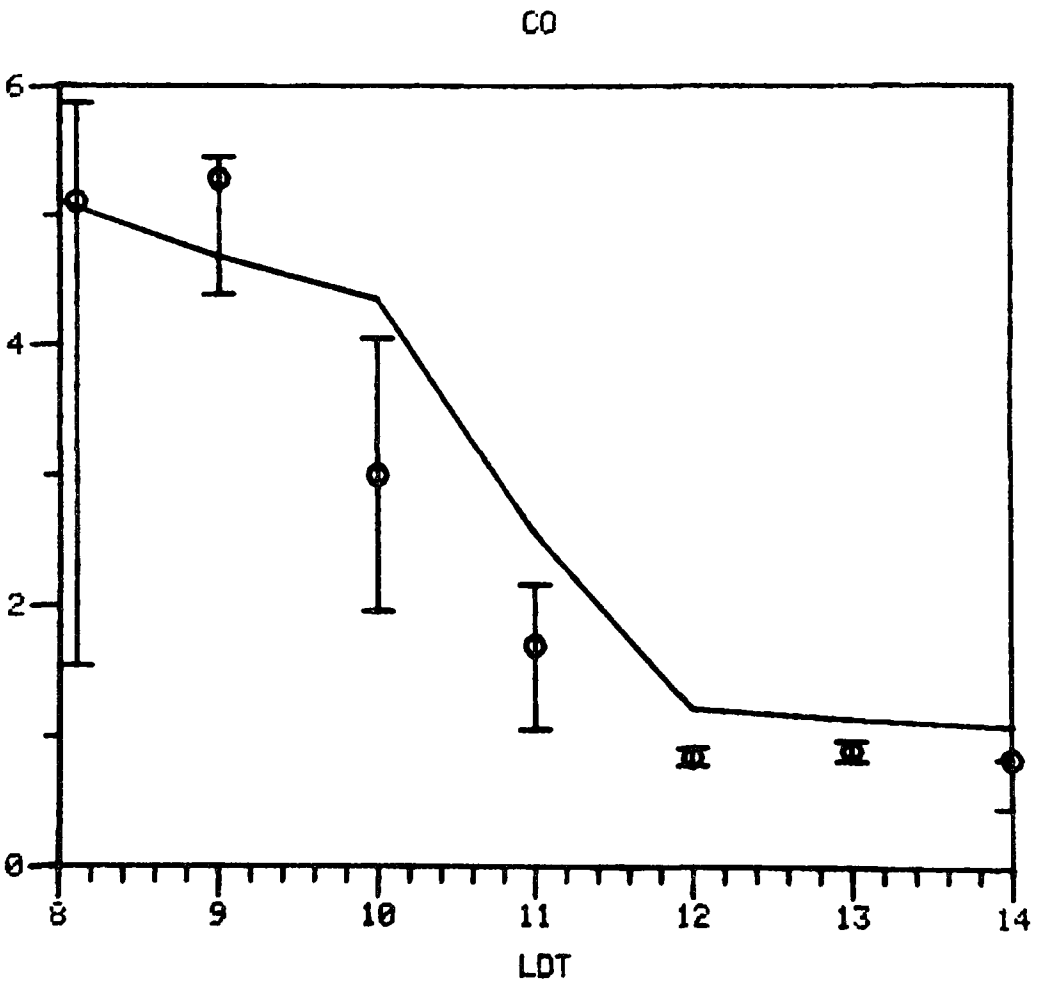

September 17, 1976
Day 261

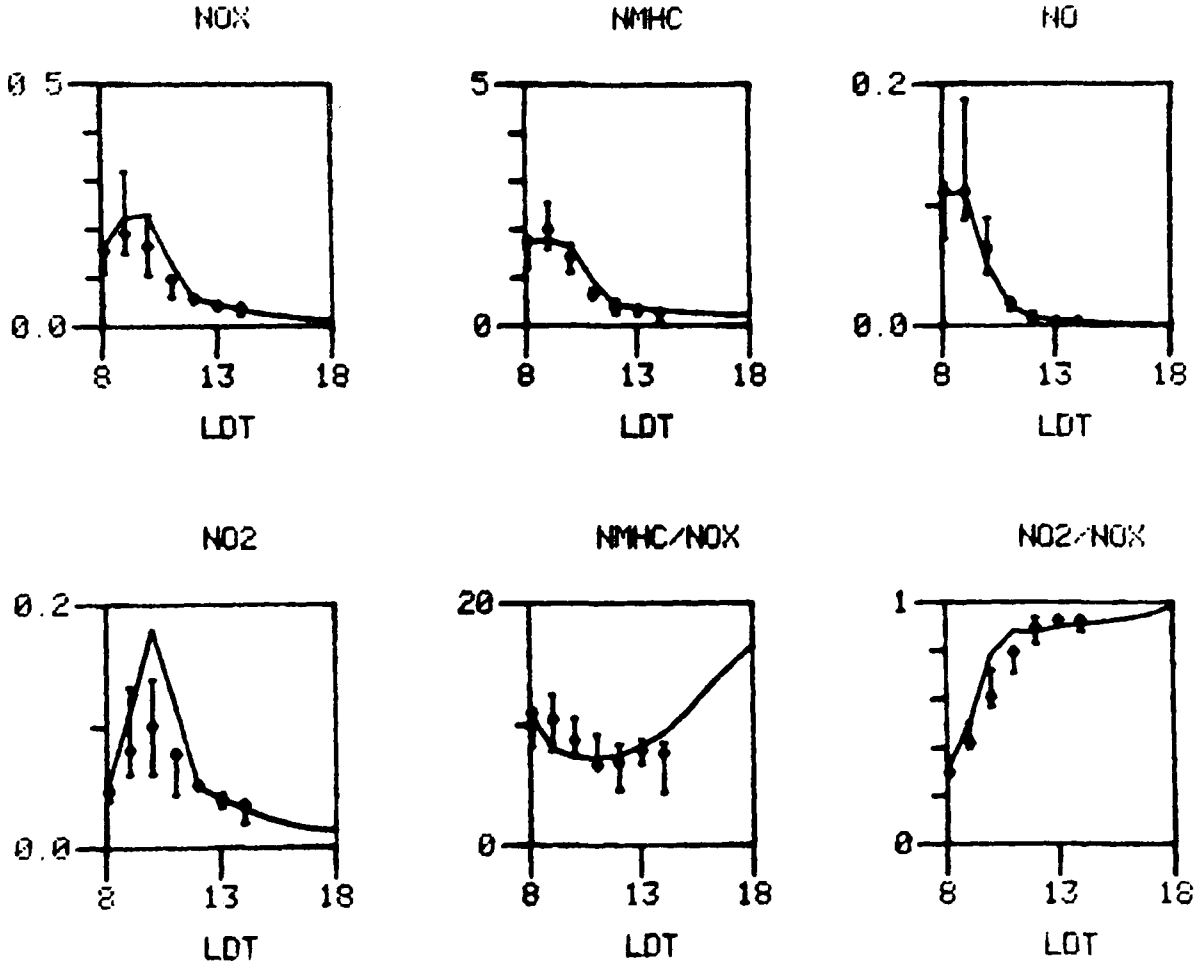

July 19, 1976
Day 201

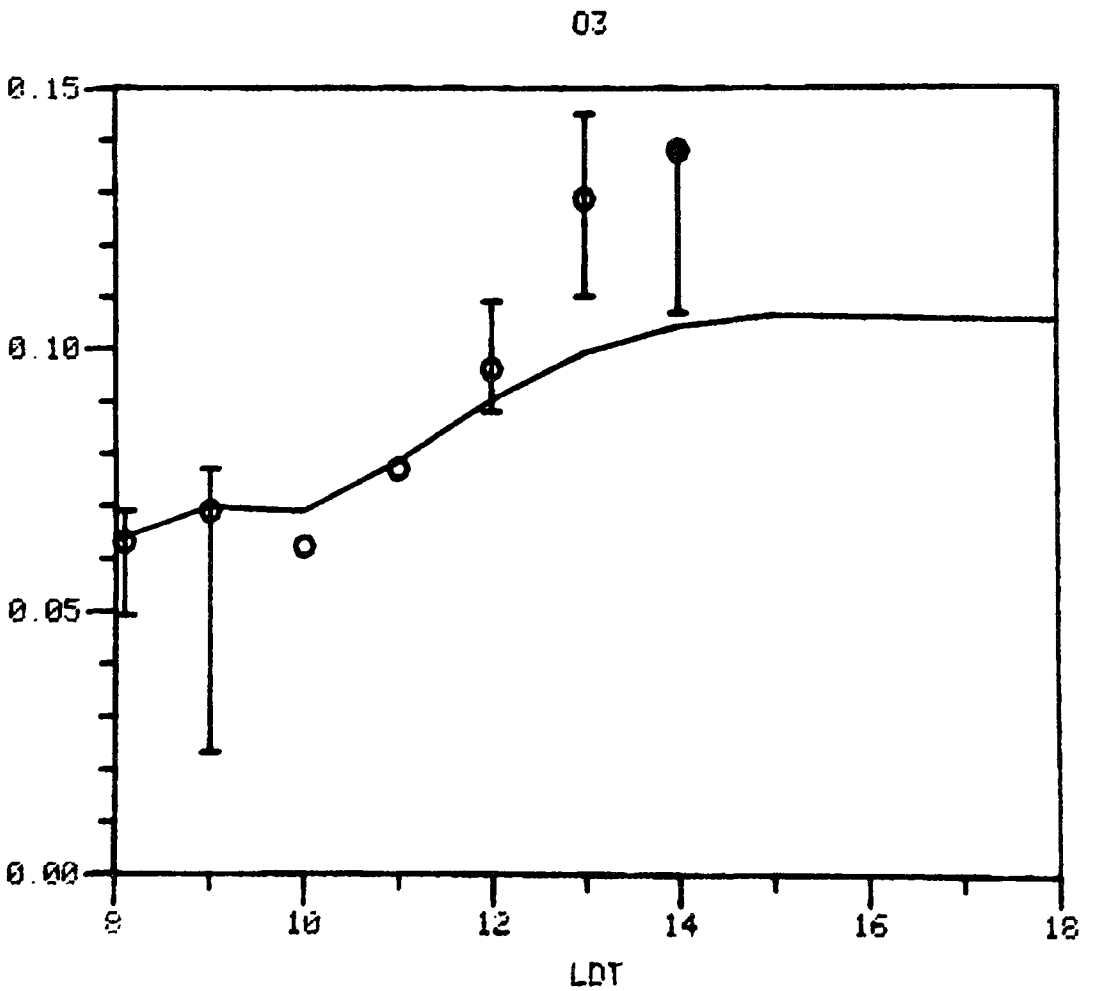

July 19, 1976
Day 201

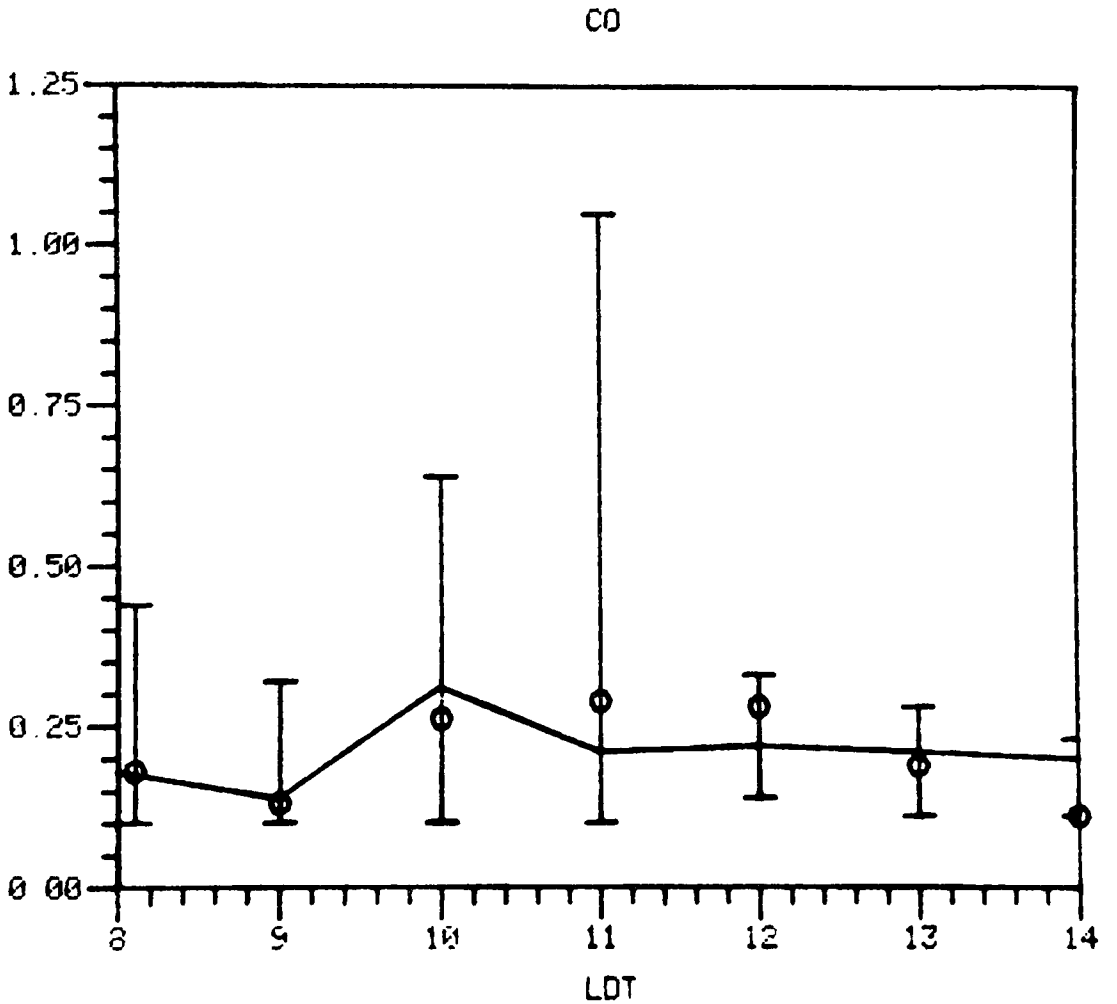

July 19, 1976
Day 201

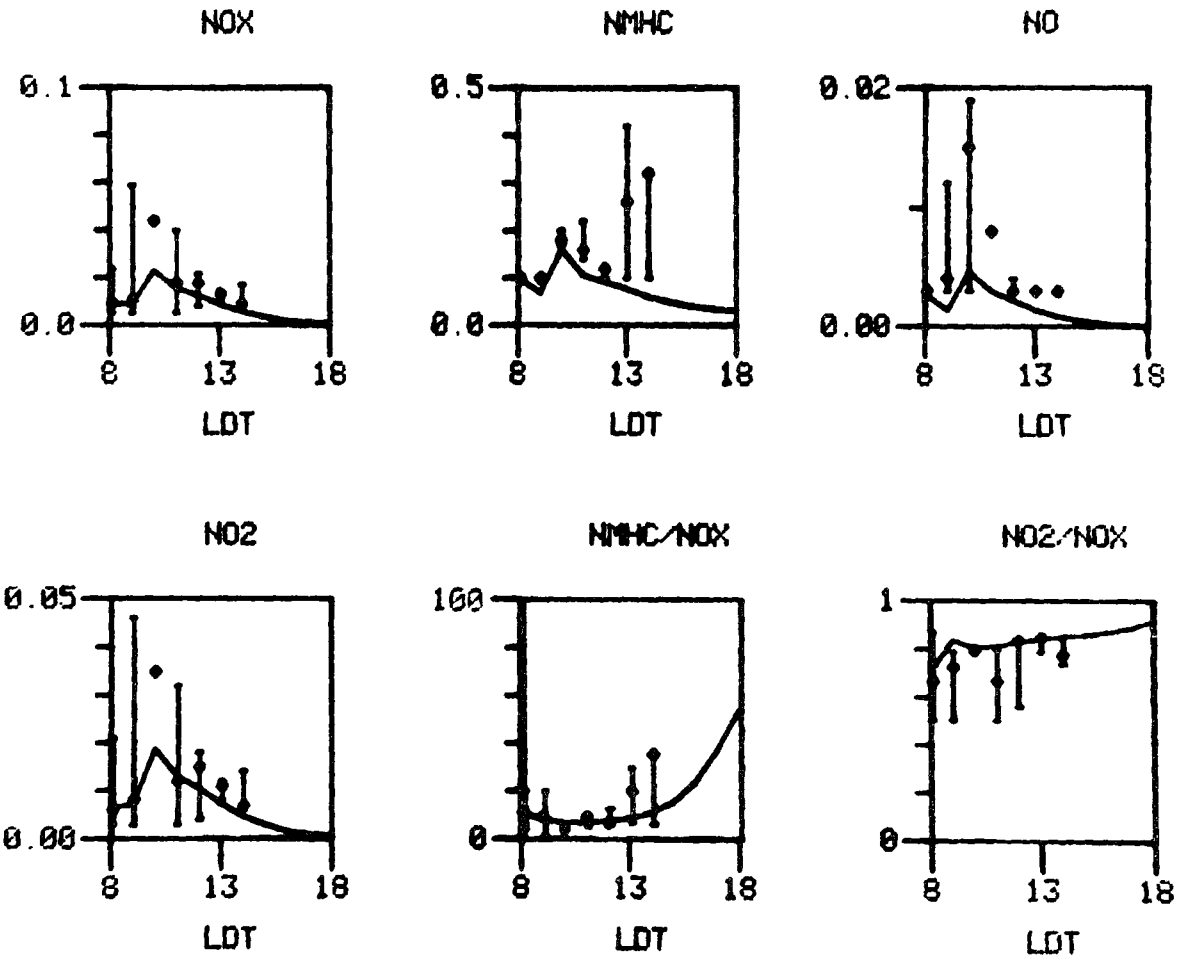

August 8, 1976
Day 221

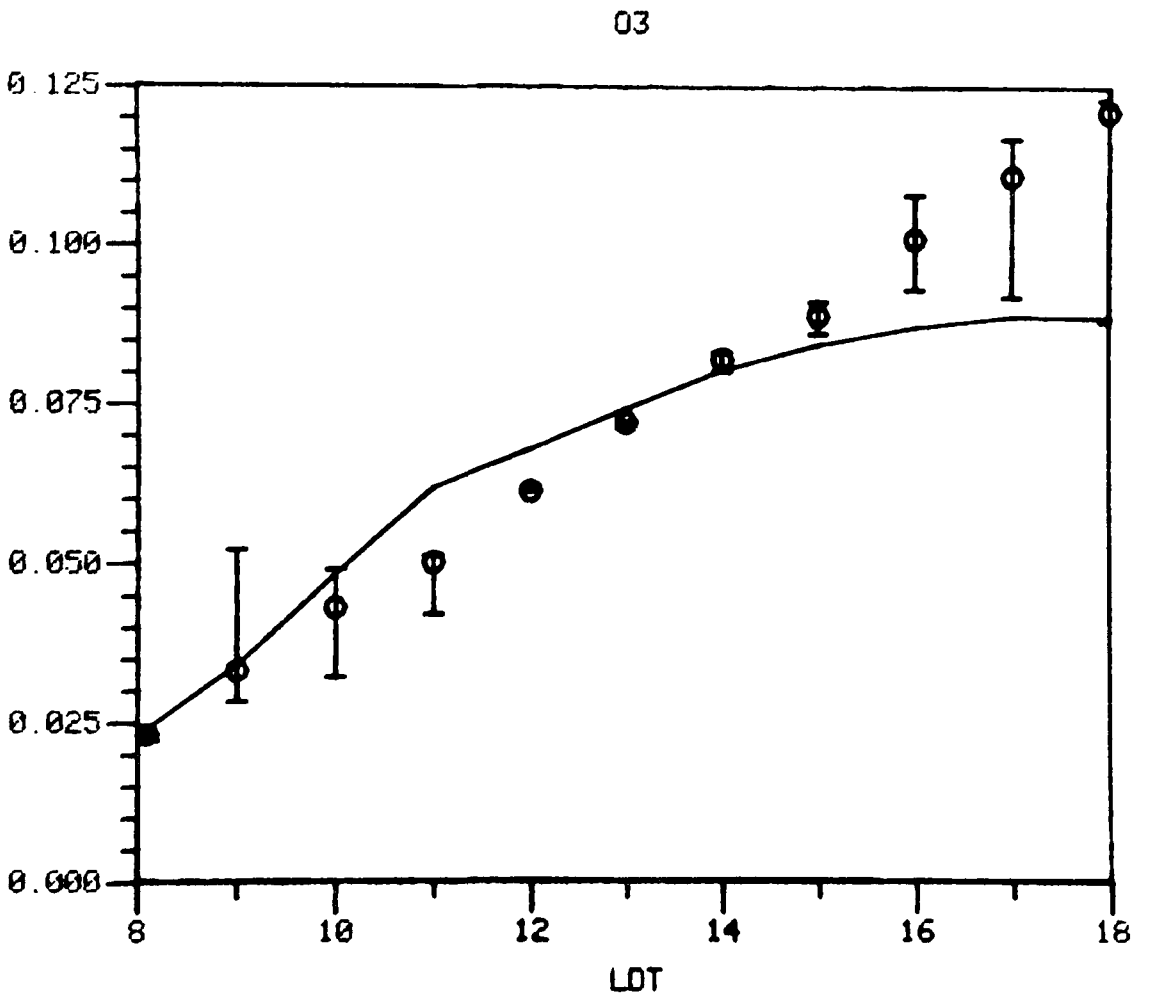

August 8, 1976
Day 221

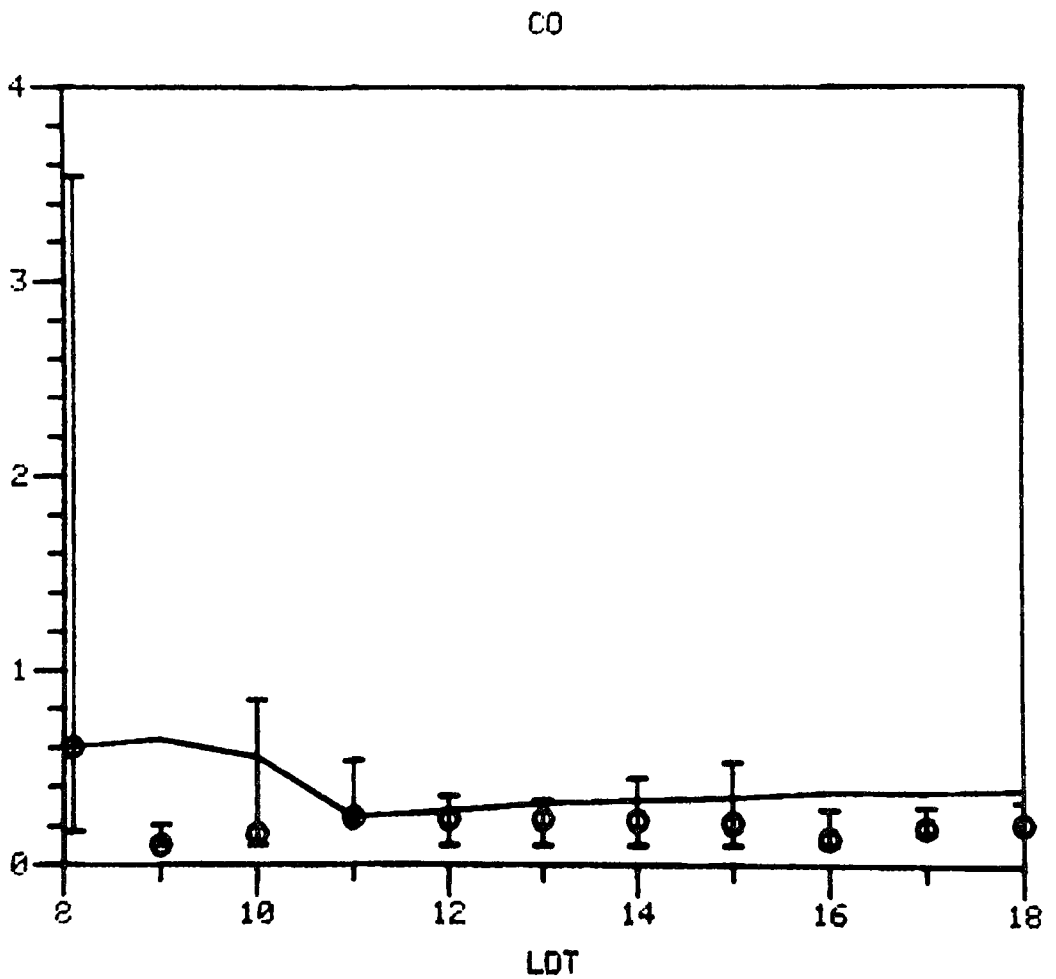

August 8, 1976
Day 221

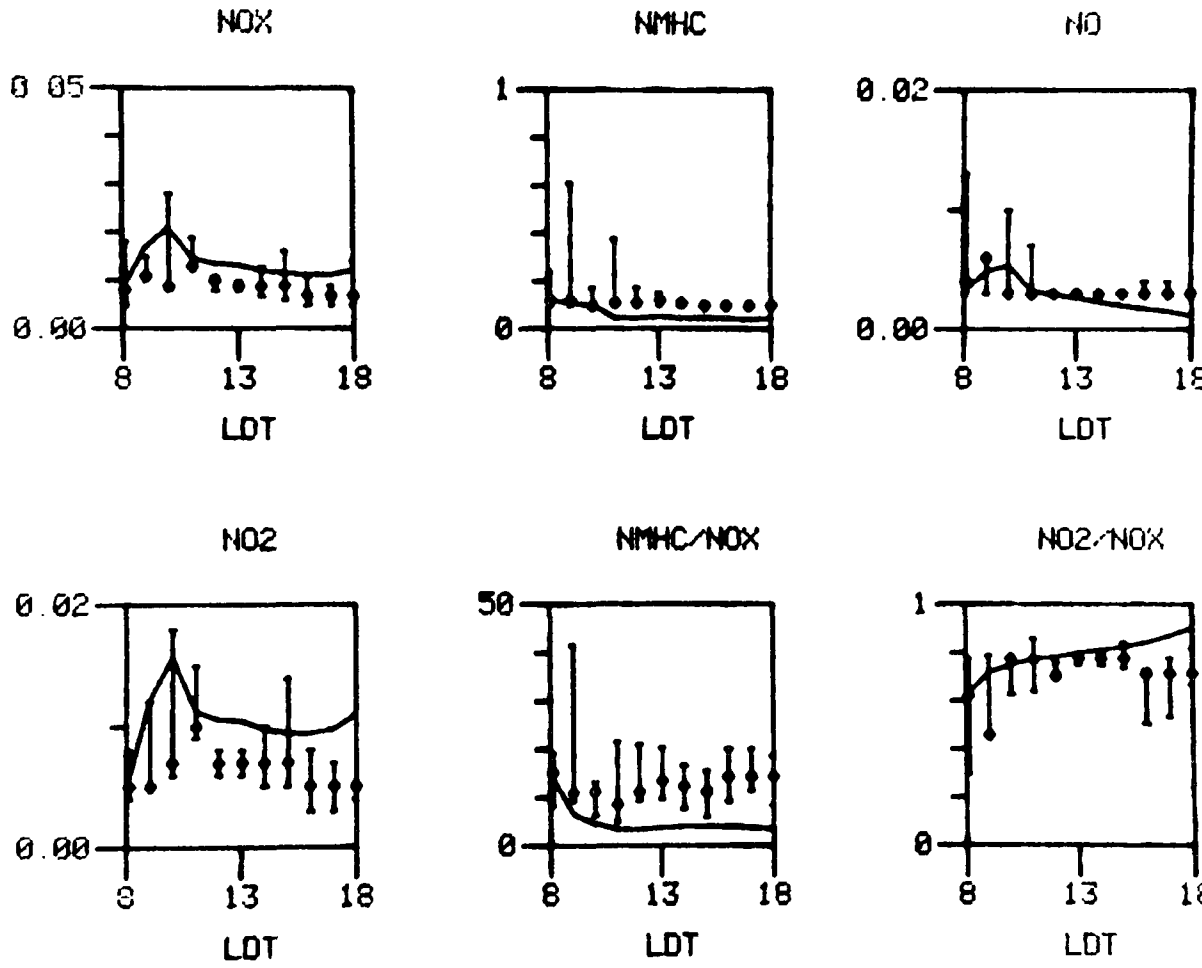

APPENDIX C

The following figures contrast the trajectories calculated from surface wind measurements using two different procedures. The solid line shows the back trajectories calculated from the vector average of all 25 RAMS sites. The dashed line corresponds to back trajectories calculated on the basis of the nearest three stations, using a $1/r^2$ weighting factor. In both cases, 10-minute average wind data were used, but only hourly intervals are shown on the trajectories. All trajectories start at 0800 LDT and end at the time of the observed peak.

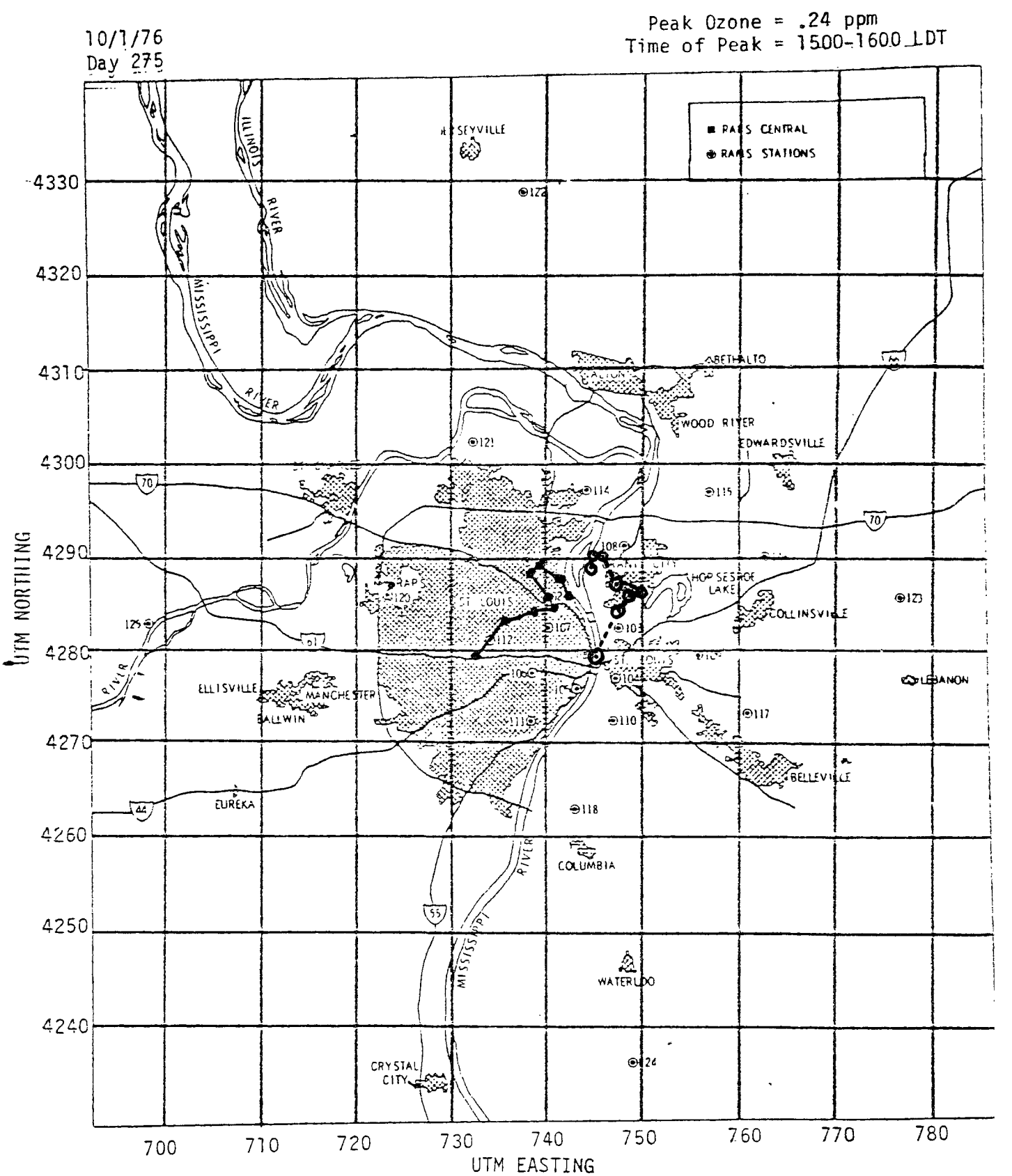
10/1/76
Day 275
Peak Ozone = .24 ppm
Time of Peak = 1500-1600 LDT
RAPS CENTRAL
RAPS STATIONS
SEYVILLE
ILLINOIS
RIVER
MISSISSIPPI
RIVER
BETHALTO
WOOD RIVER
EDWARDSVILLE
HIGHLAND
LAKE
COLLINSVILLE
LEBANON
ST LOUIS
ELLISVILLE
MANCHESTER
BALLWIN
EUREKA
BELLEVILLE
COLUMBIA
WATERLOO
CRYSTAL
CITY
MISSISSIPPI
RIVER
70
44
55
4330
4320
4310
4300
4290
4280
4270
4260
4250
4240
700
710
720
730
740
750
760
770
780
UTM NORTHING
UTM EASTING

7/13/76
Day 195

Peak Ozone = .22 ppm
Time of Peak = 1600-1700 LDT

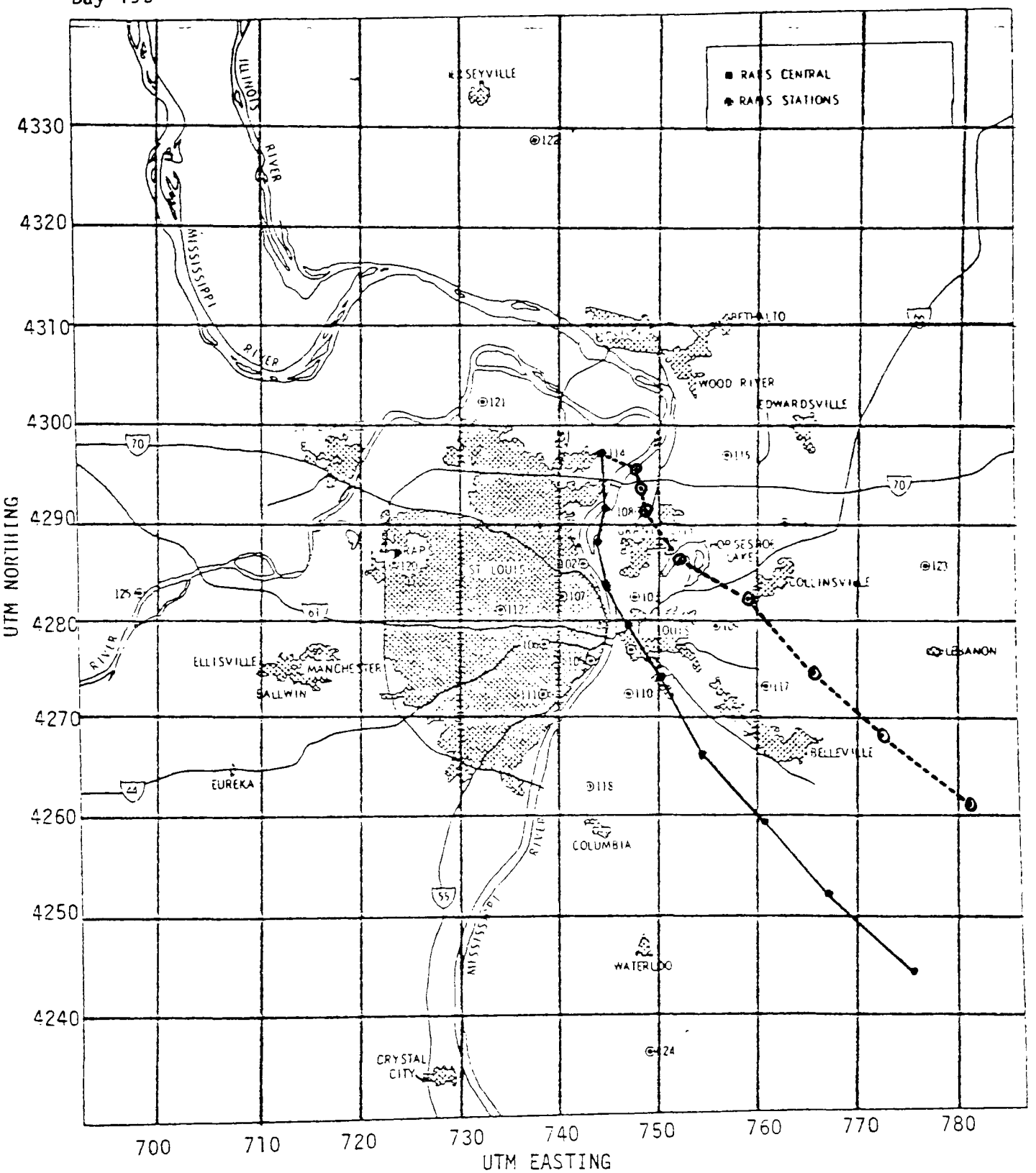

6/8/76
Day 160

Peak Ozone = .22 ppm
Time of Peak = 1700-1800 LDT

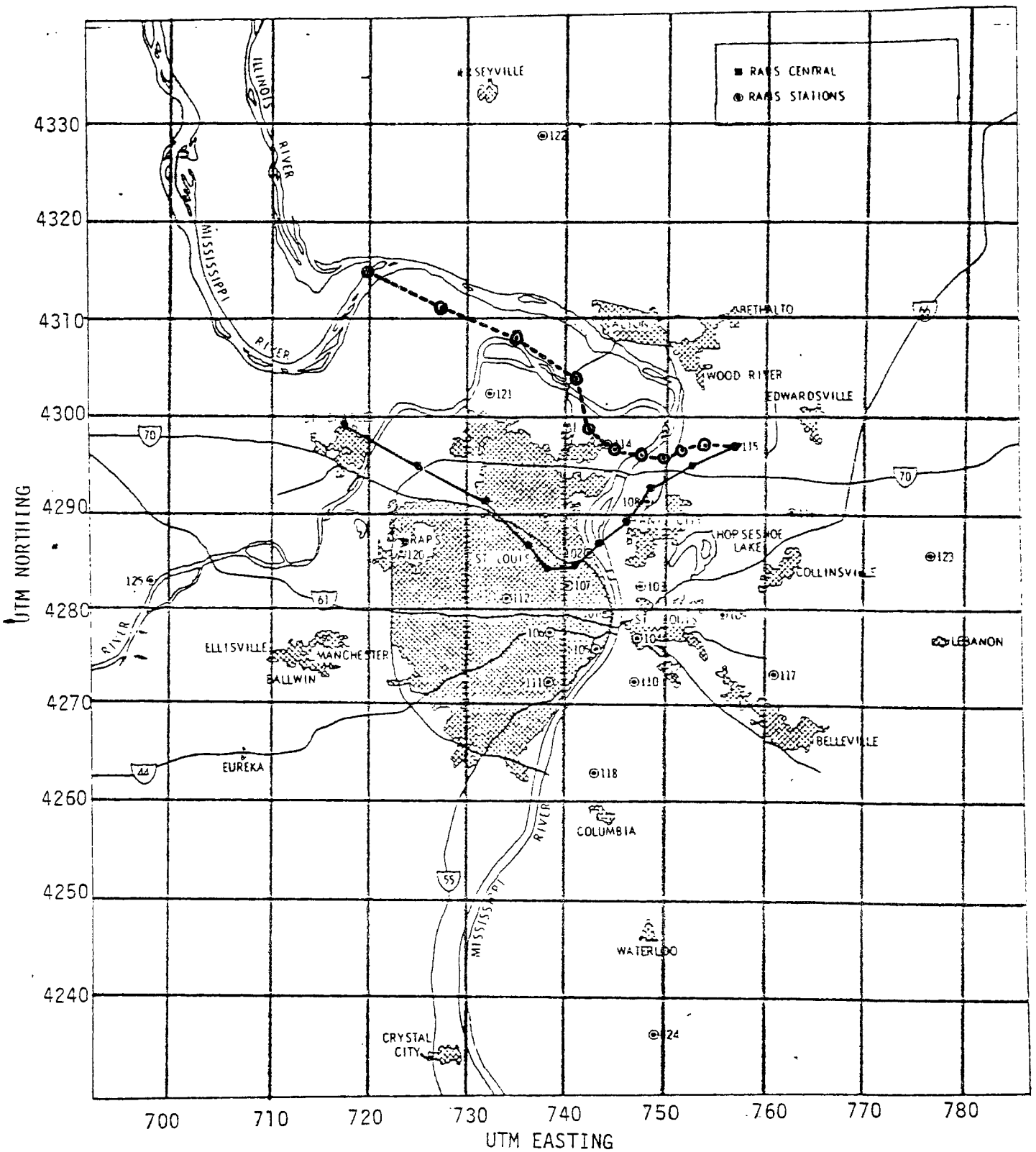

6/7/76
Day 159

Peak Ozone = .20 ppm
Time of Peak = 1600-1700 LDT

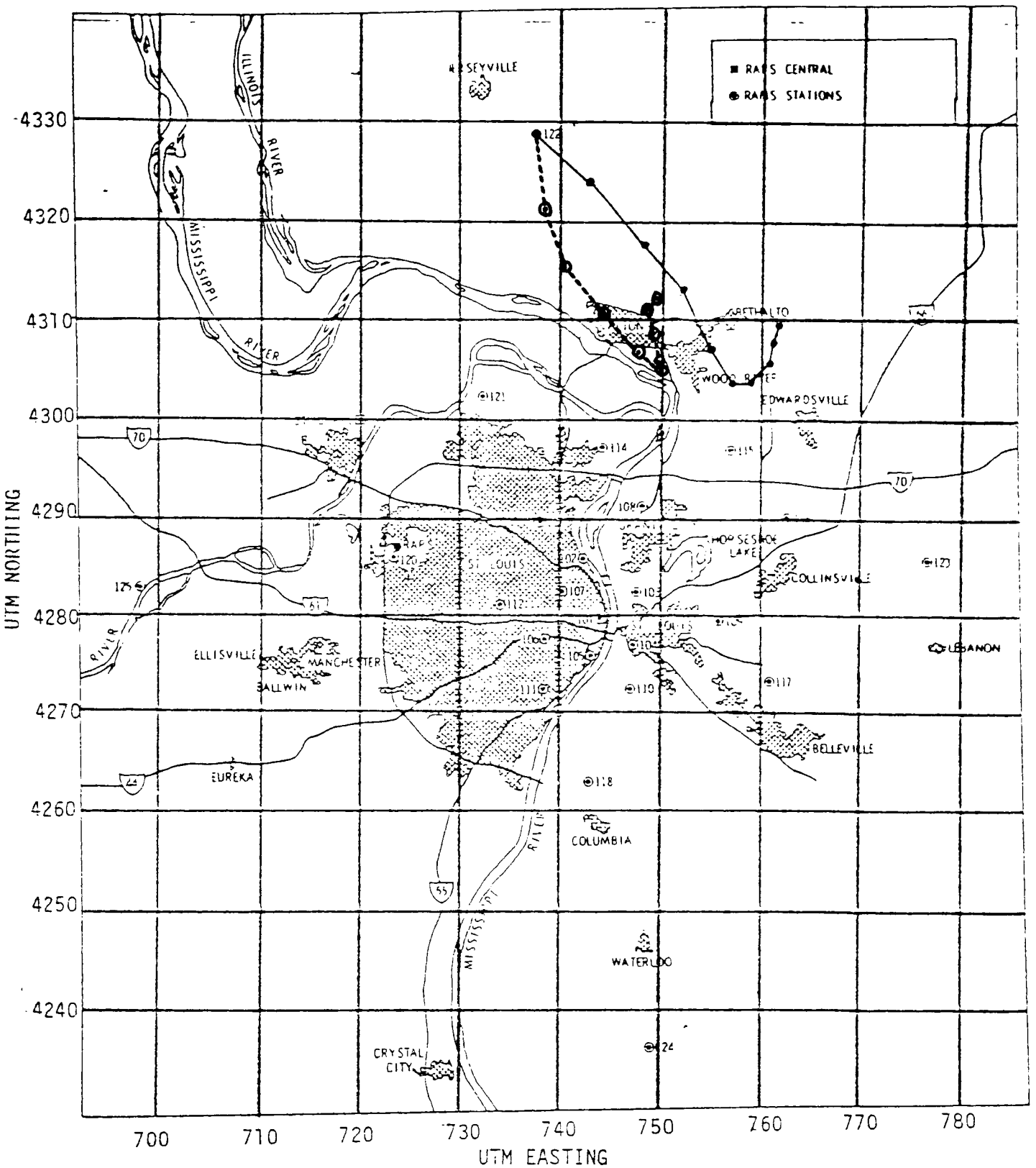

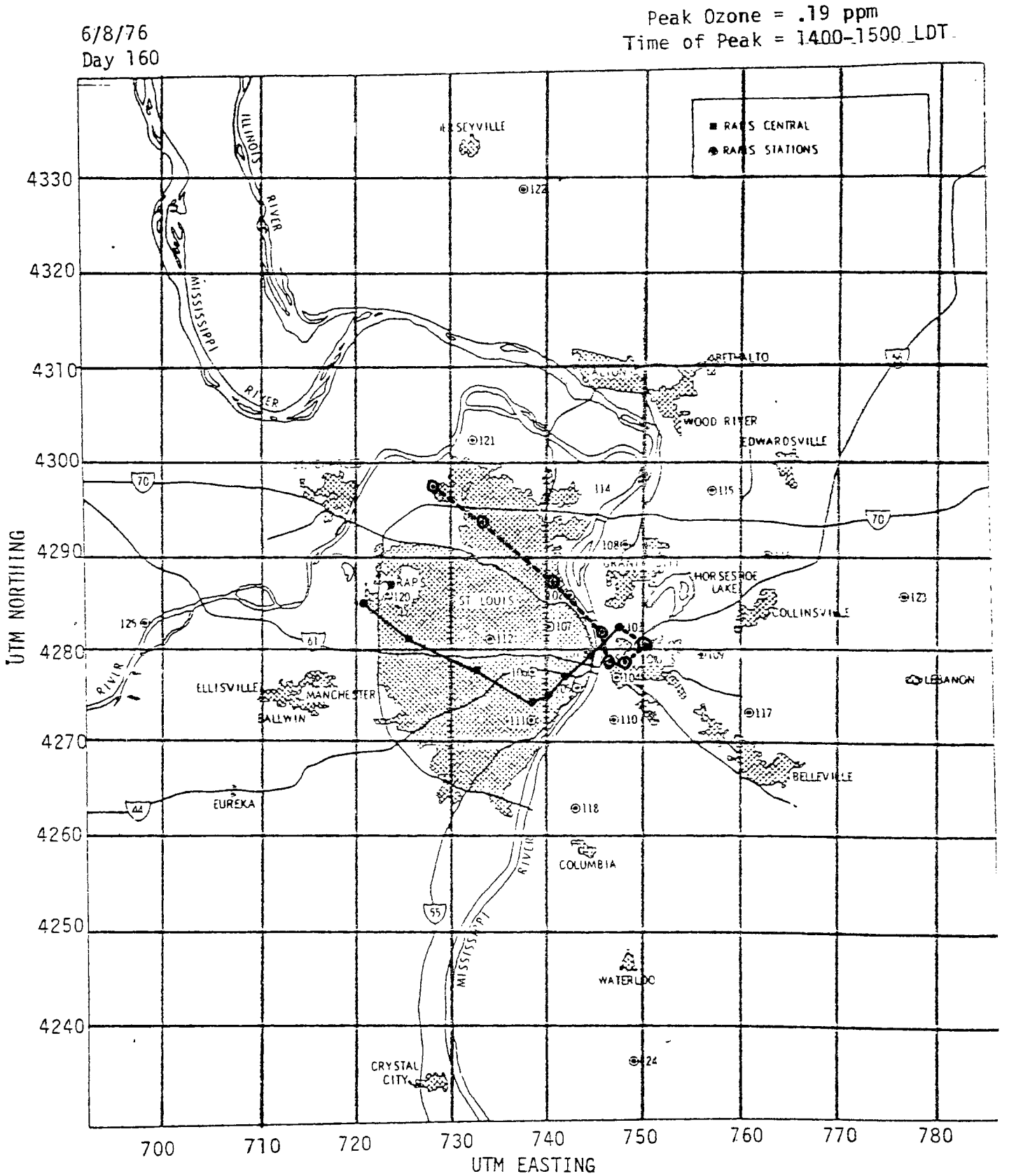
6/8/76
Day 160
Peak Ozone = .19 ppm
Time of Peak = 1400-1500 LDT
RAPS CENTRAL
RAPS STATIONS
ILLINOIS
RIVER
MISSISSIPPI
RIVER
ALTON
WOOD RIVER
EDWARDSVILLE
ST LOUIS
HORSESHOE LAKE
COLLINSVILLE
ELLISVILLE
MANCHESTER
BALLWIN
EUREKA
BELLEVILLE
LEBANON
COLUMBIA
WATERLOO
CRYSTAL CITY
70
61
44
55
4330
4320
4310
4300
4290
4280
4270
4260
4250
4240
700
710
720
730
740
750
760
770
780
UTM NORTHING
UTM EASTING

8/25/76
Day 238

Peak Ozone = .19 ppm
Time of Peak = 1400-1500 LDT

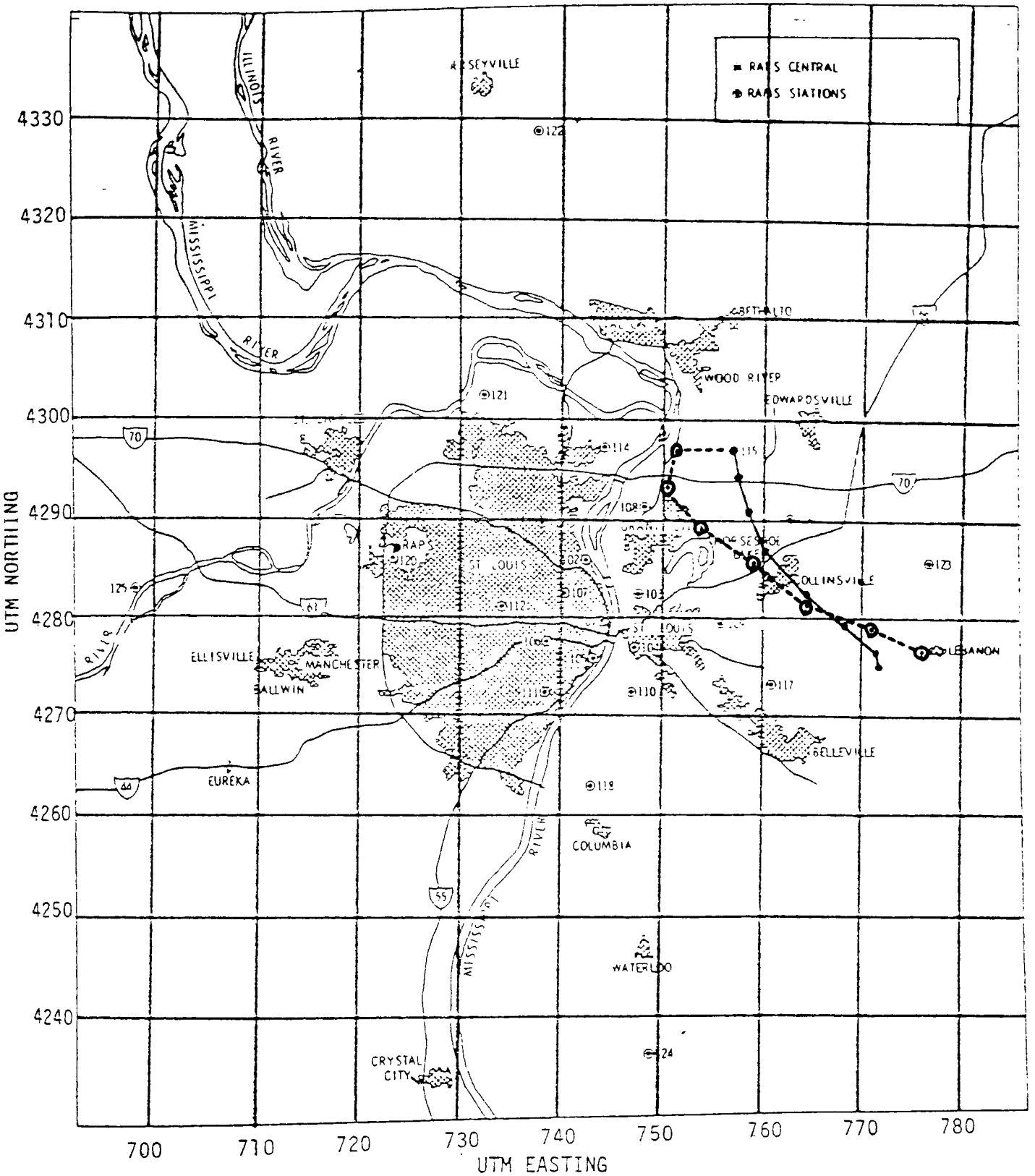

10/2/76
Day 276

Peak Ozone = .19 ppm
Time of Peak = 1700-1800 LDT

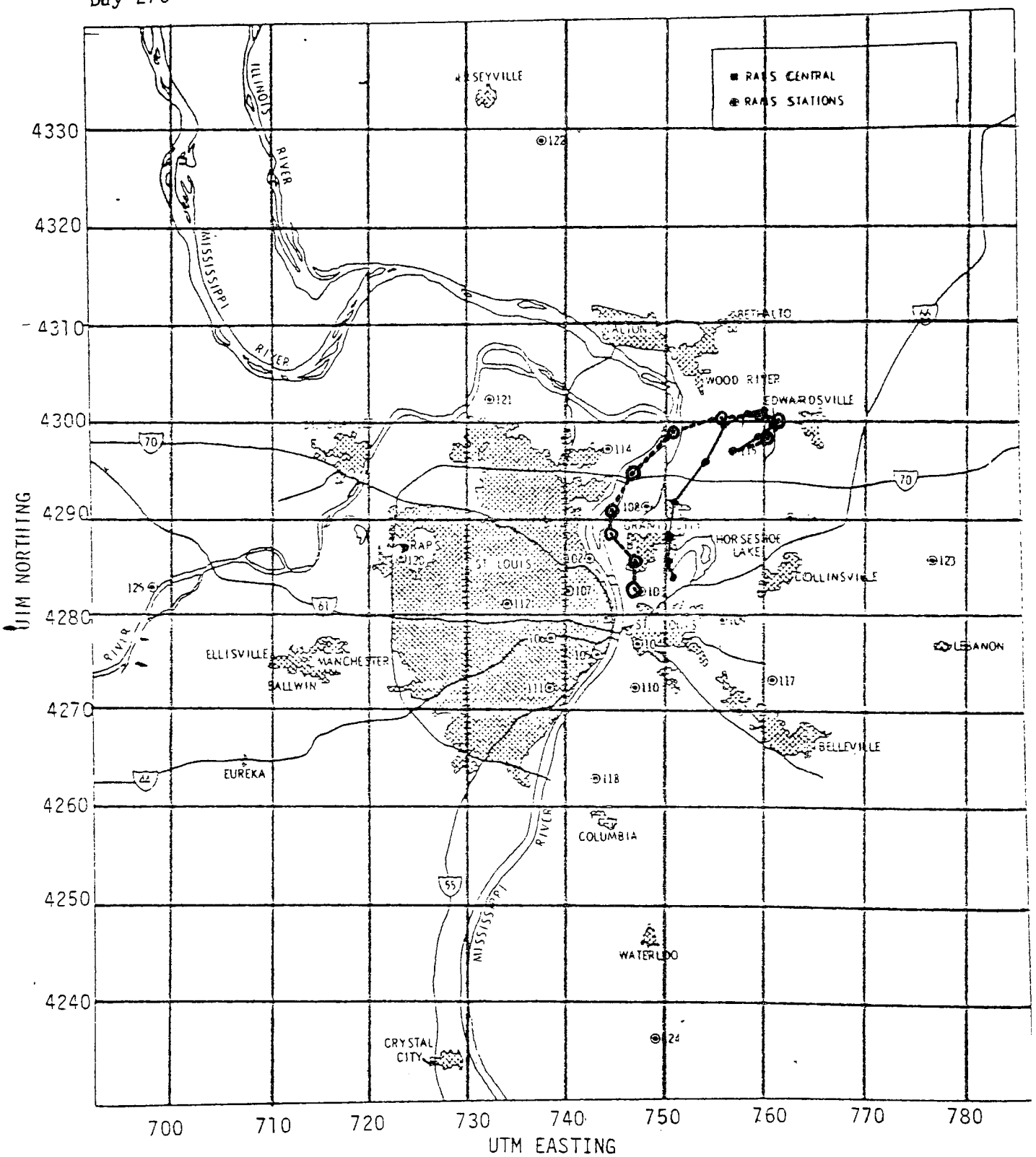

9/17/76
Day 261

Peak Ozone = .15 ppm
Time of Peak = 1300-1400 LDT

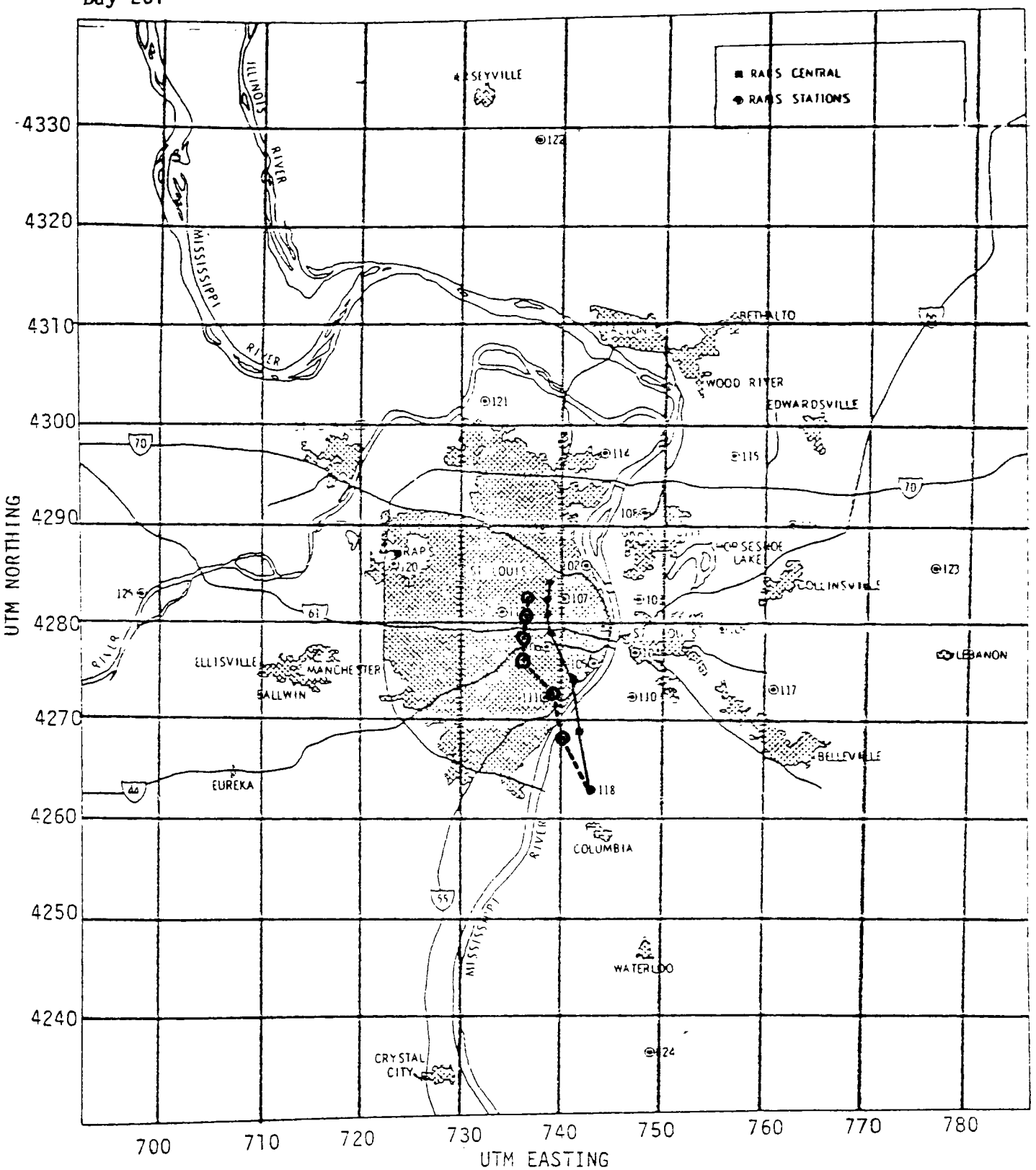

7/19/76
Day 201

Peak Ozone = .15 ppm
Time of Peak = 1300-1400 LDT

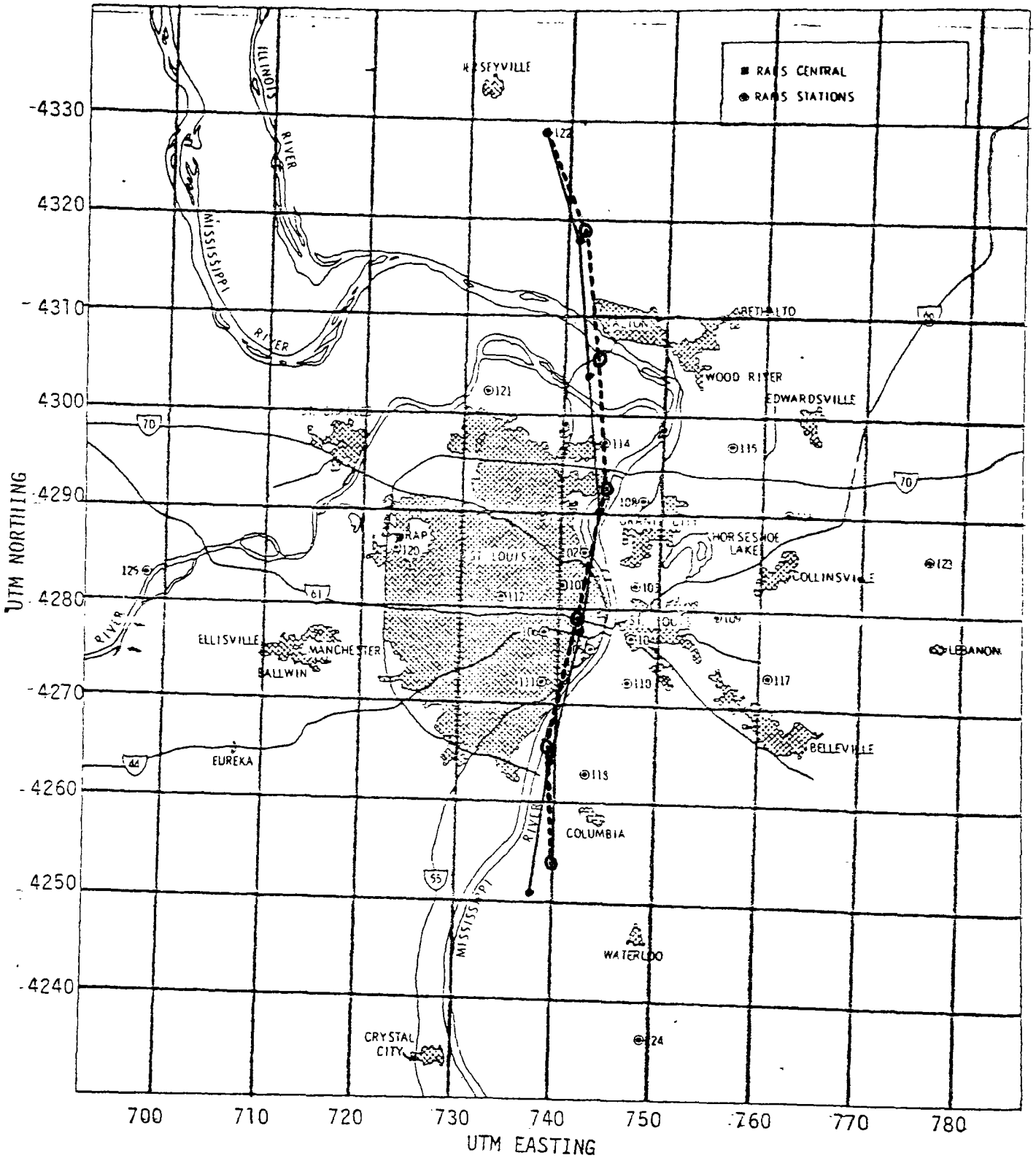

8/8/76
Day 221

Peak Ozone = .12 ppm
Time of Peak = 1800-1900 LDT

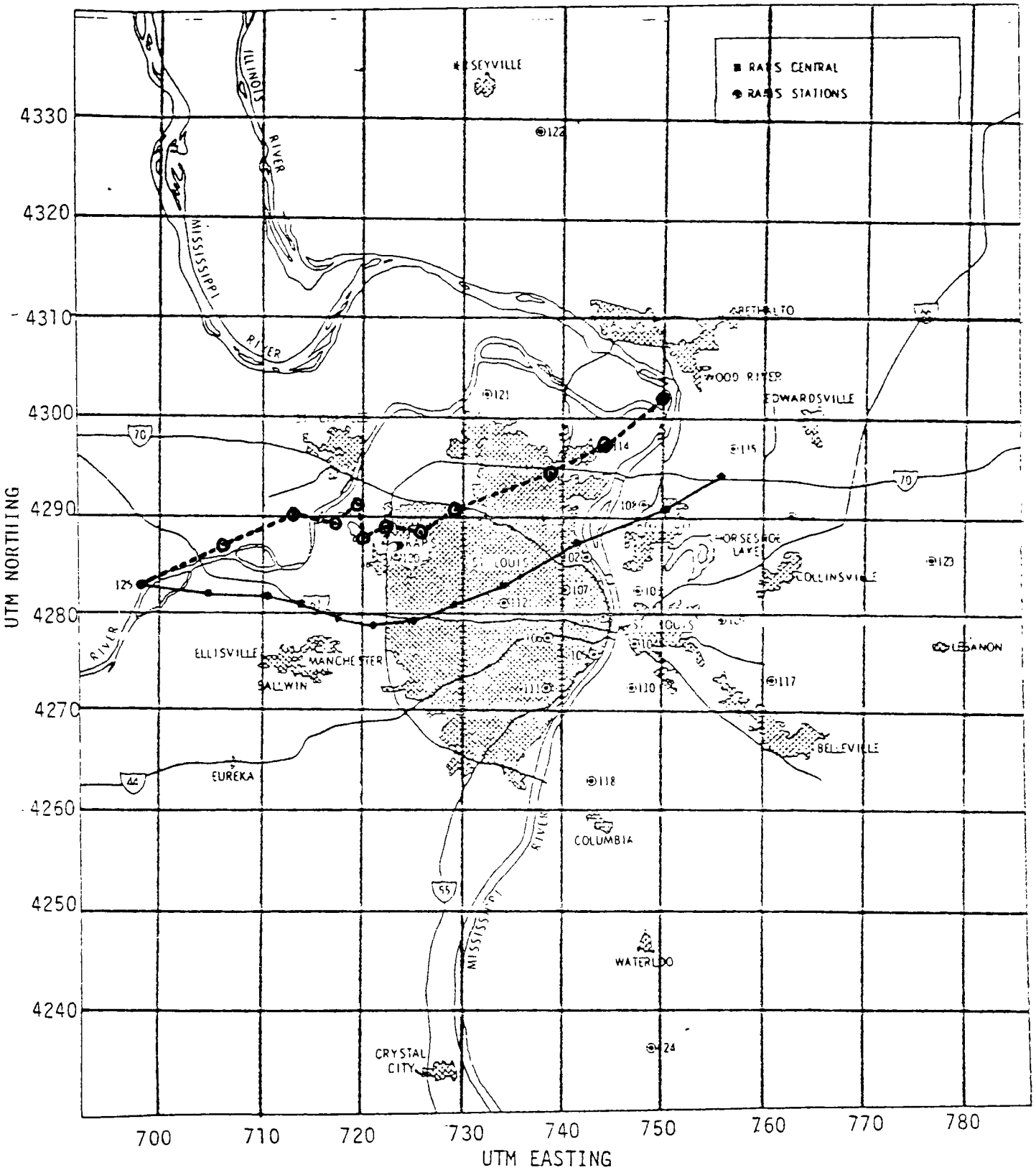

APPENDIX D

The following tables summarize the Level III inputs for each test case.

MODEL INPUT DATA

DATE: 10/01/76 JULIAN DAY: 275 SITE: 102

Simulation Start Time: 0800 LDT

Simulation End Time: 1800 LDT

Initial Concentrations:

NMHC 1.90 ppmC; NO_x 0.236 ppm; O_3 0.0 ppm; NO_2/NO_x 0.25

O_3 Aloft: 0.06 ppm

0800 LDT Mixing Height, meters: 250

Maximum Afternoon Mixing Height, meters: 950.

Post 8 a.m. Emissions:

Hour	NMOC Emission Density, kg-moles/km² hr	NMOC Emission Fraction	NO_x Emission Density, kg-moles/km² hr	NO_x Emission Fraction
1	2.716	0.139	0.465	0.192
2	2.716	0.139	0.465	0.192
3	2.716	0.139	0.465	0.192
4	2.716	0.139	0.465	0.192
5	2.716	0.139	0.465	0.192
6	2.716	0.139	0.465	0.192
7	2.716	0.139	0.465	0.192
8	2.716	0.139	0.465	0.192

MODEL INPUT DATA

DATE: 7/13/76 JULIAN DAY: 195 SITE: 114

Simulation Start Time: 0800 LDT

Simulation End Time: 1800 LDT

Initial Concentrations:

NMHC 0.26 ppmC; NO_x 0.048 ppm; O_3 0.0 ppm; NO_2/NO_x 0.25

O_3 Aloft: 0.08 ppm

0800 LDT Mixing Height, meters: 250.

Maximum Afternoon Mixing Height, meters: 1670.

Post 8 a.m. Emissions:

Hour	NMOC Emission Density, kg-moles/km^2 hr	NMOC Emission Fraction	NO_x Emission Density, kg-moles/km^2 hr	NO_x Emission Fraction
1	2.716	1.019	0.465	0.945
2	2.716	1.019	0.465	0.945
3	2.716	1.019	0.465	0.945
4	2.716	1.019	0.465	0.945
5	2.716	1.019	0.465	0.945
6	2.716	1.019	0.465	0.945
7	2.716	1.019	0.465	0.945
8	0.533	0.200	0.148	0.301
9	0.533	0.200	0.148	0.301

MODEL INPUT DATA

DATE: 6/08/76 JULIAN DAY: 160 SITE: 115

Simulation Start Time: 0800 LDT

Simulation End Time: 1800 LDT

Initial Concentrations:

NMHC 1.08 ppmC; NO_x 0.107 ppm; O_3 0.0 ppm; NO_2/NO_x 0.25

O_3 Aloft: 0.10 ppm

0800 LDT Mixing Height, meters: 250.

Maximum Afternoon Mixing Height, meters: 2220.

Post 8 a.m. Emissions:

Hour	NMOC Emission Density, kg-moles/km² hr	NMOC Emission Fraction	NO_x Emission Density, kg-moles/km² hr	NO_x Emission Fraction
1	2.716	0.245	0.465	0.424
2	0.163	0.015	0.044	0.040
3	0.163	0.015	0.044	0.040
4	0.163	0.015	0.044	0.040
5	0.163	0.015	0.044	0.040
6	0.163	0.015	0.044	0.040
7	0.163	0.015	0.044	0.040
8	0.163	0.015	0.044	0.040
9	0.163	0.015	0.044	0.040

MODEL INPUT DATA

DATE: 6/07/76 JULIAN DAY: 159 SITE: 122

Simulation Start Time: 0800 LDT

Simulation End Time: 1800 LDT

Initial Concentrations:

NMHC 1.83 ppmC; NO_x 0.205 ppm; O_3 0.0 ppm; NO_2/NO_x 0.25

O_3 Aloft: 0.11 ppm

0800 LDT Mixing Height, meters: 250.

Maximum Afternoon Mixing Height, meters: 1920.

Post 8 a.m. Emissions:

Hour	NMOC Emission Density, kg-moles/km² hr	NMOC Emission Fraction	NO_x Emission Density kg-moles/km² hr	NO_x Emission Fraction
1	2.716	0.145	0.465	0.221
2	2.716	0.145	0.465	0.221
3	2.716	0.145	0.465	0.221
4	0.533	0.028	0.148	0.070
5	0.070	0.004	0.092	0.044
6	0.163	0.009	0.044	0.021
7	0.163	0.009	0.044	0.021
8	0.014	0.001	0.003	0.001
9	0.014	0.001	0.003	0.001

MODEL INPUT DATA

DATE: 6/08/76 JULIAN DAY: 160 SITE: 103

Simulation Start Time: 0800 LDT

Simulation End Time: 1800 LDT

Initial Concentrations:

NMHC 1.08 ppmC; NO_x 0.107 ppm; O_3 0.0 ppm; NO_2/NO_x 0.25

O_3 Aloft: 0.10 ppm

0800 LDT Mixing Height, meters: 250

Maximum Afternoon Mixing Height, meters: 2220.

Post 8 a.m. Emissions:

Hour	NMOC Emission Density, kg-moles/km² hr	NMOC Emission Fraction	NO_x Emission Density, kg-moles/km² hr	NO_x Emission Fraction
1	2.716	0.245	0.465	0.424
2	2.716	0.245	0.465	0.424
3	2.716	0.245	0.465	0.424
4	0.163	0.015	0.044	0.040
5	0.163	0.015	0.044	0.040
6	0.163	0.015	0.044	0.040
7	0.163	0.015	0.044	0.040

MODEL INPUT DATA

DATE: 8/25/76 JULIAN DAY: 238 SITE: 115

Simulation Start Time: 0800 LDT

Simulation End Time: 1800 LDT

Initial Concentrations:

NMHC 2.01 ppmC; NO_x 0.162 ppm; O_3 0.0 ppm; NO_2/NO_x 0.25

O_3 Aloft: 0.09 ppm

0800 LDT Mixing Height, meters: 250.

Maximum Afternoon Mixing Height, meters: 1800.

Post 8 a.m. Emissions:

Hour	NMOC Emission Density, kg-moles/km² hr	NMOC Emission Fraction	NO_x Emission Density, kg-moles/km² hr	NO_x Emission Fraction
1	2.716		0.465	0.280
2	0.163		0.044	0.026
3	0.163		0.044	0.026
4	0.163		0.044	0.026
5	0.163		0.044	0.026
6	0.163		0.044	0.026
7	0.163		0.044	0.026
8	0.163		0.044	0.026
9	0.163		0.044	0.026

MODEL INPUT DATA

DATE: 10/02/76 JULIAN DAY: 276 SITE: 115

Simulation Start Time: 0800 LDT

Simulation End Time: 1800 LDT

Initial Concentrations:

NMHC 2.47 ppmC; NO_x 0.264 ppm; O_3 0.0 ppm; NO_2/NO_x 0.25

O_3 Aloft: 0.06 ppm

0800 LDT Mixing Height, meters: 250

Maximum Afternoon Mixing Height, meters: 1810.

Post 8 a.m. Emissions:

Hour	NMOC Emission Density, kg-moles/km² hr	NMOC Emission Fraction	NO_x Emission Density, kg-moles/km² hr	NO_x Emission Fraction
1	2.716	0.107	0.465	0.172
2	0.163	0.006	0.044	0.016
3	0.163	0.006	0.044	0.016
4	0.163	0.006	0.044	0.016
5	0.163	0.006	0.044	0.016
6	0.163	0.006	0.044	0.016
7	0.163	0.006	0.044	0.016
8	0.163	0.006	0.044	0.016
9	0.163	0.006	0.044	0.016
10	0.163	0.006	0.044	0.016

MODEL INPUT DATA

DATE: 09/17/76 JULIAN DAY: 261 SITE: 118

Simulation Start Time: 0800 LDT

Simulation End Time: 1800 LDT

Initial Concentrations:

NMHC 2.04 ppmC; NO_x 0.174 ppm; O_3 0.0 ppm; NO_2/NO_x 0.25

O_3 Aloft: 0.06 ppm

0800 LDT Mixing Height, meters: 250

Maximum Afternoon Mixing Height, meters: 1670.

Post 8 a.m. Emissions:

Hour	NMOC Emission Density, kg-moles/km^2 hr	NMOC Emission Fraction	NO_x Emission Density, kg-moles/km^2 hr	NO_x Emission Fraction
1	2.716	0.130	0.465	0.261
2	2.716	0.130	0.465	0.261
3	0.123	0.006	0.023	0.013
4	0.123	0.006	0.023	0.013
5	0.123	0.006	0.023	0.013
6	0.123	0.006	0.023	0.013

MODEL INPUT DATA

DATE: 07/19/76 JULIAN DAY: 201 SITE: 122

Simulation Start Time: 0800 LDT

Simulation End Time: 1800 LDT

Initial Concentrations:

NMHC 0.96 ppmC; NO_x 0.054 ppm; O_3 0.0 ppm; NO_2/NO_x 0.25

O_3 Aloft: 0.08 ppm

0800 LDT Mixing Height, meters: 250.

Maximum Afternoon Mixing Height, meters: 1590.

Post 8 a.m. Emissions:

Hour	NMOC Emission Density, kg-moles/km^2 hr	NMOC Emission Fraction	NO_x Emission Density, kg-moles/km^2 hr	NO_x Emission Fraction
1	2.716	0.276	0.465	0.840
2	2.716	0.276	0.465	0.840
3	0.348	0.035	0.120	0.217
4	0.117	0.012	0.068	0.123
5	0.163	0.017	0.044	0.079
6	0.014	0.001	0.003	0.005

MODEL INPUT DATA

DATE: 8/08/76 JULIAN DAY: 221 SITE: 125

Simulation Start Time: 0800 LDT

Simulation End Time: 1800 LDT

Initial Concentrations:

NMHC 0.33 ppmC; NO_x 0.033 ppm; O_3 0.0 ppm; NO_2/NO_x 0.25

O_3 Aloft: 0.07 ppm

0800 LDT Mixing Height, meters: 250.

Maximum Afternoon Mixing Height, meters: 1440.

Post 8 a.m. Emissions:

Hour	NMOC Emission Density, kg-moles/km^2 hr	NMOC Emission Fraction	NO_x Emission Density, kg-moles/km^2 hr	NO_x Emission Fraction
1	2.716	0.803	0.465	1.375
2	2.716	0.803	0.465	1.375
3	2.716	0.803	0.465	1.375
4	2.716	0.803	0.465	1.375
5	0.533	0.158	0.148	0.438
6	0.533	0.158	0.148	0.438
7	0.533	0.158	0.148	0.438
8	0.533	0.158	0.148	0.438
9	0.533	0.158	0.148	0.438
10	0.070	0.021	0.092	0.272

TECHNICAL REPORT DATA
(Please read Instructions on the reverse before completing)

1. REPORT NO.	2.	3. RECIPIENT'S ACCESSION NO.
EPA 450/4-82-009		

4. TITLE AND SUBTITLE	5. REPORT DATE
An Evaluation of the Empirical Kinetic Modeling Approach Using the St. Louis RAPS Data Base	June 1982
	6. PERFORMING ORGANIZATION CODE

7. AUTHOR(S)	8. PERFORMING ORGANIZATION REPORT NO.
Gerald L. Gipson	

9. PERFORMING ORGANIZATION NAME AND ADDRESS	10. PROGRAM ELEMENT NO.
U.S. Environmental Protection Agency Office of Air Quality Planning and Standards/MDAD/AMTB Mail Drop 14 Research Triangle Park, North Carolina 27711	11. CONTRACT/GRANT NO.

12. SPONSORING AGENCY NAME AND ADDRESS	13. TYPE OF REPORT AND PERIOD COVERED
Same	Final
	14. SPONSORING AGENCY CODE

15. SUPPLEMENTARY NOTES

16. ABSTRACT

The use of three different approaches for evaluating the Empirical Kinetic Modeling Approach (EKMA) are described. The first two approaches consist of using the model underlying EKMA to make predictions of peak ozone for comparison with observations. In one ase, the detailed St. Louis RAPS data base was used to develop model inputs. In the second, a much more simplified data base was used as the basis for model inputs. In general, the simplified approach produced better results. The final approach consisted of comparing EKMA predictions of changes in ozone with those of a more complex photochemical air quality simulation model. EKMA did not agree with the complex model over the entire range of evaluation. However, when estimating the degree of control necessary to lower peak ozone to the level of the standard, differences between EKMA and the complex model and EKMA were usually less than 10%.

17. KEY WORDS AND DOCUMENT ANALYSIS

a. DESCRIPTORS	b. IDENTIFIERS/OPEN ENDED TERMS	c. COSATI Field/Group
Ozone Control strategies Photochemical pollutants Photochemical models EKMA OZIPP		

18. DISTRIBUTION STATEMENT	19. SECURITY CLASS *(This Report)*	21. NO. OF PAGES
Unlimited	Unlimited	177
	20 SECURITY CLASS *(This page)*	22. PRICE

EPA Form 2220-1 (Rev. 4-77) PREVIOUS EDITION IS OBSOLETE